Alma Mater Studiorum – Università di Bologna

DOTTORATO DI RICERCA IN

SCIENZE BIOMEDICHE E NEUROMOTORIE

Ciclo XXX

Settore Concorsuale: 05/D1

Settore Scientifico Disciplinare: BIO/09

NEUROPHYSIOLOGICAL AND METABOLIC REGULATION OF SPONTANEOUS AND SYNTHETIC TORPOR: A TRANSLATIONAL PERSPECTIVE

Presentata da: Timna Hitrec

Coordinatore Dottorato **Supervisore**

Prof. Lucio Cocco **Prof. Roberto Amici**

Esame finale anno 2018

ABSTRACT

Torpor is an energy-saving physiological state characterized by a transient and reversible decrease in metabolic rate and core temperature, which occurs in different species in conditions of scarce food availability. At present, the mechanism underlying torpor occurrence is unknown. The attempt to imitate natural torpor is pursued in clinical practice, in order to overcome the severe side effects that follow the induction of therapeutic hypothermia. Several attempts to induce a torpor-like state (synthetic torpor) by manipulating central nervous activity have been made in rodents. Most promising are the activation of central adenosine type-1 receptors and the pharmacological inhibition of the Raphe Pallidus (RPa).

Aims of the present project were: i) to unravel the neural pathway of spontaneous torpor in mice, a species that enters daily torpor spontaneously; ii) to understand the possible mechanism of metabolic rate reduction in spontaneous and synthetic torpor, in mice and rats, respectively, by evaluating mitochondrial activity during deep hypothermia; iii) to explore the possibility to induce synthetic torpor in a large mammal, the swine, by the central manipulation of the RPa.

In summary, the results showed that: i) Paraventricular and Dorsomedial Hypothalamic nuclei showed a specific neural activation at the entrance in torpor; ii) liver mitochondria showed a reduction in maximum respiration rate in spontaneous, but not in synthetic torpor, while no major changes occurred in kidney and brain; iii) central manipulation of the RPa in swine induced physiological modifications similar to those observed in rats.

ABSTRACT

Il torpore è una condizione fisiologica caratterizzata da una diminuzione transitoria e reversibile del metabolismo e della temperatura centrale, attuata da alcune specie in condizioni di scarsa disponibilità di risorse. Attualmente, il meccanismo che sottende il torpore è sconosciuto. Tentare di imitare ciò che avviene naturalmente nel torpore spontaneo è un obiettivo perseguito dalla pratica clinica, al fine di eliminare i gravi effetti collaterali indotti dall'ipotermia terapeutica. Alcuni tentativi di indurre uno stato di pseudo-torpore (torpore sintetico) tramite una manipolazione centrale del sistema nervoso sono stati condotti nei roditori. Tra questi, i metodi più promettenti sembrano essere l'attivazione dei recettori centrali di tipo 1 per l'adenosina e l'inibizione farmacologica del Raphe Pallidus (RPa).

Gli obiettivi del progetto sono stati: i) individuare la via nervosa che sottende l'ingresso in torpore nel topo, un animale capace di entrare spontaneamente in torpore giornaliero; ii) individuare il possibile meccanismo della riduzione metabolica nel torpore spontaneo e sintetico, rispettivamente nel topo e nel ratto, valutando l'attività mitocondriale durante l'ipotermia profonda; iii) esplorare la possibilità di indurre il torpore sintetico in un mammifero di grande taglia, il maiale, tramite manipolazione centrale del RPa.

In sintesi, i risultati hanno evidenziato che: i) all'entrata in torpore si osserva una attivazione neuronale specifica nei nuclei Paraventricolare e Dorsomediale dell'ipotalamo; ii) i mitocondri del fegato mostrano una riduzione della massima capacità respiratoria nel torpore spontaneo ma non in quello sintetico, mentre non si sono osservati effetti rilevanti nel rene e nel cervello; iii) nel maiale, la manipolazione centrale del RPa induce modificazioni fisiologiche simili a quelle osservate nel ratto.

TABLE OF CONTENTS

1. INTRODUCTION 1

1.1 THERMOREGULATION 3

1.1.1 THERMOREGULATORY RESPONSES TO BODY COOLING *5*

1.1.2 THERMOREGULATORY RESPONSES TO BODY WARMING *8*

1.1.3 CURRENT UNDERSTANDINGS OF CENTRAL NEURAL PATHWAYS FOR THERMOREGULATION *9*

1.1.4 THE ROLE OF SYMPATHETIC AUTONOMIC NERVOUS SYSTEM IN THERMOREGULATION *12*

1.2 CENTRAL NERVOUS CONTROL OF ENERGY HOMEOSTASIS 16

1.2.1 CENTRAL REGULATION OF FOOD INTAKE *16*

1.2.2 HOMEOSTATIC CONTROL OF FOOD CONSUMPTION AND ENERGY EXPENDITURE *22*

1.3 TORPOR AND HIBERNATION 24

1.3.1 SPONTANEOUS TORPOR *24*

1.3.2 SYNTHETIC TORPOR *37*

1.4 THERAPEUTIC HYPOTHERMIA 43

1.4.1 CURRENT CLINICAL APPLICATIONS *43*

1.4.2 POSSIBLE FUTURE APPLICATIONS *45*

2. AIMS 47

3. MATERIAL AND METHODS 51

3.1 EXPERIMENT I 53

3.1.1 ANIMALS *53*

3.1.2 PREOPERATIVE PROCEDURES *54*

3.1.3 SURGERY *54*

3.1.4 EXPERIMENTAL SET-UP *57*

3.1.5 EXPERIMENTAL PLAN *57*

3.1.6 PERFUSION *59*

3.1.7 HISTOLOGY *59*

3.1.8 IMMUNOHISTOCHEMISTRY *60*

3.1.9 IMAGE ACQUISITION AND COUNTING *61*

3.1.10 STATISTICAL ANALYSIS *62*

3.1.11 PRELIMINARY NEURONS PHENOTIPIZATION ... *62*
3.2 EXPERIMENT II ... 62
3.2.1 ANIMALS ... *62*
3.2.2 PREOPERATIVE PROCEDURES ... *63*
3.2.3 SURGERY ... *63*
3.2.4 EXPERIMENTAL SET-UP ... *66*
3.2.5 EXPERIMENTAL PLAN ... *66*
3.2.6 MICROINJECTIONS IN THE FREE-BEHAVING RAT ... *68*
3.2.7 MITOCHONDRIA PROCESSING ... *68*
3.2.8 STATISTICAL ANALISYS ... *69*
3.3 EXPERIMENT III ... 70
3.3.1 ANIMALS ... *70*
3.3.2 PREOPERATIVE PROCEDURES ... *70*
3.3.3 SURGERY ... *71*
3.3.4 MICROINJECTION ... *72*
3.3.5 STATISTICAL ANALISYS ... *73*

4. RESULTS ... 75

4.1 EXPERIMENT I ... 77
4.1.1 EFFECTS OF TORPOR ON CUTANEOUS TEMPERATURE ... *77*
4.1.2 C-FOS POSITIVITY ... *77*
4.1.3 DOUBLE STAINING POSITIVITY ... *78*
4.1.4 TRIPLE STAINING IN LATERAL HYPOTHALAMUS ... *78*
4.2 EXPERIMENT II ... 79
4.2.1 EFFECTS OF SPONTANEOUS AND SYNTHETIC TORPOR ON CUTANEOUS AND HYPOTHALAMIC TEMPERATURE ... *79*
4.2.2 EFFECTS OF SPONTANEOUS AND SYNTHETIC TORPOR ON LIVER MITOCHONDRIA ... *79*
4.2.3 EFFECTS OF SPONTANEOUS AND SYNTHETIC TORPOR ON KIDNEY MITOCHONDRIA ... *80*
4.2.4 EFFECTS OF SPONTANEOUS AND SYNTHETIC TORPOR ON BRAIN MITOCHONDRIA ... *81*
4.2.5 EFFECTS OF SYNTHETIC TORPOR ON UNCOUPLING PROTEIN 2 EXPRESSION ... *81*
4.3 EXPERIMENT III ... 81
4.3.1 EFFECTS OF CENTRAL ACTIVATION AND INHIBITION OF THE RAPHE PALLIDUS IN THE PIG ... *81*

5. DISCUSSION ... 83

5.1 **EXPERIMENT I** 85
5.2 **EXPERIMENT II** 88
5.3 **EXPERIMENT III** 90
5.4 **CONCLUSIONS** 91

6. FIGURES 93

7. REFERENCES 175

ACKNOWLEDGEMENTS 199

INDEX OF ABBREVIATIONS

2-DG: 2-deoxyglucose

5'-AMP: 5' adenosine monophosphate

α-MSH: α-melanocyte stimulating hormone

ACSF: artificial cerebrospinal fluid

ADP: adenosine diphosphate

AGRP: agouti-related protein

ANS: autonomic nervous system

AP: arterial pressure

ARC: Arcuate nucleus

ATP: adenosine triphosphate

AVA: arterio-venous anastomoses

BAT: brown adipose tissue

BNST: Bed Nucleus of Stria Terminalis

CART: cocaine and amphetamine regulated transcript

CGRP: calcitonin gene-related peptide

CHA: N-6 Cyclohexyladenosine

CTb: Cholera Toxin b

DAP: diastolic arterial pressure

DMH: Dorsomedial Hypothalamic nucleus

ECG: electrocardiogram

H_2S: hydrogen sulphide

HR: heart rate

ICV: intracerebroventricular

IML: intermediolateral column

LH: Lateral Hypothalamus

LPB: Lateral Parabrachial nucleus

MC4R: melanocortin 4 receptor

MCH: melanin concentrating hormone

MnPO: Median Preoptic nucleus

MPO: Medial Preoptic nucleus

NAc: Nucleus Accumbens

NMDA: N-methyl-D-aspartate

NPY: neuropeptide Y

NTS: Nucleus Tractus Solitarius

PAG: Periaqueductal Gray

PBN: Parabrachial nucleus

PBS: phosphate-buffered saline

PGE2: prostaglandin E2

POA: Preoptic Area

POMC: proopiomelanocortin

PVH: Paraventricular Hypothalamic nucleus

RPa: Raphe Pallidus

RVLM: Rostral Ventrolateral Medulla

RVMM: Rostral Ventromedial Medulla

SAP: systolic arterial pressure

SCN: Suprachiasmatic nucleus

T1AM: 3-iodothyronamine

Ta: ambient temperature

Tb: body temperature

Thy: hypothalamic temperature

TRH: thyrotropin-releasing hormone

TRP: transient receptor potential channel

UCP1: uncoupling protein 1

UCP2: uncoupling protein 2

VGLUT3: glutamatergic vescicular transporter type 3

VLPAG: Ventrolateral Peraqueductal Gray

VLPO: Ventrolateral Preoptic nucleus

VTA: Ventral Tegmental Area

1. INTRODUCTION

1.1 THERMOREGULATION

Thermoregulation is a complex physiological regulatory process that allows the animal to maintain its core body temperature (Tb) at stable levels. This is achieved through the regulation of heat loss and production, in order to counteract any relevant change in below or beyond the normal physiological values, mostly induced by changes in ambient temperature (Ta) below or beyond the so-called thermoneutral zone. Maintaining a constant body temperature is a full-time necessity, and the body must be able to produce, preserve and disperse heat efficiently; all of these processes are mediated by specific effector organs.

The theory that is behind the physiology of thermoregulation is called set-point theory: the core idea is that the brain controls body temperature by modulating the reference value of core temperature, the set point (Boulant, 2005; Cerri, 2017). Accordingly, the thermal effectors operate in a fine and coordinated manner to reduce the difference between the core temperature and the set point.

Recently, the set point theory has been challenged by Romanovsky (Romanovsky, 2006), who proposed that Tb would not be regulated by a single controller, but by independent thermoeffector loops, each having specific afferent and efferent branches.

To explain the key factors involved in thermoregulation, it is important to understand how these thermoregulatory processes evolved in time.

On this behalf, animals can be divided in two major groups:

- Poikilotherms: animals that adapt their core Tb to Ta, usually keeping it at a maximum of around 35°C, with obvious consistent oscillations due to Ta variations. These animals are ectotherms, since they mostly rely on external environment to heat their own body. In this group, we find reptiles, amphibians and fishes.

- Homeotherms: animals that maintain a pretty constant internal body temperature regardless of external ambient temperature variations. The body temperature is stable at around 37°C, with minimal oscillations. These animals are mostly endotherms, since they rely on their own metabolism to heat their own body.

In this group, we find birds and mammals. A third group of animals that are called heterotherms are able to switch between homeothermy and poikilothermy. In particular, heterotherms are able to enter a peculiar poikilothermic regulated state that is called torpor. Torpor is a very efficient energy-saving physiological state, adopted by hibernating animals in conditions of scarce food availability, usually during cold periods of the year, which consists in a large decrease of metabolic rate and body temperature.

The process of maintaining a constant body temperature relies on a few physical phenomena that explain the heat exchange occurring between a body and the external environment:

- Radiation: heat is transferred through electromagnetic (infrared) radiations.
- Conduction: heat produced by the kinetic energy (vibration) of particles of a body can be transferred by contact with a cooler body whose particles have a lower kinetic energy.
- Thermal convection: heat from a body is transferred to fluids, which by heating up lower their density, creating convective motions. These convection currents create an ascending hot current and a descending cold current, which lowers the temperature of the body.
- Evaporation: change of state of matter from liquid to gaseous.

In the first three processes, the exchange can occur in both directions, whilst the last one can only occur unidirectionally from the body to the environment, because heat is transferred to the fluid, which evaporates and leaves the body in gaseous form.

The evolution of thermoregulation strictly adhered to these physical phenomena, being the pillars of the evolution of specific organs and strategies, highly specialized in the task of preserving the body temperature. From that perspective, two distinct forms of thermoregulation can be observed:

- Behavioural thermoregulation: the animal is actively modifying its body temperature, by adopting behavioural strategies (e.g. reptiles basking in the sun to absorb heat). This ancestral method can be found in all animal classes. Animals that

use this kind of thermoregulation choose their habitat considering the external ambient temperature, preferring the one that provides the temperature closest to the optimal one. Seeking for the best ambient conditions can be done by small and frequent moving: for example, snakes move several times during the day, alternating shady areas to sunny ones. On the other hand, some animals, such as migratory birds, seek for the best ambient condition by moving thousands of kilometres, travelling to climates that are more temperate during winter. Another behavioural thermoregulation strategy consists in postural adjustments that, exposing more or less body surface to the environment, respectively disperse or preserve body heat. Moreover, some mammals cover their body with saliva, allowing heat dispersion through evaporation. In scientific field, this behaviour is known as saliva-spreading.

- Non-behavioural thermoregulation: it relies on involuntary acts driven by the autonomic nervous system. Even if recently some studies showed that reptiles and fish have a form of non-behavioural thermoregulation, they mostly rely on behavioural strategies (Bicego *et al.*, 2007). Therefore, the only animals efficiently using non-behavioural thermoregulation are mammals and birds. These animals can control and regulate their temperature independently from external factors, and in comparison to other animal classes, they have a higher body temperature. Either every thermal challenge coming from the external or the internal environment is counteracted by specific autonomic strategies that can be divided in two categories: thermoregulatory responses to body cooling and thermoregulatory responses to body warming.

1.1.1 THERMOREGULATORY RESPONSES TO BODY COOLING

Thermoregulatory responses to body cooling include all those strategies aimed to preserve and/or produce heat. In these conditions, core temperature is preserved by an increase in heat production (thermogenesis), which can be the outcome of shivering or non-shivering processes, and through a reduction of heat dispersion (cutaneous vascular flow regulation and piloerection).

1.1.1.1 SHIVERING THERMOGENESIS

This thermoregulatory response is obtained by the isometric contraction of skeletal muscles, which produces heat. The contraction is driven by a neural stimulus directly driven to the muscle when the core temperature decreases, however it does not produce a finalized movement, but a shivering behaviour. This phenomenon is also very important to increase Tb during fever development.

1.1.1.2 NON-SHIVERING THERMOGENESIS

1.1.1.2.1 Chemical thermogenesis

Chemical thermogenesis is a strategy that allows animals to produce heat through exothermic biochemical reactions that occur in organs that have thermoregulatory abilities. The main organs involved are brown adipose tissue (BAT), liver and muscle.

1.1.1.2.2 Brown adipose tissue

Brown adipose tissue (BAT) was found for the first time in hibernating mammals, therefore was firstly named hibernating gland. It consists of reticular adipose tissue, rich of mitochondrial carotenoids that give the typical brown pigmentation (in opposition to the white adipose tissue). Its major function is to produce heat, and that is the reason for its anatomical distribution near blood vessels, a strategic position to release heat in the blood stream, to be diffused in the whole body. The biggest portions of BAT can be found at interscapular, periaortic and perirenal level. This adipose tissue is present in almost all mammals (rodents especially), humans included (Saito *et al.*, 2009), especially in neonatal age and in animals that have a large surface/volume ratio. The BAT's thermogenic activity relies on the function of a specific mitochondrial protein: uncoupling protein 1 (UCP1), located in the mitochondrial internal membrane. It has the ability to uncouple the oxidative phosphorylation, in this way the process does not produce ATP but heat (Cannon and Nedergaard, 2004). UCP1 is activated by fatty acids released from lipidic droplets and it consists of a channel protein permeable to protons, in this way the protons return to the matrix via the UCP1 and not the ATP-sinthethase. This creates a protonic gradient across the membrane, leading to the uncoupling from ATP

synthesis. The innervation of the brown adipose tissue consists of direct connecting fibers from the sympathetic column ganglia, the fibers release noradrenalin, which binds to β3 receptors, activating second messenger mechanisms, leading to both heat production and UCP1 expression, moreover, this stimulation also determines tropism in BAT. Plasmatic levels of thyroid hormones T3 and T4 are also crucial for the activation of BAT; the exposure to low ambient temperatures determines an increase in these hormones, this activates brown adipose tissue in order to stimulate heat production.

1.1.1.2.3 Liver

The liver is a very active metabolic organ, hosting a considerate amount of exothermic reactions. It is currently considered a thermoregulatory organ, able to increase its metabolic activity with subsequent heat production, when the body is exposed to low ambient temperatures.

1.1.1.2.4 Muscle

As previously mentioned, muscles have the ability to produce heat by shivering, but recently some isoforms of UCP have been found in the tissue, suggesting a metabolic thermogenic role. Moreover, birds express the protein avUCP, an isoform of UCP, whose expression seems to be directly related to decreases in body temperature (Dulloo and Samec, 2001; Raimbault *et al.*, 2001).

1.1.1.2.5 Heart

A prominent positive chronotropism is observed in cardiac activity during exposure to low ambient temperature. On one hand, this sustains the increased metabolic tissue demand, but on the other, it produces a discrete amount of heat.

1.1.1.3 CUTANEOUS VASOCONSTRICTION

The heat obtained from both from thermogenic organs and normal biochemical exothermic reactions, requires an efficient transport system, to assure its diffusion throughout the whole body, but in the meantime, it also has to preserve heat when needed. This important role is played by the cardiovascular system. For this purpose, the branch of the autonomic nervous system responsible of thermoregulation had to cooperate with a more ancient part of the autonomic nervous system, the one in

charge of the cardiovascular function. These two systems are alternatively in control of the cardiovascular activity, and in some conditions, thermoregulatory needs can entirely predominate on cardiovascular ones, when the control of the cardiovascular system is operated by thermoregulatory centers.

Thermoregulatory centers can modulate the cardiovascular system in two ways: by modifying the heart rate, and by adjusting the diameter of arterioles.

The increase in heart rate provides a better perfusion of the brown adipose tissue, guaranteeing a good oxygenation to support the increased activity, in addition to that, the increase in cardiac frequency optimise heat distribution in all anatomical body districts.

The variation in skin arterioles diameter is crucial in the increase (vasodilation) or decrease (vasoconstriction) of the peripheral cutaneous blood stream, which are respectively involved in heat dispersion or heat preservation.

Therefore, the exposure to low ambient temperatures causes vasoconstriction in cutaneous blood vessels to preserve heat; at the same time, there is an increase in heart rate, to maximize heat transport from thermogenic organs to the whole body.

Piloerection

Piloerection (involuntary erection or bristling of hairs) is a heat-preserving strategy of particular importance in animals covered with fur. The contraction of the arrector pili muscles helps in heat preservation by creating an insulating layer of air between the body and the external environment.

1.1.2 THERMOREGULATORY RESPONSES TO BODY WARMING

Thermoregulatory responses to body warming involve all the effectors that play a role in heat dissipation, whose activation is concomitant with the inhibition of thermogenic organs. The most important heat dissipation strategy is the regulation of cutaneous blood flow, but also some secondary mechanisms act as a support in thermodispersion, such as polypnea and sweating.

1.1.2.1 CUTANEOUS VASODILATION

Regulation of cutaneous blood flow is a crucial mechanism in body temperature defence both in cold and hot environments. In the latter, the body has to dissipate excessive amount of heat, which is obtained by increasing cutaneous blood flow (vasodilation) and by shutting down thermogenic effectors (reduction in heat production). In these circumstances, a decrease in cardiac frequency is observed, due to a lower oxygen demand by thermogenic organs.

1.1.2.2 PERSPIRATION

Perspiration (or sweating), is the secretion of fluids by sweat glands. This thermoregulatory process is based on the thermodispersion through liquid evaporation. In humans, sweat glands are localized in the whole body surface, with a major density in hands and toes. They have been found only in a few other mammals, such as camel and antelope (Bicego *et al.*, 2007), where in others have been observed only in some anatomical parts of the body (paws in dogs).

1.1.2.3 THERMAL POLYPNEA

Polypnea is a non-pathological increase in respiratory acts frequency that physiologically happens during physical activity, in response to an increase in metabolic processes and consequently in oxygen demands. Thermal polypnea (also called panting) plays an important role in thermodispersion in furry animals in hot environments, when at rest, a large increase in respiratory acts frequency, concomitant with a small tidal volume, promotes heat dissipation through evaporation of liquids on the surface of buccal and pulmonary mucous membranes with limited effects on CO_2 plasma levels. This strategy can be observed only in some mammals, and it is more intense and accentuated in animals that have thermoregulatory difficulties in hot environments (e.g. dogs with short muzzle).

1.1.3 CURRENT UNDERSTANDINGS OF CENTRAL NEURAL PATHWAYS FOR THERMOREGULATION

Homeotherms keep their body temperature constant, around 37°C – 37.5°C, regardless of external or internal (e.g. physical activity) modifications. To achieve

that, being able to measure the entity of those modifications is crucial in thermoregulation, in order to counteract any oscillations with prompt and specific actions. That makes clear how central neural pathways for thermoregulation are extremely complex and not yet entirely described. The thermoregulatory circuitry can be parted in two main branches:

1. Temperature sensation afferent pathway

2. Thermoregulatory effectors pathway

Temperature sensation consists in gathering thermal information from the body and the external environment and sending them to superior somatosensorial or autonomic thermoregulatory nuclei. Thermal information are collected by thermal receptors, which can sense temperature with specific channel proteins of the transient receptor potential (TRP) family. In particular, TRPM8 are cold-sensitive, whereas TRPV3/4 are warm-sensitive.

Their distribution is quite ubiquitarian, however three areas can be pointed out for having a higher amount of temperature sensitive receptors: the skin, the guts, and the brain.

The major organ involved in delivering information about the external environment is the skin, thus cutaneous thermoception is crucial in starting anticipatory thermic compensation, both for cold and warm stimuli. This behaviour was pointed out by studies conducted in rats (Lomax *et al.*, 1964), cats (Forster and Ferguson, 1952) and dogs (Hellstrom and Hammel, 1967), where the exposure to cold environments caused a rapid decrease in cutaneous temperature, not followed by a decrease in rectal temperature, which in fact slightly increased. Even for the exposure to warm environments there was an anticipatory response driven by cutaneous afferences (Nakamura and Morrison, 2010).

All thermal information obtained by cutaneous thermoceptors are directed to the lamina I neurons through somatosensitive fibers in the dorsal spinal horn. The spino-thalamo-cortical tract connects the lamina I neurons to the primary somatosensitive cortex, where the real thermoception occurs (Craig, 2000).

At the same time, thermal information are also transmitted through a glutamatergic pathway to different parts of the Lateral Parabrachial nucleus (LPB), the dorsolateral part for cold-sensation and the dorsomedial for warm-sensation. Afterwards signals are sent to the Preoptic Area (POA) through glutamatergic projections, targeting the Median Preoptic nucleus (MnPO).

The POA is considered the higher integrative center for thermoregulatory responses, but it also regulates several other homeostatic functions, such as energy expenditure, osmolarity and cardiovascular activity. It is thought to be the area controlling the core temperature set-point (Morrison *et al.*, 2008).

Several cold and warm thermal receptors are located in the gut, and their afferent fibers are in the vagus and splanchnic nerves, however, it is still not clear how those information reach the POA. It has been suggested that several gut stimuli, such as satiety, temperature, gastric tension, thirst, taste, and arterial pressure are transferred to the dorsal and caudal part of the LPB through the Nucleus Tractus Solitarius (NTS) (Saper, 2002). Thus, some speculations suggest that the LPB could be the integration center between thermic and visceral stimuli, which end up in the POA (Nakamura and Morrison, 2010).

As previously mentioned, the central nervous system is rich in neurons that are able to fire action potential in response to specific thermic stimuli. Among them, the most studied neuronal population is the one within the POA in the hypothalamus. POA has a subpopulation of thermosensitive neurons that display spontaneous discharge at thermoneutral temperatures, which increase their firing when the area is warmed locally (Nakayama *et al.*, 1963). In particular, it contains warm-sensitive neurons whose tonic firing is reduced by skin cooling, and the thermosensitivity is increased (Boulant and Hardy, 1974). Several scientific evidences pointed out how POA modulates thermogenesis and BAT activity (Hammel *et al.*, 1960; Imai-Matsumura *et al.*, 1984); it is still not clear how warm-sensitive neurons work, however these findings suggest that warm-sensitive neurons integrate cutaneous and local (central) thermal information, and function as inhibitory projection neurons in the Medial Preoptic nucleus (MPO), which are tonically active in thermoneutral temperatures to

suppress thermogenesis (Morrison and Nakamura, 2011). The current model of thermoregulation and cutaneous vasomotion is summarized in Fig 1.

1.1.4 THE ROLE OF SYMPATHETIC AUTONOMIC NERVOUS SYSTEM IN THERMOREGULATION

The autonomic nervous system (ANS) is anatomically and functionally divided in two branches: the sympathetic and the parasympathetic one.

Form a functional point of view; these two branches collaborate in controlling several body parts, by constantly balancing and adjusting their influence based on maintaining body homeostasis. They act on the target organs by releasing neurotransmitters that bind to specific receptors located in the organs. The main neurotransmitters involved are noradrenaline (binding to noradrenergic receptors) for the sympathetic branch and acetylcholine (binding to cholinergic receptors) for the parasympathetic one.

From the anatomical point of view, the major differences between the branches can be found in the ganglia position. In the parasympathetic system, the motoneurons or preganglia neurons (cholinergic) axons originate from the cervical and sacral part of the spinal cord; they synapse with the postganglia neurons in the ganglia, which are located in the target organ. In the sympathetic system, the preganglia neurons (cholinergic) originate from the lateral horns of toracolumbar part of the spinal cord, and synapse with the post-ganglia neurons (adrenergic) in the ganglia, that in this branch are located far from the target organs (in the proximity of the spinal cord).

All organs are controlled by both branches, except from sudoriparous glands, blood vessels smooth muscle, and BAT, which are only controlled by the sympathetic nervous system.

1.1.4.1 SYMPATHETIC AUTONOMIC CONTROL OF BLOOD VESSELS

As already previously introduced, cutaneous vasomotion regulation plays an important role in thermoregulatory responses, in both low and high ambient temperatures exposure. The crosstalk between the cardiovascular and the

thermoregulatory centres makes it a complex and key-system in body temperature defence.

The unique ability to influence both heat preservation (through vasoconstriction) and dispersion (through vasodilation) makes it very interesting from a functional and experimental point of view.

All the body is involved in this process; however, some anatomical districts are more engaged in thermoregulation, and they are called heat exchangers (e.g. tail and paws in rats, ears in cats and rabbits). The main common characteristics of these organs are the high surface/volume ratio, an extensive capillary bed and glabrous skin.

The capillary bed has numerous arterio-venous anastomoses (AVA), direct precapillary connections between small arteries and small veins.

AVA's have think smooth muscle walls, controlled directly by the ANS. Their inner diameter varies between 10 and 50 μm, when stimulated, they are able to contract and block the blood flow.

It is not completely clear which role the AVA's play in cutaneous vasomotion, however it is believed that AVA's in thermoregulatory districts reduce their muscular tone to preserve heat (the blood stream uses the AVA as a shortcut between small arteries and veins by-passing the cutaneous capillary bed); on the other hand, when heat needs to be dissipated, the AVA's close to redirect the blood flow to the surface (Gordon, 1990).

Precapillary sphincters walls are made of smooth muscle, and they are under the control of the sympathetic nervous system. The released noradrenaline binds to adrenergic receptors on the muscular cells of the vessels, causing muscular contraction and consequently a reduction in blood stream, at the opposite, the reduction in noradrenaline release widens the vessels, leading to an increase in blood stream. Thus, it is clear that vasoconstriction is an active process, whereas vasodilation is a passive process driven only by a reduction in noradrenaline release, without any specific inhibitory activity on the muscle.

However, in some vascular districts (e.g. palm of the hand) vasodilation can be driven by specific vasodilation fibers or nitric oxide release.

As said before, cell bodies of postgangliar neurons are located in paravertebral ganglia, were they have synapsing afferent fibers from pregangliar neurons. The latter ones are called sympathetic autonomic motor neurons, whose cell body is located in the grey matter of intermediolateral column (IML) in the spinal cord.

1.1.4.2 SYMPATHETIC PREMOTOR NEURONS – THE ROSTRAL VENTROMEDIAL MEDULLA (RVMM)

Sympathetic premotor neurons play a crucial role by mediating efferent signals from higher autonomic centres directly to sympathetic preganglionic neurons in the IML column of the spinal cord. These neurons can be inhibitory or excitatory, depending on the released neurotransmitter (Nakamura *et al.*, 2005).

The brain regions containing sympathetic premotor neurons have been discovered with the injection of retrograde tracers (pseudo-rabies virus) into the peripheral effector organs. This method is based on specific molecules (retrograde tracers) that are able to retrogradely and transinaptically move in the axon, the molecule migrates to central brain regions and can later be detected with molecular techniques, "mapping" the connections between the peripheral and the central nervous system.

This experimental approach led to the discovery of several brain regions containing sympathetic premotor neurons, involved in thermoregulation and vasomotion, mainly in the brainstem (medulla, pons and hypothalamus).

Particularly, for the cardiovascular regulation and consequently cutaneous vasomotion, several brain regions containing premotor neurons have been found in the rat: the Rostral Ventromedial Medulla (RVMM), the Rostral Ventrolateral Medulla (RVLM), the caudal raphe nuclei, the A5 noradrenergic neurons in the pons and the Paraventricular Hypothalamic nucleus (PVH).

• Rostral Ventromedial Medulla (RVMM)

Several scientific data point out the fact that the RVMM plays a crucial role in thermoregulation. In fact, it is the common afferent nucleus of all thermoregulatory

signals. That is supported by anatomical studies conducted with the injection of a retrograde tracer (pseudo-rabies virus) in thermoregulatory organs such as BAT (Cano *et al.*, 2003), blood vessels in heat exchanging districts (rat's tail) (Blessing and Nalivaiko, 2001; Tóth *et al.*, 2006), heart (Standish *et al.*, 1995; Ter Horst *et al.*, 1996) and muscle (Kerman *et al.*, 2006).

The RVMM is a brain region located in the brainstem above the pyramidal tracts, containing the Raphe Obscurus, the Raphe Magnus, the Raphe Pallidus and the Inferior Olivary nucleus.

The premotor neurons contained in the RVMM are involved in the regulation of BAT, cutaneous vasomotion, shivering thermogenesis through alpha motor fibers directed to the muscles, and heart rate. These neurons are rich in glutamatergic, GABA-ergic and serotoninergic receptors; however, there are several others, including orexinergic, histaminergic and αMSH receptors.

It has been found that serotoninergic neurons have EP3 receptors, particularly in the POA, that specifically bind to the inflammatory mediator prostaglandin E2 (PGE2). Studies in which PGE2 was injected in the POA show the binding between PGE2 and the EP3 receptor causes an increase in body temperature, known as fever (Stitt, 1973; Williams *et al.*, 1977). However, the functional meaning of the EP3 receptors in the RVMM has still to be clarified. The injection of PGE2 in the RVMM did not show any relevant physiological change in arterial pressure, heart rate, body temperature or cutaneous vasomotion (Tanaka and McAllen, 2005). The current hypothesis is that these neurons contribute in the hyperalgesic response by activating a pain-modulating circuitry during inflammation and fever (Heinricher *et al.*, 2004).

Several scientific studies found the glutamatergic vesicular transporter type 3 (VGLUT3), in the neurons of the RVMM. That suggests that there is a population of glutamatergic neurons that modulates thermoregulatory responses directed to the IML through excitatory outputs (McAllen *et al.*, 1982; McAllen, 1986; Morrison, 1999; Nakamura *et al.*, 2005). However, another work showed a major anatomical complexity, in fact, it demonstrates that IML projection RVMM premotor neurons

co-express glutamate, GABA and serotonin. Moreover, it has been found for the first time an inhibitory afference from the RVMM to the IML (Stornetta *et al.*, 2005).

Thermoregulation highly depends on the RVMM premotor neurons. During exposure to low ambient temperatures their excitatory signals directed to the IML activate thermogenic responses by BAT (Morrison, 2003) and probably shivering (Tanaka *et al.*, 2006; Brown *et al.*, 2008). Furthermore, they drive vasoconstriction in cutaneous blood vessels (Smith *et al.*, 1998; Blessing and Nalivaiko, 2001; Tanaka *et al.*, 2002; Nakamura *et al.*, 2004; Ootsuka and Blessing, 2005; Tóth *et al.*, 2006) to reduce heat dissipation; also, they play a role in heart rate increase, to respond to the higher oxygen demands from thermogenic organs (Fig. 2).

On the contrary, exposure to high ambient temperature causes a reduction in RVMM premotor neurons activity, which inhibits thermogenic organs, a reduction in heart rate (Morrison *et al.*, 2008), and cutaneous vasodilation (Ootsuka *et al.*, 2004; Nakamura and Morrison, 2010).

1.2 CENTRAL NERVOUS CONTROL OF ENERGY HOMEOSTASIS

1.2.1 CENTRAL REGULATION OF FOOD INTAKE

Since endothermy is very energy-demanding, mammals highly depend on food intake to survive, therefore a complex neural circuitry evolved in order to guarantee the fulfilling of this primary need. Among behavioural patterns in mammals, feeding has a high priority, where the animal does not only eat to gain energy, but feeding provides a true hedonic effect (Saper, 2002). As previously said, in conditions of scarce food availability, usually during cold periods of the year, heterotherms are able to enter torpor, which is an efficient energy-saving physiological state. The neural pathways involved in feeding are interconnected at some levels, however we can describe three circuits that have different roles in food intake regulation: i) the AGRP (agouti-related peptide) pathway; ii) the Lateral Hypothalamus (LH) pathway; iii) the CGRP (calcitonin gene-related peptide) pathway.

1.2.1.1 AGRP PATHWAY

AGRP neurons are a subpopulation in the Arcuate nucleus (ARC), which release GABA (the most common inhibitory neurotransmitter) and two possible neuromodulators: AGRP or neuropeptide Y (NPY). It has been found that stimulation of these neurons rapidly induce a voracious feeding behaviour, the degree of response depends on the amount of activated neurons: the more neurons are active, the shorter is the time lag between stimuli and effect, and more food is ingested (Aponte *et al.*, 2011). On the contrary, AGRP inhibition decreases food consumption in fasted mice (Krashes *et al.*, 2011).

The ARC contains another subpopulation, which releases different neurotransmitters, whose precursor is proopiomelanocortin (POMC): α-melanocyte-stimulating hormone (α-MSH), and cocaine and amphetamine regulated transcript (CART). These neurons, called POMC-CART, reduce food consumption and body weight when activated (Aponte *et al.*, 2011), due to the activation of their targets mediated by the melanocortin 4 receptor (MC4R). AGRP is an MC4R antagonist, POMC-CART neurons express the Y1 receptor for NPY (Fuxe *et al.*, 1997), and receive inhibitory projections from AGRP neurons(Csifáry *et al.*, 1990); is it clear that POMC-CART and AGRP neurons affect each other, there are many overlaps in hypothalamic and extra hypothalamic targets (Krashes *et al.*, 2011).

Activated AGRP neurons have different effects depending on the released neurotransmitters. When GABA and NPY are released, and acute feeding response is observed, whereas the release of AGRP is involved in the regulation of long-term hunger sensing. Some data show how after the activation of AGRP neurons where GABA and NPY release are impeded, the feeding response is much slower, and the time gap between stimuli and effect is longer. This effect seems to be mediated by the antagonist effect on the POMC neurons, both from the MC4R receptors and direct inhibitory projections (Krashes *et al.*, 2013).

AGRP neurons are organized in several subpopulations, with different target efferences, acting in a parallel and redundant manner, where each of them is sufficient to affect the feeding behaviour: some of them mostly act on the acute food

intake; others modulate the long-term feeding behaviour (Betley *et al.*, 2013). For example, to induce feeding quickly, it is sufficient to activate the AGRP efferences projecting to even just one of these structures: subfornical part of the LH, PVH, Bed Nucleus of Stria Terminalis (BNST), and Paraventricular Thalamic nucleus (Betley *et al.*, 2013). These structures are deeply interconnected. The feeding promoting effect caused by activation of the BNST seems to be mediated by the inhibitory effect of the latter on glutamatergic neurons of the LH (Sternson and Atasoy, 2014; Sternson and Eiselt, 2017). The inhibition of oxytocinergic neurons within the PVH, through projections to the Periaqueductal Gray (PAG) and dorsal Raphe, causes an increase in feeding (Stachniak *et al.*, 2014). AGRP pathways involving the Parabrachial nucleus (PBN), the Central Nucleus of the Amygdala, and the PAG, modulate the long-term regulation of food intake.

Some studies suggest that a reduction in firing rate in the AGRP neurons acts as a positive reinforcement for the behaviour causing it. In other words, when the AGRP neurons are active, the animal eats because it has learnt that food seeking and associated sensorial stimuli reduce the firing rate of the AGRP neurons. The firing rate of the latter decreases before the actual feeding and it is maintained on low levels during the meal: in fact, even some "clues" of forthcoming food are sufficient to decrease the firing rate in AGRP neurons. These data suggest that AGRP neurons induce food-seeking behaviour, more that stimulating constant food intake: this might be the first activated pathway when there is energy deficiency, even though several other circuits, mostly associated with the LH, are needed to sustain long-term food consumption (Saper, 2002).

1.2.1.2 LATERAL HYPOTHALAMUS PATHWAY

Since the LH was first studied by electrical stimulation, it has been observed that the animal does not only eat voraciously, but it shows also a behaviour of auto-stimulation of the LH, for example by pressing a lever (Delgado and Anand, 1953; Stachniak *et al.*, 2014). This reinforces the hypothesis that the LH is involved in the regulation of food intake and positive reinforcement.

As shown in other studies, LH is involved in other behaviours: lesions or stimuli within the LH affected drinking, chewing and coupling. It is interesting to observe that those behaviours are not triggered by different areas of LH, but their appearance depends on the environmental context at the time of stimulation. Thus, LH is thought to be a wake-promoting and environmental interaction nucleus.

The LH neuronal population is heterogeneous; the major subpopulations are glutamatergic and GABA-ergic, whereas other neurons produce orexin, melanin-concentrating hormone (MCH), neurotensin and galanin (Stuber and Wise, 2016).

Similarly to what happens in AGRP neurons, stimulation of LH has different effects based on which subpopulation is involved, in fact, stimulation of GABA-ergic neurons causes voracious feeding and auto-stimulation, similar to the one observed when stimulating the whole LH (Jennings *et al.*, 2015). On the contrary, the activation of glutamatergic neurons in fasted animals causes a decrease in food intake, and promotes an aversion for the context where it is delivered (Jennings *et al.*, 2015). As previously said, LH receives inhibitory projections from the BNST; the activation of those connections promotes food consumption.

Feeding behaviour and reinforcement mechanisms are also influenced by orexinergic neurons, even though their main role is involved in wakefulness maintenance: their stimulation causes a reduction in the transition from REM and non-REM sleep to wakefulness (Adamantidis *et al.*, 2007), whereas in other studies it has been shown that orexinergic neurons within the LH are activated when seeking for "consummatory rewards", such as food (Harris *et al.*, 2005).

MCH neurons are involved in promotion of REM sleep, possibly by inhibitory efferences that act on wake-promoting nuclei, such as the Tubero-mamillar (Jego *et al.*, 2013). These neurons are also involved in feeding regulation, probably with a similar role as the orexinergic ones, promoting food consumption. Recent studies have shown that overexpression of MCH causes obesity, whilst underexpression causes hypophagia (Qu *et al.*, 1996). This might be because orexinergic and MCH neurons are only contributing in the behavioural responses mediated by LH, and do not have a major role. Therefore, feeding behaviours triggered by LH stimulation

might be ascribed just to the physiological behavioural pattern that occurs during wakefulness (Stuber and Wise, 2016). Neurotensinergic neurons, which 95% also produce galanin, seem to be involved in reduction of food consumption: administration of neurotensin drastically reduces food consumption (Levine *et al.*, 1983), and ablation of leptin receptors in neurotensinergic neurons causes hyperphagia and obesity (Leinninger *et al.*, 2011).

Several anatomical and functional studies have demonstrated a role of the LH in hedonic control of food intake, and more in general, of the rewarding system. In fact, LH in connected to several brain regions that are known to be involved in attributing an appetitive role to environmental stimuli, to predict and recognize "rewards", in motivation for seeking and drug addiction: the Nucleus Accumbens (NAc) and the Ventral Tegmental Area (VTA), which make the mesolimbic dopaminergic system (Volkow and Morales, 2015). Both GABA-ergic and glutamatergic neurons of the LH send projections to the VTA, and NAc sends inhibitory efferences to the LH GABA-ergic neurons. The latter project mostly on the GABA-ergic neurons within the VTA, which in turn inhibit the dopaminergic neurons of the VTA; the activation of this pathway promotes feeding.

LH glutamatergic neurons project to the glutamatergic neurons of the lateral habenula (LHb), which activate the GABA-ergic VTA neurons, this inhibits the dopaminergic efferences; the activation of this pathway causes food aversion (Stuber and Wise, 2016). All these data are coherent with what previously found by optogenetic and chemogenetic investigation of the LH. The VTA project dopaminergic fibers to the NAc. The NAc contains two major neuronal subpopulations: one expresses the D1 receptor, associated with excitatory G proteins, and the other expresses the D2 receptor, associated with inhibitory G proteins. The efferences going from NAc to the LH are mostly expressing D1 receptors, and their activation promotes food consumption (Zhu *et al.*, 2016).

As previously mentioned, LH modulates positive reinforcement and rewarding mechanisms, and its involvement in food palatability is additionally confirmed by the finding of afferent connections from NTS, providing gustatory information, and PBN. In fact, the dorsolateral region of the PBN projecting to the LH, is

preferentially activated by sweet-tasting stimuli (Tokita *et al.*, 2014). The involvement of the LH in the central circuits of hedonic control of food consumption is summarized in Fig. 3.

Feeding is promoted by positive feedback mechanisms driven by the LH, where the consumption of palatable food stimulates for more food consumption. However, to avoid overfeeding, a mechanism that block the positive feedback system is needed: this role is played by the CGRP neurons within the PBN.

1.2.1.3 CGRP PATHWAY

As previously mentioned, the PBN is an important region for transmission of sensitive and gustatory information, which are provided by the NTS through excitatory fibers. Since PBN activation is related to nausea and gastric distention, it is hypothesized that it is involved in satiety feeling (Alhadeff *et al.*, 2014); moreover, its inhibition increases the meal time without increasing the food intake, that means that in the same time period, there are less meals, but they are more consistent (Campos *et al.*, 2016).

Recently, a subpopulation within the PBN was discovered expressing CGRP, which seems to be involved in overfeeding driven gut sickness, in toxins exposure (lithium chloride) and infection after a lipopolysaccharide injection (Yamamoto *et al.*, 1994; Carter *et al.*, 2013). When activated, CGRP neurons drastically reduce food consumption, however, their inhibition does not increase food consumption but in conditions where there is reduced feeding (injection of toxins, LPS). This seems to support the idea that CGRP neurons play a role in Conditioned Taste Aversion, a mechanism where the animal avoids specific foods related to previous sickness or nausea episodes (Campos *et al.*, 2016). That is probably driven by excitatory efferences from CGRP neurons to the Central Nucleus of Amygdala, a brain region associated with processing of unpleasant emotions and environmental stimuli (both positive and negative) (Carter *et al.*, 2013).

1.2.2 HOMEOSTATIC CONTROL OF FOOD CONSUMPTION AND ENERGY EXPENDITURE

Homeostatic control of food consumption relies on the three previously described pathways. However, to coordinate such a complex physiology, those systems need constant information about the content and activity of the gastrointestinal tract, blood glycaemia and energy availability. These information are delivered to the central nervous system through nerves and hormones produced by metabolic organs. The most relevant ones are leptin and ghrelin.

Leptin is a hormone produced by the white adipose tissue produced in situations of positive energy balance, and it is commonly called the "satiety hormone". Mice lacking leptin or its receptor (LepR) display hyperphagia, reduced energy expenditure and extreme obesity (Zhang *et al.*, 1994; Ingalls *et al.*, 1950).

The ARC expresses high levels of LepR, the binding of leptin to the receptors causes inhibition of AGRP neurons and activation of POMC neurons, promoting their anorecting effect (Cowley *et al.*, 2001). Hypothalamic response to circulating leptin in the ARC is summarized in Fig. 4. As previously mentioned, POMC and AGRP neurons project to the PVH, which promotes the release of pituitary hormones such as the thyrotropin-releasing hormone (TRH), gonadotropin-releasing hormone (GnRH) and corticotropin-releasing hormone (CRH).

The TRH promotes the synthesis of the thyroid-stimulating hormone (TSH), which promotes the synthesis of thyroid hormones thyroxine (T4) and triiodothyronine (T3). The efferences from the ARC to the PVH are the major neural substrate used in the modulation of metabolic rate depending on its nutritional state. Leptin is able to modulate this pathway, modifying the synthesis of TRH and therefore the metabolism; in fact, mice lacking leptin often display hypometabolism and hypothyroidism (Seoane *et al.*, 2000)

Leptin receptors can be found in other bran regions, such as the LH, VTA, Dorsomedial Hypothalamic nucleus (DMH), NTS, PBN, PAG, and Dorsal Motor Vagal nucleus (Hosoi *et al.*, 2002).

Leptin inhibits MCH and neurotensinergic neurons in the, this effect causes a decrease in the rewarding system of food when the energy is restored or excessive. Moreover, leptin can modulate satiety sensation by acting on the PBN and NTS (Leinninger *et al.*, 2011). All these data bring out the fact that leptin, by acting on all three food intake regulatory pathways, is crucial in control of food consumption.

Ghrelin, known as the "hunger hormone", is mainly synthetized in the stomach, by specialized endocrine cells. Fasting increases and food consumption decreases the synthesis and blood concentration of this hormone (Klok *et al.*, 2007). Ghrelinemia doubles before the meal, and drops down to basal levels within an hour from its consumption. The reduction is directly proportional to the calorie intake, which also affects the dynamics of the time and amount of the next peak of ghrelinemy (Foster-Schubert *et al.*, 2008).

In rats, intracerebroventricular administration of ghrelin strongly stimulates food consumption (Schéle *et al.*, 2016). Several hypothalamic and brainstem regions involved in regulation of food consumption are rich in ghrelin receptors: AGRP neurons of the ARC, PVH, LH, Ventromedial Hypothalamic nucleus, NTS; and several brain regions involved in positive reinforcement and gratification, such as the VTA, hippocampus and amygdala (Cowley *et al.*, 2003). Ghrelin seems also to promote ingestion of food rich in fats and carbohydrates (Shimbara *et al.*, 2004).

Moreover, since ghrelin is produced during fasting periods, it also plays a role in metabolic homeostasis, in terms of leading to a state of energy saving: lowers body temperature by directly regulating the expression of UCP1 in BAT in mice (Tsubone *et al.*, 2005) and indirectly modulating the sympathetic nervous system (Yasuda *et al.*, 2003); also, reduces spontaneous locomotor activity in rats (Tang-Christensen *et al.*, 2004).

All these data confirm the major role of ghrelin in homeostatic regulation of food intake and energy balance.

Food consumption is also regulated by information coming from the stomach, such as its distention and its content; those sensitive visceral information are sent to the medial and dorsomedial part of the NTS through the vagus nerve. An important area

in sensing gastrointestinal hormones is Area Postrema, detecting the levels of glucagon-like-peptide 1, peptide YY and cholecystokinin; this area sends projections to the NTS, the latter also gets information from the arcuate nucleus about adiposity-related signals, such as insulin and leptin. These information are integrated in higher regulatory centres, such as LH, DMH, PBN, ARC, thalamus, and projected to the cortex (Schwartz *et al.*, 2000; Williams and Elmquist, 2012).

1.3 TORPOR AND HIBERNATION

1.3.1 SPONTANEOUS TORPOR

Torpor is a physiological phenomenon characterized by a transient and reversible metabolic suppression, caused by a reduction in core temperature, metabolic rate and other physiological functions (Geiser, 2004). Several animal species are able to enter this hypothermic and hypometabolic state during unfavourable environmental conditions without any compensatory response. Torpor occurs with various patterns and frequency across the animal kingdom, in fact, in some animals the reduction in energy expenditure occurs daily; whereas in others it can last for days or weeks (the so-called torpor bouts), with occasional short (usually less than 24h) arousals. The latter is known as hibernation, which is usually a seasonal phenomenon, starting in late summer or autumn and ending in late winter or spring.

While hibernation and torpor are relevant in cold climates, another physiological adaptation occurs in several animals in hot climates, the so-called estivation.

All these conditions represent the ability of some mammals to temporarily adopt a "partial" heterothermy in conditions where maintaining a constant body temperature is too energy-demanding compared to food availability and ambient temperature.

During torpor, animals core temperature can decrease to around 30°C and lower, reaching even 0°C some species, a value very close to the ambient temperature, however, for extremely low ambient temperatures, the core temperature is maintained around 0°C (Barnes, 1989; Arnold *et al.*, 1991). Moreover, it has been showed that when ambient temperature decreases, torpid animals increase their metabolic rate to counteract the process and maintain the body temperature at

constant levels (Buck and Barnes, 2000). These evidences suggest that even in torpor some form of thermoregulatory control is maintained, and the minimum set-point is species- or population-specific (Florant and Heller, 1977).

During torpor, metabolic rate decreases to 5-30% of the basal metabolic rate. It is getting more and more clear how this reduction is not a secondary natural consequence of temperature reduction, but it is rather an active reduction that starts before the actual drop in body temperature (Heldmaier *et al.*, 2004).

The graph reported in Fig. 5 shows the metabolic rate suppression and the body temperature reduction occurring during daily torpor in the Djungarian hamster (Phodopus sungorus).

Torpor does not only reduce energy expenditure, but also provides other benefits: it facilitates energy saving for migration in some bird species (Carpenter and Hixon, 1988); plays a role in reproduction strategies, by allowing sperm storage in some bats and other mammals, and during pregnancy, eases fat storage (Geiser et al., 1994); it is a water saving strategy; and ultimately it is associated with a reduction in risk of extinction (Geiser and Brigham, 2012).

1.3.1.1 PHYLOGENETIC BACKGROUND OF TORPOR

Currently 214 hibernating animal species are known: 43 birds and 171 mammals (Ruf and Geiser, 2015), including a primate (Dausmann *et al.*, 2004). As showed in Fig. 6, these species are widespread across different animal orders: judging by the heterogeneity of torpor distribution in the animal kingdom, it is likely that it is a characteristic inherited by an ancient protomammal. Thus, it would be a plesiomorphic feature maintained only in species that take advantage of hibernation in very cold climates or that go through food shortage. Consequently, it is possible that the gene pool necessary for torpor is preserved in all mammals including humans, whereas the regulatory mechanisms are not active (Cerri, 2017).

1.3.1.2 DAILY TORPOR AND HIBERNATION

As previously said, torpor is an efficient energy-saving physiological state, adopted by hibernating animals in conditions of scarce food availability, usually during cold periods of the year.

While some studies suggest that hibernators and "daily heterotherms" are just a big functional group of heterotherms in a homogeneous physiological continuum (Boyles *et al.*, 2013), others recently demonstrated that the separation between hibernation and daily torpor is not merely based on the torpor bouts length, but also on substantial differences in other physiological parameters, such as: i) the relative and absolute minimum metabolic rate during torpor (TMRmin); ii), the relative minimum metabolic rate (TMRrel, as a percentage of the basal metabolic rate), and; iii) the minimum body temperature (Tmin) (Ruf and Geiser, 2015). According to Ruf and Geiser, in a typical 30g weight mammal, Tmin and TMRmin were respectively 13°C and 16.7% lower in hibernators in comparison to daily heterotherms.

Howsoever, the major difference can be seen in the torpor bouts length: between 3 and 12 hours in daily torpor, with intercurrent arousals where the animal actively seeks for food, and approximately more than a week for hibernation. Thus, it is thought that, although the central hypothalamic control of body temperature could be the same, the physiological mechanisms that underlie the temporal frameworks of daily torpor and hibernation may be different.

In hibernating animals, the physiological circadian clock seems to disappear, and more of a seasonal rhythm appears, dictating the start of hibernation; whereas in daily torpor, the temperature seems even following the circadian rhythm and no particular rigorous seasonal pattern is observed (Körtner and Geiser, 2000).

The marmot (Marmota marmota) is a common seasonal hibernating rodent that lives in cold climates. The torpid season starts in late September-early October, and ends in late March-early April. Throughout this whole period, the marmot displays cycles of torpor bouts and arousals, every 8-10 days. A cycle is characterized by: i) torpor onset – BMR and core temperature decrease, ii) few days of deep torpor, iii) arousal, iv) euthermic period lasting 1-2 days. The whole hibernating season lasts 6-7 months

(mean value 193 days), and around 15-20 cycles of torpor bouts-arousals are observed. TMR drops down to 0.014 mlO2 g^{-1} h^{-1}, that represents 1/25 of the BMR, core temperature stays around 1.5-3°C above the ambient temperature. During arousal, the marmot rapidly increases its core temperature, and reaches normothermia in about 3 hours. The torpor onset time, arousal time and euthermic periods are quite similar in every cycle, but the torpor bout length strictly depends on the core temperature. Similar patterns have been observed in marsupials and other mammals (Geiser, 2004).

Arousal happens in a short timeframe, but is very energy-demanding. The 72% of all stored fat is used for the 17% in arousals and for the 57% for maintaining euthermia. Some speculations on the role of arousal have been made, but its role is still not completely clear. However, it is demonstrated that the longer and profound is the torpid period, the more the arousal is energy-demanding (Heldmaier *et al.*, 2004)

The Djungarian hamster (Phodopus sungorus) is a common daily heterotherm rodent, brought here as an example of the torpor-arousal patterns in daily torpor. The events are similar to those observed in hibernating animals: torpor onset, torpor maintenance, arousal and euthermia, and they all happen in a much shorter period. During normothermia, it has a resting metabolic rate of 2.01 $mlO2g^{-1}h^{-1}$, which at the onset of torpor drops down to approximately 0.7 $mlO2g^{-1}h^{-1}$ (1/3 of the BMR) in about 40 minutes. Body temperature decreases from 35.6°C to 15.5°C, and torpor is maintained for about 9 hours. From the onset of the arousal, the hamster reaches normothermia in about 30 minutes. Overall, daily homeotherms show a milder reduction in core temperature and BMR than hibernators do (Geiser, 2004).

While in some species daily torpor is a mandatory process depending on the photoperiod length (Lynch *et al.*, 1978; Ruf *et al.*, 1993), in others is optional and only adopted in conditions of food shortage. An example of the latter is the mouse (Mus musculus), which goes into a torpid state only during food shortage, or a combination of fasting and cold ambient temperature (Hudson and Scott, 1979).

It is appropriate to address a few considerations about torpor length. In daily homeotherms, a short torpor (within 24 hours) is the only possible option, because

the rest of the time has to be used to actively seek for food and eat. In hibernators, torpor bouts can be extended through the so-called “hourglass mechanism”(French, 1985). According to this theory, arousal is determined by a metabolic imbalance, possibly due to metabolic waste or shortage that causes cell damage. The imbalance can be corrected much more efficiently during euthermia, speeding up the recovery process.

This connection was demonstrated: the bigger the TMR, the shorter the bout; and the bigger the euthermic metabolic rate, the shorter the arousal length (Ruf and Geiser, 2015).

Another difference between daily homeotherms and hibernators can be seen in body mass and habitat latitude (Ruf and Geiser, 2015). Overall, hibernators have a bigger body mass, and that could be explained with the fact that while daily homeotherms frequently seek and eat food during arousal, hibernators rely only on their endogenous fat, stored during summer: bigger animals are able to store more fat; a small animal has very limited fat storage and could not rely only on it.

Regarding the geographical distribution, daily homeotherms live around 24.5 ± 1.1° latitude, hibernators live around 35.0 ± 1.4°, a latitude closer to the poles, where seasonal food shortage is much longer: therefore, hibernation is an efficient survival strategy in animals that do not feed for months (Ruf and Geiser, 2015).

1.3.1.3 ESTIVATION

Torpor is not only seen in cold ambient, but it can be a surviving strategy also in warm environments, this process is called estivation (Wilz and Heldmaier, 2000). Estivation is characterized by the ability to survive arid environments, often associated with water and food shortage, and high ambient temperatures. Vertebrates (some fish, amphibians, reptiles, small mammals) and some invertebrates adopt this strategy. Also, a tropical primate able to enter estivation was reported (Dausmann *et al.*, 2004).

Estivation period varies a lot, usually is 9-10 months, but it can go up to two years in some species.

An example about annual estivation is given by a North American spadefoot toad (Scaphioupus couchii), which usually spends only around 20 nights per year in active state, mainly devoted to food seeking and mating. The main factors that make estivation possible are the ability to store energy and water that is achieved also by behavioural changes, such as seeking for shady, covered places that minimize water loss and hide from predators. Water preservation is of particular importance: since it is lost during breathing and body surface, animals enter estivation with huge water accumulation; some frogs for example can store a lot of water in the bladder.

During estivation, body metabolism is mainly based on aerobic oxidation of fats, together with protein catabolism, with a little contribution of carbohydrates. Metabolic rate drops down to 10-30% of BMR, the lower is the metabolic rate, the longer can the estivation last (Storey and Storey, 1990).

It is likely that daily torpor, hibernation and estivation all rely on similar physiological mechanisms (Ruf and Geiser, 2015).

1.3.1.4 METABOLIC REGULATORY ASPECTS OF TORPOR AND HIBERNATION

As previously said, torpor and hibernation are characterized by a drastic decrease in body temperature, which is likely driven by a previous active decrease of metabolic rate. This is obtained by combining changes in physiological values (decrease in heart and respiratory rate, digestion, renal function, locomotion) and biochemical modulations (suppression of non-basal vital functions, switch of metabolism from glucose to lipids consuming) (Quinones *et al.*, 2014). In particular, metabolic rate decreases to 5-30% of the basal level (Heldmaier *et al.*, 2004). The reduction in metabolic rate during hibernation could be driven by four different mechanisms: 1) changes in thermal conductance, by acquiring the ability to disperse heat more efficiently; 2) inhibition of thermogenesis, by the central inactivation of the hypothalamic set point; 3) a direct consequence of the fall in brain temperature (through a passive mechanism) 4) active regulated modulation of metabolic central circuits. The role of each process on the overall phenomenon is still being debated (Brown *et al.*, 2007).

Speaking from a metabolic point of view, the ability of surviving during energy shortage periods and accumulating adipose tissue during energy abundance are indicators of a very efficient metabolism. Metabolic efficiency can be defined as a measure of the ability to obtain energy, by producing high-energy molecules (adenosine triphosphate, ATP), from the nutrients obtained by feeding. Thus, metabolic efficiency could justify the tendency of some organisms to accumulate fat tissue, and those organisms are more efficient in surviving energy shortage periods. The molecular and cellular mechanisms regulating metabolic efficiency are not entirely known, changes in organs and tissues that largely contribute to the metabolic rate directly reflect on the overall body energy expenditure. On a cellular level, variations of mitochondrial metabolic efficiency considerably affect metabolic rate. Thus, understanding the metabolic mechanisms involved in particular situations such as fasting, and the drastic metabolic reduction observed during torpor, could highlight the importance and role of the modulation of metabolic suppression.

Many scientific studies have tried to elucidate the existence of an active metabolic suppression mechanism, rather than a merely passive effect of hypothermia, occurring in torpor and hibernation, by studying the changes in primary energy producing organelles in the cell, mitochondria.

1.3.1.4.1 Mitochondrial function in hibernation and torpor

Mitochondria are membrane-delimited organelles located in all animal eukaryotic cells, which have the ability to convert energy in molecules used to promote cellular reactions. Through mitochondrial respiration, cells completely oxidize organic substrates using oxygen, producing CO_2 and H_2O, and obtaining usable energy. Mitochondrial respiration specifically consists of the citric or tricarboxylic acid cycle, whose reactions occur within the mitochondrial matrix, and oxidative phosphorylation, consisting of two steps: electron transport chain, on the inner membrane of the mitochondria, where electrons transported by $FADH_2$ and NADH maintain a protonic transmembrane gradient, and ATP synthesis, by phosphorylation of ADP (adenosine diphosphate) through ATP synthase.

In oxidative phosphorylation, ADP and phosphate are necessary for electron transport from NADH to oxygen. In fact, in isolated mitochondria, the electron

transport is considerably faster when the environment is saturated with ADP and phosphate.

When isolated mitochondria are added to the measurement solution and the designed substrate, a certain degree of respiration due to endogenous ADP, proton leakage, and reactive oxygen species (ROS) production is observed – this state is called State 2 respiration (Puente-Maestu *et al.*, 2009).

In absence of ADP, respiration is very slow, no phosphorylation occurs because a phosphate acceptor is missing, and thus, no ATP is produced. This condition, known as State 4 of respiration (non-phosphorylating), is the resting state of respiration. By adding a saturating quantity of ADP to an isolated mitochondria system in State 4, oxygen consumption rapidly increases reaching a threshold and concomitantly all the ADP is converted to ATP – this condition goes under the name of State 3 (phosphorylating), and is characterized by active respiration. When all the ADP has been phosphorylated, oxygen consumption decreases, and mitochondria goes back to State 4 respiration.

The speed of electron transport chain is directly controlled by ADP concentration, and this mechanism is called acceptor or respiratory control. Mitochondria have a high affinity to ADP, which they keep phosphorylating until its concentration decreases considerably. The respiratory acceptor control ratio (RCR) is the ratio between the mitochondrial respiratory velocity in presence or in absence of ADP (State 3/State 4). This ratio is usually high, around five or more, in undamaged mitochondria. However, if mitochondria are damaged or not well preserved, this value decreases. Thus, RCR is a great indicator of mitochondrial integrity.

Moreover, State 4 can be influenced by the presence of uncoupling proteins in the mitochondrial membrane, which have the ability to augment the permeability of the inner mitochondrial membrane, by allowing protons in the mitochondrial intermembrane space to return to the matrix. This process decreases the proton gradient generated in oxidative phosphorylation, and thus promotes rapid substrate oxidation with energy diverted to heat generation, instead of ATP production. In particular, the most relevant is UCP1 within the brown adipose tissue (Cannon and

Nedergaard, 2004). Other isoforms of UCP, such as UCP2 (in several tissues) and UCP3 (in muscle), have been found to be increased in hibernating ground squirrel (Boyer *et al.*, 1998). UCP2 has been addressed as neuroprotective against oxidative stress in vivo and in vitro (Mattiasson *et al.*, 2003).

In hibernation and torpor, the decrease in metabolic rate is likely caused by some kind of modification occurring at mitochondrial level. Modulation of mitochondrial activity suppression could happen in three potential sites: changes in substrate oxidation, changes in phosphorylation, or changes in proton leak. Likely, modifications in State 4 respiration during torpor would probably be due to a change in substrate oxidation and/or proton leak, whereas a change in State 3 would likely be caused by modifications of substrate oxidation and/or phosphorylation (Staples and Brown, 2008). In Syrian hamster, State 3 respiration in isolated liver mitochondria is drastically reduced during hibernation(Roberts and Chaffee, 1973). In Djungarian Hamsters, State 3 respiration in isolated liver mitochondria is again reduced, however without any changes in State 4 (Brown *et al.*, 2007); a more recent study showed that respiration is not depressed in kidneys, skeletal muscle and heart, whereas in liver, State 3 and State 4 directly correlate with body temperature, likely due to an inhibition related to torpor depth and degree of metabolic rate reduction (Kutschke *et al.*, 2013). In 13-lined ground squirrels, respiration rates in liver in State 3 and 4 decrease by up to 70% (Armstrong and Staples, 2010). Since the liver is the major contributor to rodents metabolism (around 15%), an active suppression in this organ leads to a consistent decrease in metabolic rate, promoting energy saving (Fuhrman *et al.*, 1961; Staples and Brown, 2008).

Recently, a suppression of State 3 respiration in isolated mitochondria has also been confirmed in skeletal and cardiac-muscle mitochondria in 13-lined ground squirrels, whereas no difference has been found in brain cortex (Brown and Staples, 2014; Gallagher and Staples, 2013).

An extensive analysis of the biochemical structure of mitochondria is beyond the scope of this thesis, however the current state of knowledge hypothesizes that during hibernation, liver mitochondrial metabolism is reversibly downregulated, mostly by a suppression of substrate oxidation upstream of electron transport chain complex

IV (cytochrome c oxidase) (Staples and Brown, 2008). It is interesting to note how H2S, a hypothermia-inducing compound later discussed in this thesis, is a potent inhibitor of complex IV, and administration H2S induces a torpor-like state in mice (Blackstone *et al.*, 2005). However, even though the current evidences suggest an active maintenance of a hypometabolic state through mitochondrial metabolism suppression, it is still not clear whether these changes might be a passive consequence of temperature decrease. To assess this question, mitochondrial respiration was also studied in non-hibernators in situations of forced hypothermia. In rats, artificial hypothermia (Tb, 15°C) obtained under conditions of hypoxia, hypercapnia and low ambient temperature was not accompanied by a reduction in State 3 respiration in isolated liver mitochondria (Komelina *et al.*, 2015).

Analysing the above presented data, even though a considerable amount of studies have investigated changes in transcription, translation and modifications of key enzymes for substrate oxidation, and an active metabolic suppression is hypothesized, the mechanism of induction of hypometabolism occurring in hibernation is still unclear (Staples and Brown, 2008).

1.3.1.5 CURRENT UNDERSTANDINGS OF CENTRAL NEURAL PATHWAYS FOR TORPOR

Even though the central neural pathway for torpor is not yet known, recent studies suggest a possible role for the autonomic nervous system and, especially, for the hypothalamus (Drew *et al.*, 2007).

Torpor is an energy-preserving strategy, used during periods of lack in resources; thus, the onset of the process has to be regulated by a complex circuit, which should have the ability to integrate information about energy balance and the external environment, and to modulate body's metabolic and behavioural activity.

Since the autonomic nervous system regulates the overall energy balance, the physiological regulation of the onset (by the parasympathetic branch) and arousal (by the sympathetic branch) from torpor possibly relies on modifications induced by the ANS: heart and respiratory rate, oxygen consumption (Milsom *et al.*, 1999; Drew *et al.*, 2007).

Moreover, intracerebroventricular injection of TRH, which activates the sympathetic nervous system, induces arousals when injected during the entrance or the maintenance of torpor (Tamura *et al.*, 2005), confirming the hypothesis that torpor is only possible with concomitant sympathetic inhibition.

Usually, the major role in those processes is played by the hypothalamus, so it is likely that it has some sort of modulating ability on the entrance, maintaining and arousal from torpor. As a matter of fact, at the onset of torpor, progressively lower body temperature is needed to trigger thermogenesis; that means that even during torpor, the POA is actively regulating the set-point temperature (Heller, Colliver and Beard, 1977). Moreover, the POA could have a role in inhibiting or deactivating wake-promoting centres in the lateral hypothalamus (Krilowicz *et al.*, 1994).

The hypothalamic area responsible of the circadian rhythms of physiological variables, the Suprachiasmatic nucleus (SCN), shows an increased oxygen consumption and c-Fos expression (a marker of neural activity) in deep torpor and arousal (Drew *et al.*, 2007; Zee and Manthena, 2007); that suggests a role of this area in torpor. The SCN efferences project to the DMH and the Sub-Paraventricular Zone (SPZ); the latter is divided in a ventral (vSPZ), which seems to be involved in the regulation of the wake-sleep activity, and a dorsal (dSPZ) part, that is implicated in thermoregulation through its efferences to the MPO.

The DMH sends projections to hypothalamic nuclei involved in sleep-wake regulation, such as the Ventrolateral Preoptic nucleus (VLPO), THE LH, and the PVH. It is believed that the projections from SCN to SPZ and DMH integrates circadian rhythms with environmental stimuli, such as food shortage (signalled by structures sensible to leptin and ghrelin, the ARC and Ventrolateral Hypothalamic nucleus, that send projections to the DMH), visceral sensory stimuli and cognitive information from the prefrontal cortex (Saper *et al.*, 2005).

Some studies suggested a role for endogenous opioids in torpor maintenance (Margules *et al.*, 1979), and μ opioid receptors could affect thermal sensitivity by controlling the activity of warm-sensitive neurons in the POA (Yakimova *et al.*,

1996); moreover, the opioidergic system seems to be involved in the regulation of respiratory rate during torpor.

Another structure that is possibly involved in torpor is the hippocampus, since it is the last structure that displays an electroencephalogram weakening during the entrance in torpor, and the first one that gains back EEG power during arousal (Drew *et al.*, 2007).

Many efforts in the scientific world have been made to discover not only the anatomical circuitry of torpor, but also possible chemical mediators involved in the process.

One of the most studied one is adenosine, a nucleoside produced by ATP metabolism, whose concentration is determined by the metabolic rate. Adenosine plays an important role in many districts; it can decrease heart activity, increase oxygen perfusion and promote vasodilation, balancing energy demands and distribution.

Centrally, adenosine acts as a neuromodulator, by affecting the glutamatergic system. It has an inhibitory effect on neurons that express A1 receptors, when the latter are activated by adenosine. It is believed that adenosine is involved in many pathophysiological processes, such as sleep-wake regulation, regulation of brain perfusion, epilepsy, neuroprotection in ischemic events and amphetamine driven neuronal damage (Latini and Pedata, 2001).

Several scientific evidences have proved that adenosine plays a role in torpor, in fact one of the side effects of its administration is a mild hypothermia (Miller and Hsu, 1992); in rodents, hypoxia-induced hypothermia is milder when the adenosine antagonist aminophylline is administered (Barros *et al.*, 2006).

In rodents, peripheral injection of adenosine causes a torpor bout, bradycardia and a decrease in metabolic rate, a pattern similar to the one observed in spontaneous torpor; during deep torpor, subcutaneous injection of aminophylline promotes arousal (Iliff and Swoap, 2012).

Recently, synthetic torpor was induced in the rat, a non-hibernating mammal, by intracerebroventricular administration of adenosine (Tupone *et al.*, 2013).

Other studies explored the role of several other chemical mediators, in particular, the "hibernation protein complex" (HPc) has been found in ground squirrels. It is made by four proteins: HP20, 25 and 27 that make the HP20c complex, which binds to the fourth protein, HP55, in the blood.

At the beginning of the hibernating season, the HPc blood concentration decreases, due to a reduction in its synthesis and because the HP55 detaches from the complex, making it permeable for the central nervous system. Therefore, the concentration of cerebrospinal fluid HP20c increases during the beginning of torpor and during cyclic arousals; intracerebroventricular administration of anti-HPc antibodies promotes arousal. All these data suggest that HPc, whose blood concentration is regulated on a seasonal rhythm, in the necessary, but not the only one, hormonal signal for induction and maintenance of torpor (Drew *et al.*, 2007).

1.3.1.5.1 Considerations about the possible role of the Raphe Pallidus in torpor

Thermogenesis, as described before, has a complex central circuitry, where the higher centre, the POA, controls thermogenic effectors through the Raphe Pallidus (RPa), a nucleus situated within the RVMM. During torpor, thermogenic organs are inhibited, so it is likely that during torpor neurons within the Raphe Pallidus are not active. The functional inactivity of those neurons can be caused by either inhibition, where the neurons should be specific inhibitory neurons that act directly and tonically, or by disfacilitation, where the RPa neurons should have connections to excitatory or modulatory neurons that when inactive, do not provide the RPa with the necessary input.

Even though all the excitatory inputs to the RPa have yet to be discovered, it is reasonable that some of them are coming from the DMH.

The RPa neurons should be disfacilitated in three possible ways: i) a circulating factor may inhibit the excitatory nuclei; ii) a higher inhibitory nucleus could act on the excitatory nuclei; iii) a combination of these two conditions.

Even if there are no data available to confirm that, another consideration has to be made about the possible disfacilitation of the RPa: its neurons must not be spontaneously active when there is no excitatory or modulatory input (Cerri, 2017).

1.3.2 SYNTHETIC TORPOR

As previously described, torpor is a physiological strategy that allows to survive long periods of food shortage and extreme climatic conditions through metabolic suppression and decrease in body temperature. This phenomenon is well preserved across several animal orders, so it is possible that every mammal has the necessary gene pool, but in some animals, natural selection favoured the ones not expressing it. Therefore, it might be possible to induce a torpor-like state in non-hibernating mammals (synthetic torpor).

At present, physiological mechanisms underlying torpor are unknown. A combination of environmental factors (shorter light-time, lower ambient temperature, diet changes) and endogenous factors (shift in fuel utilization, from glucose to lipids and change in hormones, mostly in leptin concentration and effects) seem to be involved in its onset and maintenance (Carey *et al.*, 2003).

Regarding this topic, the scientific community has always been very interested in researching a method for artificially inducing torpor for experimental and clinical applications, and several pharmacological and environmental manipulations have been studied. At current state of knowledge, the most promising ones are the activation of central adenosine A1 receptors and the pharmacological inhibition of the RVMM.

1.3.2.1 HYDROGEN SULPHIDE (H_2S)

Hydrogen sulphide is an endogenous molecule, produced in small quantities, that acts as a signalling compound for the central nervous system and the cardiovascular system. It is also a powerful reversible inhibitor of the Complex IV (cytochrome-c oxidase) of the oxidative phosphorylation in the mitochondria. H_2S competes with O_2 to bind to the Complex IV, causing a decrease in oxygen consumption and a

reversible inhibition of cellular metabolism. It was also found its involvement in anti-apoptotic and anti-oxidant mechanisms (Calvert *et al.*, 2010).

Moreover, in mice, H_2S seems to prevent kidney damage and protect against lethal hypoxia (Dugbartey *et al.*, 2015). These characteristics made the H_2S considered a good candidate for torpor induction.

Mice exposed to gaseous H_2S showed a big reduction in metabolic rate (up to 90%) and the body temperature dropped to about 2°C above ambient temperature (with a minimum of 15°C). Mice returned to euthermia six hours after exposure (Blackstone *et al.*, 2005).

However, the attempt to induct torpor-like state with H_2S in bigger animals brought inconsistent data, experiments performed in pigs and sheeps did not display the appearance of torpor after the exposure to H_2S (Drabek *et al.*, 2011; Derwall *et al.*, 2011). This might be because bigger animals have a different metabolic regulation that better counteracts the effects of H_2S. Moreover, as previously said mice are daily heterotherms, therefore the drop in core temperature might be just a defence strategy against the Complex IV blockade and subsequent hypoxia (Bouma *et al.*, 2012).

1.3.2.2 3-IODOTHYRONAMINE

3-iodothyronamine (T1AM), a by-product of the T4 thyroid hormone, is a high-affinity agonist for the trace amine-associated receptor TAAR1, a G protein-coupled receptor, and is the most powerful known TAAR1 agonist. Its physiological role is still not clear, but its injection in mice caused a dose-dependent reduction in body temperature and heart rate, and in mice and djungarian hamsters (Phodopus sungorus) caused a reduction in metabolic rate (Scanlan *et al.*, 2004; Braulke *et al.*, 2008). However, a few differences between T1AM induced torpor-like state and spontaneous torpor must be pointed out: after administering T1AM, body temperature rapidly decreases and after the torpid period the animal regains normothermia slower; T1AM induces a metabolic depression followed by a rapid glycolysis inhibition, which is less pronounced in spontaneous torpor; the temperature bout in T1AM treated animals is shallower, reaching 33°C and 30°C in hamsters and mice respectively (Braulke *et al.*, 2008; Bouma *et al.*, 2012).

Some data showed how fat diet delivery, for four weeks prior to the intraperitoneal injection of T1AM caused multiple days torpor bouts in mice (Ju *et al.*, 2011). However, the action and the possible use of this compound have still to be clarified.

1.3.2.3 REDUCTION OF ENERGY AVAILABILITY

Several studies have been testing the effects of 2-deoxyglucose (2-DG), a powerful glycolytic inhibitor, when administrated intraperitoneally. In Siberian Hamsters, 2-DG caused a drop in body temperature below 30°C approximately 50 min after the injection (Dark *et al.*, 1994).

Also, two inhibitors of fatty acids oxidation have been investigated: methylpalmoxirate and mercaptoacetate: the first caused a mild hypothermia in siberian hamsters, while the second was ineffective in inducing torpor (Stamper *et al.*, 1999; Dark *et al.*, 1994; Bouma *et al.*, 2012). It is still not clear whether these compounds act as torpor inducers or their effect is aspecific and not related to spontaneous torpor.

1.3.2.4 NEUROPEPTIDE Y

Neuropeptide Y (NPY), a common neurotransmitter and a strong orexigenic agent, induces a decrease in metabolic rate in mice (Walker and Romsos, 1993), and mild hypothermia in Siberian hamsters when injected intracerebroventricularly. It has still to be clarified if NPY has a comparable effect on hibernating mammals. It is hypothesized that NPY injection might activate hypothalamic regions that physiologically initiate and regulate spontaneous torpor (Paul *et al.*, 2005; Bouma *et al.*, 2012).

1.3.2.5 5'-ADENOSINE MONOPHOSPHATE

5'-adenosine monophosphate (5'-AMP) is a nucleotide obtained by hydrolysis of ATP. In fasted mice kept at constant darkness, injection of 5'-AMP caused moderate bradycardia and hypothermia (Tao *et al.*, 2011), however the effects of 5'-AMP are different from those observed is spontaneous torpor. This could be ascribed to the dephosphorylation of 5'-AMP that produces adenosine, which reduces heart rate and core temperature, or because 5'-AMP causes an activation of the AMP kinase

(AMPK), that senses the [AMP]:[ATP] ratio and plays a crucial role in metabolic regulation (Bouma *et al.*, 2012).

In rats, 5'-AMP injection was not completely successful, as it induced mild hypothermia accompanied by metabolic and cardiovascular side effects (Zhang *et al.*, 2009).

It is currently thought that AMP does not induce torpor (Swoap *et al.*, 2007), however it still may be an interesting compound for other clinical applications.

1.3.2.6 ACTIVATION OF CENTRAL ADENOSINE A1 RECEPTORS

Adenosine is a nucleoside that has inhibitory neuromodulating characteristics, and such as other purinergic molecules (ATP, cAMP), acts as an important signalling molecule in extracellular and intracellular environments. The presence of adenosine affects excitable tissues (heart and brain) and induces vasodilation, acting as a co-factor in regulation of energy homeostasis. In particular, the brain has plenty of adenosine receptors, and it has been demonstrated its involvement in arousal, sleep homeostasis, epilepsy and in neuroprotection : caffeine, a psychoactive molecule commonly used, promotes wakefulness by acting as an antagonist of adenosine receptors (Fredholm and Lindström, 1999; Dunwiddie and Masino, 2001).

Even though adenosine receptors are widespread in the central nervous system, they are more densely expressed within the Nucleus Tractus Solitarius (NTS) (Carrettiero and Fior-Chadi, 2008); a complex modulatory and integrating region that plays a role in cardiovascular, gustatory, thermoregulatory, respiratory, and metabolic functions (Grill and Hayes, 2012; Tupone *et al.*, 2013).

In hibernators, a fluctuating sensitivity to A1-adenosine receptor (A1AR) signalling has been observed, in particular, the increase in sensitivity is concomitant with the beginning of the hibernating season, which may also influence sleep drive and body temperature (Olson *et al.*, 2013).

The fact that adenosine plays a role in torpor is widely demonstrated, in fact some studies investigating its potential in improving brain ischemia had as a side effect a mild hypothermia (Miller and Hsu, 1992); in rodents, hypoxia-induced hypothermia

is milder when the adenosine antagonist aminophylline is administered (Barros *et al.*, 2006).

A similar condition to spontaneous torpor can be induced in rodents, where the peripheral injection of adenosine causes a torpor bout, bradycardia and a decrease in metabolic rate; during deep torpor, subcutaneous injection of aminophylline promotes arousal (Iliff and Swoap, 2012).

In particular, the A1-receptor (A1AR) seems the one involved in hypothermia inducing effects, since the administration of other receptors subtypes agonists did not cause any decrease in body temperature in mice (Anderson *et al.*, 1994).

In hamsters, the intracerebroventricular administration of N-6-cyclohexyladenosine (CHA), a A1-receptor agonist, causes a decrease in core temperature similarly to what is observed when spontaneously hibernating (Tamura *et al.*, 2005), comparable results have been shown in arctic ground squirrels (Olson *et al.*, 2013).

Recently, Tupone and colleagues have demonstrated that the intracerebroventricular injection of CHA induces a torpor-like state in a non-hibernating mammal, the rat. In rats exposed at an ambient temperature of 15°C, immediately after the injection, the heart rate decreases quickly, lowering to about 200 bpm, followed by a decrease in core temperature to about 28°C. In addition, the BAT temperature decreases, all these phenomena are accompanied by a decrease in EEG power (Fig. 7). The bradycardia and decrease in BAT temperature (which is innervated by sympathetic nerves) are likely due to a sympathetic inhibition. The NTS has a sympatho-inhibitory activity, which is tonically inhibited by GABA-ergic projections. It is likely that CHA, binds to inhibitory A1AR receptors of the GABA-ergic projections, removes the inhibitory drive to the sympatho-inhibitory activity of the NTS, ultimately activating that branch. However, the mechanism of the sympatho-inhibitory effects of the NTS are still not clear, and a direct connection of the NTS to sympathetic premotor neurons have still not been found. There might exist a multi-synaptic pathway that inhibits the RPa or its excitatory efferences (Tupone *et al.*, 2013).

Overall, current data suggest that activation of central adenosine A1 receptors may be a promising target in inducing synthetic torpor.

1.3.2.7 PHARMACOLOGICAL INHIBITION OF THE RAPHE PALLIDUS

As previously extensively described, the RPa within the RVMM, a region containing sympathetic premotor neurons, modulates the activity of several thermoeffectors (BAT, shivering, cutaneous vasomotion), thereby playing an important role in thermoregulation.

The microinjection of the GABA-A agonist, muscimol, within the RPa in the RVMM causes a massive peripheral vasodilation in the anaesthetized (Blessing and Nalivaiko, 2001) and the free-behaving rat; whereas the microinjection of the GABA-A antagonist bicuculline methiodide caused vasoconstriction (Cerri *et al.*, 2010). MRI investigations showed that in humans, skin cooling induces the activation on the RPa (McAllen *et al.*, 2006).

These data brought the idea that the inhibition of the RPa could be a promising target for synthetic torpor, by blocking thermogenic effectors and impeding the appearance of sympathetic compensatory responses (shivering, tachycardia).

In 2013, Cerri and colleagues induced a torpor-like state in a non-hibernating animal, the rat, by multiple microinjections of muscimol within the RPa. Prolonged 6-hours RPa inhibition caused a state of deep hypothermia, where EEG power and heart rate drastically reduced, but arterial pressure was maintained constant throughout the torpid state. A few hours after suspending the injections, animals regained normothermia and did not display any observable autonomic or behavioural abnormalities (Cerri *et al.*, 2013) (Fig. 8).

The physiological role in thermoregulation of the RPa is common in many hibernating and non-hibernating species, which makes it a promising target for human therapeutic hypothermia.

1.4 THERAPEUTIC HYPOTHERMIA

The idea that cooling the body could bring beneficial effects in several clinical conditions is very ancient: the first written testimonies are from ancient Egypt, about 5000 years ago, where a treatise on medicine recommended the use of therapeutic hypothermia. Hippocrates (460-365 A.C.), in his piece De veteri medicina, suggested treating of haemorrhagic states with cold ice packs, and body cooling was advised for tetanus treatment.

In recent times, therapeutic hypothermia was extensively studied during 90s, and it showed neuroprotective effects in several clinical conditions, both in animal models and humans (Karnatovskaia *et al.*, 2014).

1.4.1 CURRENT CLINICAL APPLICATIONS

The therapeutic effect of hypothermia has been tested in all those situations where the patient could benefit of a reduction in metabolic rate, such as in conditions where oxygen and metabolic demands of the whole body or a specific organ exceed their availability: cardiac arrest, brain stroke or hypoxic-ischemic encephalopathy. In all these pathological conditions, the inability to provide enough oxygen and/or nutrients because of the decreased or absent blood perfusion in infarctuated tissues causes a rapid and non-reversible tissue necrosis. Thus, timing is crucial in preventing further damage when treating these conditions. Hypothermia, by directly interfering with the enzymatic reactions occurring in the tissue, decreases the metabolic rate and therefore oxygen and glucose consumption; moreover, it seems to prevent the damage caused by reperfusion following ischemic events: free radical production, dysregulation of ionic concentration and distribution, altered membrane permeability, intracellular acidosis and several others (Polderman, 2004).

Hypothermia also showed anti-inflammatory and anti-edemigenous effects, by inhibiting phagocytosis and cytokine release, and by decreasing cellular membrane permeability in blood vessels and hematoencephalic barrier (Jurkovich *et al.*, 1988; Huang *et al.*, 1999). At present, hypothermia is being studied and implemented in various clinical trials to test its possible protective effects in other clinical situations.

In clinical practice, therapeutic hypothermia can be induced in two ways. The first method relies on peripheral cooling, which uses convection, conduction, evaporation or radiation to subtract heat from the body (cooling blankets, ice packs, cooling helmets, alcohol and water based sprays, immersion in cold water). The second option consists of central cooling, where heat is subtracted by conduction, through intravascular catheters, cold fluids infusions and external body circulation.

However, all of these methods have a common side effect: since the hypothermia is induced by an exogenous approach, the neural circuitry that controls thermoregulatory homeostasis is still active, thus, the body fights the decrease in body temperature by attempting to keep normothermia: even in mild hypothermia, there is a major sympathetic activation, by means of cardiac effects (tachycardia), vasoconstriction and increase in arterial pressure (MacLaren *et al.*, 2014; Lee, 2008). By fighting the temperature drop, the body increases glucose, protein and fat consumption, this thereafter increases oxygen consumption and decreases systemic pH (due to the presence of ketone bodies) and leads to metabolic acidosis. Moreover, another powerful thermogenic response is activated: shivering, which can increase muscular oxygen consumption from 40 to 100% (Polderman, 2004). Lastly, there is an increase in catecholamines and cortisol, and hyperglycaemia and insulin resistance are often observed. That is particularly dangerous in heart failure or atherosclerotic patients, where the severe vasoconstriction and increase in heart rate could cause a myocardial infarction (Frank *et al.*, 2003).

Moreover, the increase in metabolic rate is the exact opposite of what is needed in some circumstances, to decrease the metabolic rate in situations where the oxygen and glucose demands cannot be fulfilled: it is clear how in these situations therapeutic hypothermia is counteractive. The insulin resistance causes hyperglycaemia, which increases the risks of kidney failure and infection. Sedatives, analgesics, and muscle relaxants are administered to prevent shivering; thus, the patient must be intubated (Soleimanpour *et al.*, 2014).

Since exogenous hypothermia is a very stressful condition, only mild hypothermia (32-34°C) can be safely induced in clinical practice nowadays.

Some studies have focused on trying to modulate the thermoregulatory pathway centrally: acting on the CNS would provide an endogenous and active decrease in body temperature, and subsequent decrease in metabolic rate, without any counteracting sympathetic activation. This would probably be safer and more efficient, since the central inhibition of thermogenic responses would permit to induce a much deeper hypothermia with a further reduction in metabolic rate, bringing effects that are more beneficial in clinical practice. Moreover, this would open a scenario of extending possible applications of hypothermia to several other situations that could benefit of a drop in metabolic rate and core temperature.

1.4.2 POSSIBLE FUTURE APPLICATIONS

As previously said, some animals are able to actively decrease their metabolic rate and body temperature when it is energetically costly to maintain normothermia. They go through several biochemical, tissue and organic changes, in particular, some studies pointed out how hibernating animals, when torpid, have a higher radiations tolerance (Kuskin *et al.*, 1959; Baird *et al.*, 2011). Even though it is still not known if that phenomenon is due to a more active resistance (radiations are less damaging), or the repair process is faster (the damage is repaired more efficiently); it is a very interesting phenomenon with possible applications in two fields:

i) In patients with radiotherapy treated tumours, hypothermia may induce a selective radioprotection, preserving the rest of the body from radiation, and thus minimizing collateral effects.

ii) Inducing a state of deep hypothermia could facilitate long-duration space exploration: astronauts are exposed to powerful cosmic radiations, which makes current space travels limited in time. Inducing hypothermia would not only have a radioprotective effect, but it would decrease food amount required for survival. Astronauts also suffer from muscle atrophy and bone fragility, which could also be reduced by hypothermia.

All these reasons brought the European Space Agency to support researches in this field.

Other interesting phenomena observed during torpor are reversible hyperphosphorylation of tau protein, synaptic plasticity dynamics and immunomodulation; understanding the mechanisms underlying those phenomena could be beneficial in developing new clinical applications and treatments.

In conclusion, hibernation and torpor are hypothermic and hypometabolic states used as a survival strategy by several animals; the neural and biochemical mechanisms underlying these mechanisms are yet not known, and the many studies have tried to answer these questions, but without any certain and clear proposed mechanism. The interest in hibernation and torpor is mostly driven by the fact that that inducing a hypometabolic state similar to hibernation in humans, could be beneficial in clinical practice. Thus, the understanding of physiological and biochemical mechanisms of spontaneous torpor and the study of possible mechanisms of induction of synthetic torpor are crucial in the attempt to reproduce it in humans. In the present study, those phenomena have been investigated.

2. AIMS

This project aims at investigating the mechanism of spontaneous torpor and evaluating the translational aspects of such mechanism. More in detail, the project consists of three main parts:

i) **Unravelling of the neural substrates of spontaneous torpor**. In this part, the neural substrates driving spontaneous torpor will be investigated in mice. The mouse is a facultative heterotherm that well serves as animal model for spontaneous torpor. Since neurons within the RPa region are key to maintain a euthermic state in mice, neurons specifically activated at torpor entrance and projecting to the RPa will be identified by immunoistochemical techniques. The results of this experiment may lead to the identification of other brain regions, besides the RPa, that could serve as new targets for synthetic torpor induction procedures.

ii) **Evaluating the role of cellular metabolism in spontaneous and synthetic torpor.** In this part of the study, the potential for spontaneous torpor to induce a direct inhibition of the mitochondrial respiratory chain will be evaluated in mice, and will be compared with the changes in mitochondrial functions induced by synthetic torpor in rats. Whereas the first part of this study is focused on how the brain initiates the entrance into torpor, this second part is focused on how cells respond to the brain commands to reduce metabolism. To evaluate the hypothesis that the overall reduction in metabolic rate in torpor is caused by a direct inhibition of the mitochondrial respiratory chain, isolated mitochondrial will be studied in peripheral tissues such as the liver and the kidney, and in the brain. Moreover, the experiment will investigate potential differences in mitochondrial activity between spontaneous and synthetic torpor. The identification of a specific inhibition of cellular metabolism could provide new insight in the understanding of torpor physiology and for the safety of synthetic torpor.

iii) **Testing a preliminary procedure to translate the synthetic torpor induction method to mammal larger than the rat**. In this part of the study, an attempt to translate to swine the methodology used to induce synthetic torpor in rats will be presented. As a first step in such direction, it will be evaluated whether the role of RPa neurons in controlling the activity of the sympathetic nervous system is consistent with what was described for rats.

3. MATERIAL AND METHODS

All the experiments were conducted in accordance to the DL 26/2014 and the European Union Directive 2010/63/EU under the supervision of the Central Veterinary Service of the University of Bologna, after the approval by the National Health Authority (decrees: 291/2013-B; 124/2015-PR; 219/2013-B).

3.1 EXPERIMENT I

3.1.1 ANIMALS

Experiments were performed on 16 C57BL/6J female mice ((13-15 week old; The Jackson Laboratory, stock number 000664 | Black 6), weighting approximately 17-24g. After their arrival, animals were housed for one week under standard laboratory conditions: light-dark cycle (LD cycle) 12h:12h (L 9:00-21:00) with ad libitum access to food (4RF21 diet, Mucedola, Settimo Milanese, Italy) and water, at an ambient temperature (Ta) of 25 ± 1°C; light intensity of 150 lux at cage level. During the adaptation, animals were housed in groups of four and kept in plexiglass cages (Techniplast) containing dust-free wood shavings; and (the bedding was changed every two days).

According to Oelkrug and colleagues (Oelkrug *et al.*, 2011), mice adapted at a high ambient temperature, when food deprived for 36 hours and then acutely exposed to a low ambient temperature, display torpor shortly after (with longer bouts in dark phases). A similar protocol for torpor induction was observed here; after one week of adaptation to standard laboratory conditions, mice were moved to a different room, with the same ambient conditions as before, apart from the ambient temperature (Ta, 28 ± 1°C) and the 12h:12h LD schedule (L 15:00-3:00), in order to create favourable (and comfortable) conditions for inducing torpor at around the 8th hour of the D period (11.00). Mice were kept in these laboratory conditions for two weeks. after that period of time they underwent surgery.

3.1.2 PREOPERATIVE PROCEDURES

Micropipette preparation

The system allowing the injection of the retrograde tracer was set up before starting the surgical procedure. Every injection was performed using a disposable glass micropipette (Borisilicate Glass Capillaries, 1B100-4, WPI). The micropipette was pulled with a micropipette puller (Vertical pipette puller 700C, David Kopf Instruments) and then carefully broken on the tip to reach approximately 30 µm of diameter; it was then sterilized, mounted on the stereotaxic frame and tightly connected to a Toohey Spritzer pressure system (Toohey Company, Fairfield, NJ, USA), a device that drives compressed air in precise and adjustable time frames, allowing finely controlled microinjections.

Using a syringe, the micropipette was filled with a solution containing NMDA (N-methyl-D-aspartate, a glutamatergic receptor agonist) 0.2 mM, leaving the meniscus easily visible. Lastly, occasional bubbles were removed from the solution and the micropipette was tested to determine correct functioning.

3.1.3 SURGERY

After two weeks of adaptation to the switched LD cycle and the higher ambient temperature, in agreement with the experimental plan (see Experimental plan), mice underwent surgery.

All the surgical instruments were autoclaved for 10 minutes at 134°C (Beta 35 Easy-lock, PBI, Milano, Italy).

Firstly, anaesthesia was induced by placing the mouse in an anesthetizing chamber, which was supplied with a continuous stream of anesthetizing gas (isoflurane 1-2%, Abbott S.p.a., Pomezia Roma, Italy, nitrous oxide 70%, in oxygen). Once the animal lost its righting reflex, it was removed from the chamber and the anaesthetic mixture thereafter was delivered through a custom-made nose cone. The mouse was then positioned on a heating mat that maintained the body temperature at 37°C throughout the whole procedure, which was performed in sterile conditions. After confirming the surgical plane of anaesthesia by the absence of blink and toe-pinch reflexes, a

lubricating ointment was applied to the eyes to prevent corneal drying, afterwards, the mouse was injected with 200 µl of Rimadyl (Carprofen 5mg/ml, Pfizer).

Using a small animal shaver, the cranic surface was shaved and the exposed skin was disinfected with iodine solution to avoid bacterial contamination of the surgical field.

Subsequently, the animal was positioned on a stereotaxic frame (Kopf instruments) by gently inserting the ear bars in the ear canals, in order to keep the head firm. Since the stereotaxic frame is not endowed with a gas delivery system, from that moment on the anaesthesia was administered intraperitoneally (Ketamine, Imalgene 1000, Merial 100mg/kg and xylazine, Xilor, Bio 98 Srl, 20 mg/kg).

The mouse electrocardiogram (ECG) and heart rate were obtained by positioning the anterior paws on two copper plates covered with a drop of electrode gel, connected with an electrophysiological amplifier. The amplified signal was then converted in digital signal and displayed on a PC trough a specific software (Spike 7) that digitally derived the heart rate from the ECG.

Once a good and stable ECG signal was obtained, the scalp was incised in the midline from the frontal bone to the nuchal muscles with a surgical sterile blade. The periosteum was gently removed, and the skull surface was cleaned to make the bone sutures clearly visible. Using a 1 mm rounded drill tip, a craniotomy was made on the interparietal bone, -6.3 caudally from bregma, following the Raphe Pallidus coordinates (-6.3 mm AP, -5.2 mm DV, from bregma) obtained from the "The Mouse Brain in Stereotaxic Coordinates" (Paxinos and Franklin, 2004) (Fig. 9). The craniotomy was made being careful not to damage the dura mater underneath. Using a Zeiss microscope at 16X magnifications, the dura thus exposed was carefully incised and parted.

Subsequently, the micropipette, previously filled with an NMDA agonist and fixed on the stereotaxic apparatus, was moved on the midline of the skull, -6.3 mm caudally from bregma, above the craniotomy. Before inserting the micropipette in the brain, its correct functioning was double-checked and afterwards, the pipette was slowly lowered down ventrally in the brain -5.2 mm from the dura.

The injection was made gradually, driving the compressed air in multiple 20ms periods. After every 20ms delivery, to assess the quantity of injected drug, the meniscus of the micropipette was observed through a Zeiss microscope at 40X magnifications. The approximate injected total volume was about 60 nl.

Since the NMDA-agonist delivered in the RPa should cause a consistent, rapid and reversible increase in the heart rate, the position of the micropipette was considered correct if that phenomenon occurred within two minutes from the end of the injection. In the eventuality of no physiological answer to the drug, the micropipette was removed, and the coordinates were adjusted until the right position was found.

After obtaining a successful RPa localization, the pipette was removed and filled with a solution containing a monosynaptic retrograde tracer (Cholera Toxin b, CTb), added with fluorescent microbeads, to allow the localization of the injection site. The micropipette was inserted again in the brain, according to the same coordinates of the first injection, and the second injection procedure was carried out as described above.

Once the injection was over, the micropipette was left in place for 5 mins, to avoid any spillage from the tip while extracting the pipette. Finally, the micropipette was carefully extracted, and the skin incision was sutured with a 5-0 suture silk thread and covered with an antiseptic cream (10% Betadine gel, Meda Pharma Milan), followed by intramuscular administration of a prophylactic broad spectrum antibiotic (30 µl of veterinary Rubrocillin, Intervet, Schering-Plough Animal Health, Milano; benzathine benzylpenicillin 12500 U.I./kg + dihydrostreptomycin sulphate 5 mg/kg: 140 U.I./mouse + 60 µg/mouse diluted in 800 µl of saline solution). Finally, the animal was kept under observation until the appearance of the first signs of recovery from general anaesthesia and then was placed in its cage and back to the LD switched (L 15:00-3:00) and Ta=28°C, for a week, to recover from surgery. The animal's pain, distress or suffering symptoms were constantly monitored and evaluated using the Humane End Point (HEP) criteria. Animals that displayed some degree of suffering symptoms were administered, as needed, with 200 µl of Rimadyl (Carprofen 5mg/ml, Pfizer).

3.1.4 EXPERIMENTAL SET-UP

During the experiments, mice were kept in a custom-made cage, consisting of a 40-cm high plexiglass cylinder filled with dust-free wood shavings, divided in two semicircles by a removable plexiglass panel. This allowed to house mice in couples, each in one semicircle, impeding their interaction; also, the top of the cylinder was left without grids, in order to record their body temperature with a thermal camera placed above the cage.

The cage containing the animal was placed inside a freezer box, modified to control efficiently the ambient temperature. The fine temperature regulation was obtained by connecting a thermostat to the compressor of the freezer and an electric heater (1800W) placed inside the latter. When the temperature deviates from the one set by the operator, the thermostat switches on the compressor or the heater to adjust the ambient temperature. The modified freezer box was also equipped with a ventilation system, an illumination system consisting of optical fibers (100 lux at the level of the cage) controlled by a timer; lastly, an infrared thermal camera (Thermovision A20, Flir Systems) was placed on a pedestal above the cages and was used to assess the presence or absence of torpor. Cutaneous temperature in mice was calculated as mean value ±SEM of cutaneous temperature recorded every 10 minutes on the cutaneous surface, on the lower back.

3.1.5 EXPERIMENTAL PLAN

Mice were divided in three experimental groups (Fig. 10):

1) Torpor Group (n=4): the torpid state was induced by following, with some slight modifications, a protocol that was shown as effective by Oelkrug and colleagues in 2011 (Oelkrug *et al.*, 2011), consisting of:

- Days 1-20: adaptation to 28°C of ambient temperature, with food and water ad libitum (on Day 14 mice underwent surgery for injection of the retrograde tracer).

- Day 20: mice were deprived of food at 21:00 for 36 hours before exposing them to a lower ambient temperature.

- Day 22: at 9:00 in the morning, mice were moved to a lower ambient temperature, Ta of 15°C.

The 36-h fasting combined with the exposure to a lower ambient temperature (Ta of 15°C) caused the appearance of torpor usually within two hours (11:00 am, approximately).

2) Cold Control Group (n=5): To assess whether the observed effects were due to cold exposure, these mice underwent the same protocol as described for the Torpor Group, except from the fact that they were not food deprived; so they were subjected to Ta of 15°C with free access to food. None of them displayed a torpid state.

3) Warm Control Group (n=7): To assess whether the observed effects were due to food deprivation, these mice underwent the same protocol as described for the Torpor Group, except from the fact that they were maintained at a high ambient temperature (Ta of 28°C) throughout the whole experiment. Therefore, they were food deprived for 36 hours, but not exposed to low Ta. None of them displayed a torpid state.

After confirming the presence of torpor in the Torpor Group, by visually observing the infrared recording of the mouse (usually around 11:00 am) (Fig. 11), the condition was maintained and constantly monitored for an hour and a half.

The recording was stopped after 90 minutes of torpor. This time was used because the expression of the early gene c-Fos (a marker of neuronal activation is known to peak in active neurons around 90 min after the beginning of neuronal activation) (Kovács, 2008).

For the two Control Groups, the time frames were adjusted as according to those of the Torpor Group, to avoid any circadian discrepancy.

3.1.6 PERFUSION

Mice were collected from the recording cage around 12:30. After being deeply anesthetized with isoflurane (1-2%, Abbott S.p.a., Pomezia Roma, Italy, nitrous oxide 70%, in oxygen) animals underwent thoracotomy to expose the heart. A 26G needle connected to a peristaltic pump was inserted through the left ventricle into the aorta and blocked with a haemostatic clamp. After puncturing the right atrium in order to allow the excess liquid to drain, the pump was switched on and the animals were perfused with 50 ml of cold phosphate-buffered saline (PBS) (0.1 M, pH 7.4), followed by 50 ml of 4% paraformaldehyde (Sigma-Aldrich, St Louis, MO, USA) in phosphate buffer (0.1 M, pH 7.4) solution. The entire mouse brains were collected.

3.1.7 HISTOLOGY

The collected brain was post-fixed at 4°C in 4% paraformaldehyde (Sigma-Aldrich, St Louis, MO, USA) in phosphate buffer (0.1 M, pH 7.4) solution for 60 mins; subsequently it was moved to a cryoprotectant solution made of 30% sucrose (Sigma-Aldrich, St Louis, MO, USA) in phosphate buffer (0.1 M, pH 7.4) additioned with sodium azide (NaN3) to avoid bacterial contamination. The brain was left in the latter until sinking (24 hours minimum – 7 days maximum) and kept in fridge.

After this treatment, the brain was ready for the cryostat cutting: it was sectioned coronally in two portions using a sharp blade. The portions were fixed to a mounting plate with an inclusion media (Killik, Bio-Optica Milano s.p.a.), and positioned in the cryostat (Reichert-Jung, 2800 Frigocut-N). The latter consists of a rotating microtome with adjustable cutting depth, positioned in a refrigerated chamber. The temperature was set at -21°C; the fast freezing and the low temperature impede damage in the brain structures caused by freezing crystals formation. After assessing the brain was completely frozen, it was entirely cut in 35 μm coronal sections: the sections were collected in rotation in 6 separate wells, allowing homogenous sampling of the entire brain in each well. Each set of sections was then rinsed in

phosphate-buffered saline (PBS 10 mM), moved to a cryoprotectant solution in a 2ml cryotube and stored at -70°C for subsequent immunohistochemistry analysis.

3.1.8 IMMUNOHISTOCHEMISTRY

The immunohistochemistry procedure was aimed to assess the presence of two antigens: c-Fos, a transcription factor located in the nucleus, used as a marker of neural activation, and CTb, a cytoplasmic non-trans-synaptic retrograde tracer, used to individuate direct afferences to the injection site.

After rinsing the sections in PBS 10mM, the protocol consisted in a 2-hour pre-incubation in an Antibody Dilution Solution made with normal donkey serum (Sigma-Aldrich, St Louis, MO, USA) followed by a 12-16-hour incubation in primary antibodies diluted in ADS. The following primary antibodies were used:

- anti-c-Fos rabbit polyclonal primary antibodies (Calbiochem, 1:10000 dilution), to localize the activated neurons during the experimental procedure;
- anti-CTb goat polyclonal primary antibodies (List Biological Laboratories Inc, 1:10000 dilution), to detect direct afferences to the Raphe Pallidus (injection site).

After 12-16 hours, the sections were rinsed in PBS 10mM additioned with Triton X-100 0.3% (v/v), in order to remove any excess of non-conjugated antibodies.

To localize and mark the conjugated primary antibodies, the sections were moved in a second incubation solution made with secondary antibodies conjugated with fluorochromes in ADS for 2 hours. The following secondary antibodies were used:

- anti-rabbit donkey green fluorochrome-conjugated (Alexa-488) antibodies;
- anti-goat donkey yellow fluorochrome-conjugated (Alexa-555) antibodies;

After the 2-hour incubation, paying attention not to expose the sections to bright light to avoid fluorescence fading, the sections were once again rinsed in PBS 10mM, mounted on glass slides in rostro-caudal order and left to dry overnight.

The slides were covered with cover slips and a mounting-media that dampens the spontaneous fading of fluorochromes in time (Pro-long Gold anti-Fade), and stored in a dark place.

3.1.9 IMAGE ACQUISITION AND COUNTING

A Nikon Eclipse 80i microscope, connected to an image acquisition camera, was used to collect all the images.

Every area of interest was photographed twice; each photo was taken with a specific filter to detect green or yellow fluorescence. Several areas involved with food consumption, thermoregulation and energy homeostasis have been examined: in particular, e the Dorsomedial nucleus (DMH), the Arcuate nucleus (ARC); the Paraventricular nucleus (PVH) and the Lateral Hypothalamus (LH) at hypothalamic level, and the Ventrolateral Periaqueductal Gray (VLPAG) and the Lateral Parabrachial nucleus (LPB) at extrahypothalamic level.

All the collected pictures were elaborated with the open-source program "GIMP-2", the yellow and green fluorescence pictures were overlapped to detect any double-stained neurons. The images were analysed blindly by using Image Pro Analyser 7.0 (IPA, Media Cybernetics) software, without applying any adjustment for brightness or contrast. In detail, for every image were counted: green-labelled neurons, representing those activated during the experimental procedure (expressing c-Fos); yellow-labelled neurons, indicating those directly communicating with the Raphe Pallidus (presence of injected retrograde tracer); and double-labelled neurons, indicating the ones that are both activated during the experiment and in direct connection with the RPa.

Since the injection site was labelled with fluorescent beads, it was possible to assess whether the injection site was in the RPa. Yellow-labelled neurons (retrograde tracer) and double-labelled ones in animals that showed a misplaced injection site were excluded from the study of the double labelling, but not of c-Fos activation. The exclusion of those animals led to the exclusion of one animal for the Cold Control group (final group total n=4), no excluded animals for the Torpor group (n=4), and, unfortunately, six animals from the Food Control group (final group total n=1).

3.1.10 STATISTICAL ANALYSIS

To compare left vs. right areas of interest, all the structures were studied bilaterally; a paired t-statistic was used, taking into consideration separately each experimental condition, in order to avoid biases in the resulting sample variances.

Since there was no difference between the left and right side, the counting process was carried on without assessing the side. For every nucleus, neurons c-Fos+ and double stained CTb+/c-Fos+ were counted and the mean value of positive neurons was calculated in each of the nuclei studied, for each of the three experimental groups. The results, expressed as mean ± SEM (Standard Error of the Mean), were analysed using the one-way Univariate Analysis of Variance (ANOVA) (SPSS 21.0) test. The modified t-test (t*) was used to compare the mean values of the Torpor Group, Cold Control Group and Warm Control Group; significance levels were set at $p<0.05$.

3.1.11 PRELIMINARY NEURONS PHENOTIPIZATION

After obtaining the results from the above-mentioned nuclei, the aim was to try to characterize the role of each one, in terms understanding which neurons are activated in each experimental group. At present, this is an ongoing study, focusing for the moment on the Lateral Hypothalamus. In particular, this nucleus was triple stained with CTb, c-Fos and orexin, since it is a major neurotransmitter in the LH involved in the control of energy balance and metabolism (Sakurai, 2014; Sakurai *et al.*, 1998), to individuate if the activated neurons were orexinergic, and if they were directly connected to the Raphe Pallidus.

3.2 EXPERIMENT II

3.2.1 ANIMALS

Experiments were performed on 16 C57BL/6J female mice (13-15 week old; The Jackson Laboratory, stock number 000664 | Black 6), weighting approximately 17-24g, and 16 male Sprague-Dawley rats (Charles River), weighting approximately 250-300g. After their arrival, animals were housed for one week at standard

laboratory conditions: light-dark cycle (LD cycle) 12h:12h (L 9:00-21:00) with ad libitum access to food (4RF21 diet, Mucedola, Settimo Milanese, Italy) and water, at an ambient temperature (Ta) of 25 ± 1°C, light intensity of 150 lux at cage level. During the adaptation, animals were kept in plexiglass cages (Techniplast) containing dust-free wood shavings, housed in groups of four mice/two rats; and the bedding was changed every two days.

Mice: after one week of adaptation to standard laboratory conditions, mice were moved to a different room, under the same ambient conditions, , with the exception of the ambient temperature (Ta, 28 ± 1°C) and the 12h:12h LD schedule (L 15:00-3:00), in order to create favourable conditions for inducing torpor, as previously described. Mice were kept in these laboratory conditions for three weeks.

Rats: After one week of adaptation, rats underwent surgery.

3.2.2 PREOPERATIVE PROCEDURES

Rats: Hypothalamic temperature (Thy) was measured using resin insulated thermistors (NTC Thermometrix) of 0.3 mm diameter. The thermistors were inserted in a 21G needle welded to a 2-pin connector; insulated with electrode resin. The day before the surgery, thermistors were calibrated to evaluate their sensibility and linearity; to achieve that, the tip of the thermistor was introduced in a heated bath at 37°C, and was connected to the same amplifier in direct current that will be used during the experiment. The impedance was then measured at three different temperatures (37.0, 38.0, 39.0°C), and the three values were interpolated.

Cannulas for intracerebroventricular (ICV) and Raphe Pallidus injections were obtained from Bilaney Consultants GmbH and were disinfected in 70% alcohol solution prior to use.

3.2.3 SURGERY

Rats: animals underwent surgery after one week of adaptation to standard laboratory conditions. Animals were pre-anaesthetized with Diazepam (Valium Roche, 5 mg/Kg intramuscular) and anaesthetized with Ketavet (Ketamine-HCl, Parke-Davis, 100 mg/Kg intraperitoneally). After confirming the surgical plane of anaesthesia by

the absence of blink and toe-pinch reflexes, using a small animal shaver, the cranial surface was shaved, and the exposed skin was disinfected with iodine solution to avoid bacterial contamination of the surgical field. Afterwards, the animal was positioned on a stereotaxic frame (Kopf instruments) by gently inserting the ear bars in the ear canals, in order to keep the head firm; the scalp was incised in the midline from the frontal bone to the nuchal muscles with a surgical sterile blade. The periosteum was removed, and the brain surface was cleaned, making the cranial sutures clearly visible. Using a 0.5 mm drill tip, four craniotomies were made, two on the left and right frontal bones (in antero-lateral position), and two on the left and right parietal bones (in postero-lateral position), to implant four stainless steel screws to ensure all the inserted probes in place. The craniotomies were performed being careful not to damage the dura mater underneath. Another hole of the same dimensions was made above the right anterior hypothalamus to insert the calibrated thermistor to record deep brain temperature.

The animals were then divided in two groups and underwent different procedures:

i) RPa injection (n=9): paying attention not to damage the dura and using a rounded tip 1mm drill, a hole was made on the occipital bone, approximately −3.9 mm posterior to lambda. A microinjection guide cannula (C315G-SPC; Plastics One; internal cannula extension below guide: +3.5 mm) was stereotactically implanted at Raphe Pallidus cohordinates -3.4 AP from interaural, 0.0 LL, -9.5 DV, obtained from "The Rat Brain in Stereotaxic Coordinates", (Paxinos and Watson, 2007) (Fig. 12). To assess the correct positioning of the guide cannula, a functional intraoperative test was carried: the selective GABA-A agonist muscimol (100nl 1mM) was injected, and the tail temperature was monitored through a temperature probe positioned at 1/3 of the length of the tail on the skin surface. Previous scientific studies showed how the inhibition of Raphe Pallidus neurons causes massive vasodilation (Blessing and Nalivaiko, 2001). Thus, the positioning was assumed correct if consistent increase in tail surface temperature was observed within 5 minutes from muscimol injection. If the test failed, the cannula

was extracted and the DV and LL coohordinates were adjusted. Correct positioning was always achieved within the second attempt.

ii) ICV injection (n=6): paying attention not to damage the dura and using a rounded tip 1mm drill, a hole was made on the left parietal bone, above the left lateral ventricle. A microinjection guide cannula (C315G-SPC; Plastics One; internal cannula extension below guide: +1 mm) was stereotactically implanted in the left lateral ventricle coohordinates - -1.2 AP, 1.3 LL, -4 DV, obtained from "The Rat Brain in Stereotaxic Coordinates", (Paxinos and Watson, 2007) (Fig. 13).). The positioning was considered successful when progressive cerebrospinal fluid withdrawal was achieved during surgery. If there was no cerebrospinal fluid withdrawal, the cannula was extracted and the DV and LL coohordinates were adjusted. No further control of the correct placement of the cannula was carried out, neither during the experimental procedure (to avoid any kind of interference with normal animal behaviour) nor immediately before the sacrifice of the animal not to interfere with brain cellular activity.

In both groups, when the cannula was considered to be in the right position, it was fixed with dental resin (ResPal), covering the whole surgical field, incorporating the thermistor and the screws.

Lastly, rats were administered with wide-spectrum antibiotics (1 µl/g Ampicilline 500mg/5ml; 0.2 µl/g di Amikacin 500mg/10ml) to prevent any infections, with 5 ml subcutaneous saline solution to prevent dehydration, and with analgesic therapy (Rimadyl - Carprofen 5mg/ml, Pfizer – 5mg/kg). Animals were constantly monitored until regaining of consciousness and then left to recover for 1 week under standard laboratory conditions. The animal's pain, distress or suffering symptoms were constantly evaluated using the Humane End Point (HEP) criteria. Animals that displayed some degree of suffering symptoms were administered, as needed, with 5mg/kg of Rimadyl (Carprofen 5mg/ml, Pfizer).

3.2.4 EXPERIMENTAL SET-UP

Mice: see Experimental set-up in Experiment I.

Rats: After one week of recovery after surgery, rats were moved to the experimental box. The cage containing the animal was placed inside a thermoregulated box, consisting in a freezer that was modified in order to permit a precise control of Ta. The fine temperature regulation was obtained by connecting a thermostat to the compressor of the freezer and an electric heater (1800W) placed inside the latter. When the temperature deviates from the one set by the operator, the thermostat switches on the compressor or the heater to adjust the ambient temperature. The modified freezer box was also equipped with a ventilation system, an illumination system consisting of optical fibers (100 lux at the level of the cage) controlled by a timer. The cage was instrumented with a rotating swivel, connected to the external amplifiers. 48 hours prior to the experiment, using a copper wire, the animals' thermistors were connected to the swivels, in order to acquire baseline deep brain temperature (Thy) and animals were exposed to a lower ambient temperature of 15°C, to favour hypothermia appearance in the experimental day.

The hypothalamic temperature (Thy) acquired, was amplified (mod. Grass 7P511L, Astro-Med Inc, West Warwick (RI), USA) and filtered at 0,5 Hz (high-pass) and then analog to digital converted to 12 bit (CED Micro MK 1401 II). It was then acquired on a digital hard drive with a 50 Hz acquisition rate. Hypothalamic temperature was calculated as mean value ±SEM of 30 minutes time frames.

3.2.5 EXPERIMENTAL PLAN

Overall, animals were divided in six experimental groups, where Groups 1, 3 and 5 were Treatment Groups, while Groups 2, 4, and 6 were the corresponding Control Groups:

1) Mouse Torpor (n=8): These animals underwent the same protocol as the one shown in 1) Torpor Group in Experimental Plan in Experiment I. All animals showed torpor shortly after the exposure to the torpor favouring conditions (within 2 hours).

2) Mouse Control (n=8): These animals underwent the same protocol as the one shown in 2) Cold Control Group in Experimental Plan in Experiment I. (Fig. 14)

3) Rat RPa MUS (n=4): After a 7-day recovery from surgery, starting at Light onset, at 9:00 am, animals were injected with the GABA-A agonist muscimol into the Raphe Pallidus (RPa). Each animal received, starting from 09:00, a total of five injections (1/h) (see below, Microinjections in the free behaving rat). All animals entered a torpor-like state shortly after the first injection.

4) Rat RPa ACSF (n=5): After a 7-day recovery from surgery, starting at Light onset, at 9:00 am, animals were injected with artificial cerebrospinal fluid (ACSF) into the RPa. Each animal received, starting from 09:00, a total of five injections (1/h) (see below, Microinjections in the free behaving rat) (Fig. 15).

5) Rat ICV CHA (n=3): After a 7-day recovery from surgery, at Light onset, at 9:00 am, animals were injected in 2 min, with 5 μl of the A1AR agonist N6-cyclohexyladenosine (1mM) (see below, Microinjections in the free behaving rat). All animals entered a torpor-like state shortly after the injection.

6) Rat ICV ACSF (n=3): After a 7-day recovery from surgery, at Light onset, at 9:00 am, animals were injected in 2 min, with 5 μl of ACSF (see below, Microinjections in the free behaving rat). (Fig. 16)

To minimize any environmental difference, animals underwent experiment in couples: each animal from one of the Experimental Groups (1, 3, 5) underwent the procedure the same experimental day as its corresponding Control (Groups 2, 4, 6). At the end of the experiments (in correspondence with the nadir of spontaneous and synthetic torpor), all animals were euthanized with an overdose of Ketavet (Ketamine-HCl, Parke-Davis), in the time frame between 13:30 and 15:00.

After assessing the absence of vital signs, the animals were dissected, and organs of interest were collected for mitochondrial analysis (see tissue processing below):

Liver and kidney were collected in all experimental groups, whereas brain was collected for Mouse Torpor, Mouse Control, Rat ICV Adenosine and Rat ICV

groups. All the organs were stored in a phosphate buffered solution and immediately processed at the Biochemistry facility (see Mitochondria processing below).

3.2.6 MICROINJECTIONS IN THE FREE-BEHAVING RAT

All microinjections were performed using a method developed in this laboratory. A 1m Teflon tube, with constant diameter (D.I.0.2mm, FEP-Tubing 4001005 10X1m Microbiotech/se AB, Stockholm, Sweden) was tightly connected from one side to a Hamilton 5 µl syringe (Hamilton Company, Bonaduz, Switzerland) and on the other side to the internal cannula (fitted to implanted guide cannula). The syringe was placed on a microinjection pump (Harvard Apparatus), with an infusion rate set at 0.3 µl/min. The tube and the cannula were filled with the solution containing either a drug (muscimol or CHA) or ACSF only, whilst the syringe was filled with coloured mineral oil. The oil-drug interface, observed with the microscope, allowed the operator to detect the drug movement in the tube and to control the injected volume. After the injection, the internal cannula was left in place for about 10 minutes and then was gently removed. To minimize the interaction with the animal, the pump, the syringe and the operator are located outside the experimental box (Fig. 17).

3.2.7 MITOCHONDRIA PROCESSING

The mitochondria processing was entirely carried out by the members of the research group coordinated by Prof. Giancarlo Solaini at the Biochemistry Division of the Department of Biochemical and NeuroMotor Sciences of the University of Bologna.

Liver, brain, BAT and kidney mitochondria were isolated from rats and mice according to Barogi et al., 1995. Briefly, tissue was homogenized in buffer solution (0.22 M Mannitol, 0.07 M Sucrose, 2 mM Tris, 1 mM EDTA and 20 mM Hepes, pH 7.2 at 37°C, containing 0.4% albumin) and then centrifuged at 2000 rev./min for 80 s. in a rotor JA20-Beckman (for liver: 5000 rev./min for 1.5 min.) to remove nuclei and plasma membrane fragments. The crude nuclear fraction was re-extracted, and the two supernatants were mixed. The mitochondrial pellet was obtained by centrifuging the mixture at 12 000 rev./min for 2.5 min. Albumin contamination was avoided with two additional washes in buffer solution. Mitochondrial protein

determination was performed with a biuret method (Gornall *et al.*, 1949) with the addition of 10% Na deoxycholate and using bovine serum albumin as standard.

Using a Clark-type oxygen electrode, respiratory rate of mitochondria (1 mg/ml) was assayed polarographycally with 10 mM glutamate/malate respiratory substrate; under this condition, which goes under the name of State 2 respiration, mitochondria respires at a relatively high rate (Aleardi *et al.*, 2005). State 3 respiration was induced by adding 0.5 mM ADP to the solution, and incubated for 3 min at 30°C (under this condition oxygen is consumed at the highest rate and coupled to the phosphorylation of ADP to adenosine triphosphate (ATP), which is driven by the energy obtained from the electron transfer chain; this state is fully coupled) (Sgarbi *et al.*, 2011). When ADP is finished, mitochondria continue respiration at a much lower rate, the so-called State 4 respiration ("resting state") (Fig. 18).

Moreover, the expression of uncoupling protein 2 (UCP2) was evaluated in rats ICV CHA and ICV ACSF in brain, liver and kidney. UCP2 assessment was made by means of an elettrophoresis gel and a subsequent western blot to detect the protein in tissue homogenate.

3.2.8 STATISTICAL ANALISYS

The differences in cutaneous temperature in mice and hypothalamic temperature in rats were statistically analysed by means of the paired Student's t-test.

The results for each state (State 2, State 3 and State 4 mitochondrial respiration) and the respiratory control ratio (State 3/State 4 or State 3/State 2), were statistically analysed independently by comparing the treated animals (torpid mice and hypothermic rats) vs. the control groups (euthermic animals) by means of a paired Student's t-test. Independent comparison of multiple parameters between control and treated animals represent a more conservative approach compared to that by ANOVA. For all data, statistical significance was set at $p<0.05$.

3.3 EXPERIMENT III

3.3.1 ANIMALS

Experiments were performed on four young female pigs, weighting approximately 35-70 Kg. The surgical protocol was implemented according to the requests from the Local Ethical Committee for animal Care to reduce as much as possible animal distress.

Some of the requested drugs that were used, such as Fentanyl, are known to induce autonomic effects (Cao and Morrison, 2006). To reduce the confounding effects of such drugs, that were infused continuously during the experiment, the experimental plan was structured so to use each animal as control of itself, by comparing pre-injection with post-injection parameters.

Animal's health and well-being was constantly monitored before starting every experimental procedure.

Experiments were carried out in collaboration with Dr. Mino Zucchelli, a neurosurgeon from the I.R.C.S.S. Neurological Sciences of Bologna, and with the research group coordinated by Prof. Maria Luisa Bacci, Dept. of Medical Veterinary Sciences, Alma-Mater Studiorum University of Bologna.

3.3.2 PREOPERATIVE PROCEDURES

On the day of the experiment, animals were pre-anesthetized with an intramuscular (IM) injection of the sedative agent Tiletamine-Zolazepam (5 mg/kg; Zoletil, Virbac, FR). After assessing a good grade of sedation, approximately 15 minutes later, animals were moved to the surgical table. The left ear was disinfected with an iodine solution, and after the auricular vein was individuated, it was catheterized by the insertion of an over-the-needle catheter (Delta Ven 1; Delta Med S.r.l., Mantova, Italy), for delivery of general anaesthesia or any other necessary fluid therapy. General anaesthesia was induced by thiopental sodium (5 mg/kg; Pentothal Sodium, MSD, IT) through the auricular vein catheter. After oro-tracheal intubation, anaesthesia was maintained with isoflurane (2.5%, Isoflo, Esteve, IT) in a 1:1

mixture of oxygen and air. Throughout the entire procedure, animals were administered with a Constant Rate Infusion of fentanyl (10 mcg/kg/h, Fentanest, Pfizer, US) to ensure analgesia, alongside with regular fluid therapy (Lactated Ringer, 10 ml/kg/h). An intra-arterial catheter was implanted in the femoral artery and connected to the anaesthesia delivery unit (ADU) in order to monitor blood pressure. A rectal thermocouple probe, connected to the same ADU, was used to monitor the core temperature (Tcore). Other standard parameters including: oxygen saturation, $ETCO_2$, HR, ECG, respiratory rate, and non-invasive blood pressure were constantly monitored. Body temperature was maintained around 37°C by the use of a forced air-warming device.

3.3.3 SURGERY

After confirming the surgical plane of anaesthesia by the absence of blink and reflexes, and a stable condition was achieved, the animals were positioned on the surgical table in ventral position; the head was securely fixed with tapes and slightly flexed to permit to make the brainstem more accessible. The skin surface over the occipital bone was tricotomized and disinfected with iodine solution to avoid bacterial contamination, and a linear occipito-cervical incision was performed with a scalpel. The skin was retracted, and the fascia was identified and opened. The underlying muscular structures were dissected, and the periosteum of the occipital bone was exposed from the lambda to the foramen magnum. The periosteum was then opened and the posterior arch of the first cervical vertebra (C1) exposed. A complete C1 laminectomy was performed and the dura mater was exposed. A small occipital craniotomy was obtained by drilling and by utilization of a Kerrison rongeur. Particular attention was directed in preserving the integrity of the dura, especially near the cranio-cervical passage and far from the midline, to avoid the damage of large dural venous sinuses. The dura was delicately opened with a small vertical incision at the level of the foramen magnum; the dural edges were suspended with retraction sutures to the muscles, to assure good exposure of the brainstem, and the arachnoid of the cisterna magna was opened. The procedure was ultimate when a progressive cerebrospinal fluid withdrawal was achieved. In order to visualize the foramen of Magendie and the fourth ventricle floor, the cerebellar tonsils were gently

dissected and retracted cranially by using cottonoids. This procedure permitted to have a good surgical visibility of the desired portion of brainstem (Fig. 19).

3.3.4 MICROINJECTION

Since the size of the skull in the pig can considerably vary in proportion with body weight, the use of the available stereotaxic atlas of the pig brain was not reliable. To therefore identify a responsive area, an injection of the GABA-A antagonist GABAzine (Tocris, 10 mmol; 30µL) with a 100-µL syringe (Hamilton) was performed by using some reference points of brain regions, starting with the following set of coordinates, from the calamus scriptorius and with the head tilted of 45° from the plane of the dorsal surface of the fourth ventricle : +0.5 mm on the anteroposterior axis, 0 mm on the latero-lateral axis, -17 mm on the dorsoventral axis. If no effects were observed, the anteroposterior coordinate was increased by 0.5 mm in each subsequent injection. A response was always obtained within the 4th injection. A period of at least 30 minutes was left between each injection.

Initially, the dose of microinjected GABAzine was derived by the dosage/Kg used in rats, but almost no effects were evoked. Since accordingly to several authors (Messier *et al.*, 2004; Darnall *et al.*, 2005; Hoffman *et al.*, 2007) the dosage of drugs to be used in piglets is larger than that calculated by the simple adjustment by their weight, the dose of GABAzine injected was therefore increased.

After an effective GABAzine injection, and at the peak of such response, approximately 15 to 30 minutes after the injection, the GABA-A agonist muscimol (10µL, 10mmol) was injected in the same location using a 100-µL syringe (Hamilton), to assess whether it would counteract the effect of GABAzine and possibly induce a mild hypothermia.

An operator according to the following arbitrary unit (AU) visually assessed shivering during the experiment: 0 = no shivering; 10 = modest shivering in the region of the nuchal muscle; 20 = shivering of the nuchal muscle and of the anterior limbs; 30 = extensive shivering of the entire body.

At the end of the experiment, in order to verify the exact location of the injections, the injection site was marked with fluorescent microbeads. Although most of the fluorescence faded away during the fixation process, a small microsphere residue was still visible in the targeted area.

At the end of the experiment, all animals were euthanized with an intravenous injection of Tanax (0.3 ml/kg, Intervet Italia, IT). The brainstem was collected and fixed for 10 days with 4% paraformaldehyde and then cryoprotected (30% 200 g/L of sucrose, Sigma Aldrich) until sinking. The medulla was cut coronally in sections of 60 μm on a cryostat (Reichert-Jung, 2800 Frigocut-N). The latter consists of a rotating microtome with adjustable cutting depth, positioned in a refrigerated chamber. The temperature was set at -21°C; the fast freezing and the low temperature impede damage in the brain structures caused by freezing crystals formation. The location of the injection sites was then visually verified on the microscope.

3.3.5 STATISTICAL ANALISYS

Baseline values were calculated as the average of the 10-min period preceding GABAzine injection. Post GABAzine-injection values were calculated as the average of the 10-min period preceding muscimol injection. Post muscimol-injection values were calculated as the average of the 10-min period, which started 20 minutes after GABAzine injection. The effects induced by the microinjection of either GABAzine or muscimol were statistically analysed by comparing the post-injection levels of each variable with those of the baseline by means of a paired Student's t-test. Statistical significance was set at $p<0.05$.

4. RESULTS

4.1 EXPERIMENT I

4.1.1 EFFECTS OF TORPOR ON CUTANEOUS TEMPERATURE

Cutaneous temperature was monitored during the experimental day by means of a thermal camera. Cutaneous temperature in mice was calculated as mean value ±SEM recorded every 10 minutes on the cutaneous surface on the lower back, a spot already used in other papers (Carrive *et al.*, 2007; Marks *et al.*, 2009; Vianna and Carrive, 2005). The infrared emission of torpid animals (Torpor Group) significantly decreased shortly after the exposure to low ambient temperature in comparison with Cold Control animals, reaching the mean value at nadir of 17.44 ± 0.5°C (Fig. 20).

4.1.2 C-FOS POSITIVITY

All three experimental conditions (Torpor, Cold Control, Food Control), showed some degree of c-Fos positivity in the studied brain regions (Fig. 21-26). As shown in Fig. 27 he mean value/slide (± SEM) of c-Fos positive neurons in Torpor is increased in almost all structures in comparison with the experimental control groups. Particularly, within in the Dorsomedial Hypothalamic nucleus (DMH) (Torpor group 67.91 ± 6.61; Food Control group 34.11 ± 6.60; Cold Control group 30.48 ± 6.37) and Paraventricular Hypothalamic nucleus (PVH) (Torpor group 57.58 ± 8.15; Food Control group 20.74 ± 8.80; Cold Control group 27.56 ± 7.91) the Torpor group has a significantly higher ($p<0.05$) number of c-Fos positive neurons in comparison with both control groups. The Arcuate nucleus (ARC), displayed the highest level of c-Fos positive neurons in the Torpor group (69.99 ± 7.14) among all studied nuclei, which was significantly ($p<0.05$) higher than the Cold Control group (32.78 ± 9.31), but not significantly different from the Food Control group (49.12 ± 10.01), where, as expected, an intense c-Fos positivity was observed. The Lateral Hypothalamus (LH) shows a high c-Fos positivity in all experimental conditions, and there are no significant differences between groups (Torpor group 54.85 ± 5.18; Food Control group 38.59 ± 7.18; Cold Control group 53.34 ± 16.53). Regarding the extrahypothalamic structures considered, in the Lateral Parabrachial nucleus (LPB) c-Fos positivity is significantly ($p<0.05$) higher in Torpor (46.28 ± 7.99) in comparison with the Food Control Group (14.65 ± 5.93). In the Ventral

Periaqueductal Gray (VLPAG), no significant differences have been observed between experimental groups (Torpor group 51.46 ± 3.00; Food Control group 38.82 ± 7.13; Cold Control group 45.49 ± 10.68).

4.1.3 DOUBLE STAINING POSITIVITY

All animals that displayed a misplaced injection of the retrograde tracer Cholera Toxin b (CTb) were excluded from the study of the double staining. The exclusion of those animals led to the exclusion of one animal for the Cold Control group (final group total n=4), no excluded animals for the Torpor group (n=4), and, unfortunately, six animals from the Food Control group (final group total n=1).

CTb positivity was observed in all considered structures, indicating a direct projection to the Raphe Pallidus, even though the number of CTb positive neurons was considered sufficient in VLPAG (14.1 ± 4.7), DMH (22.5 ± 7.9), LH (15.7 ± 5.2) and PVH (9.1 ± 3.0), but not in LPB (4.6 ± 1.5) and in ARC (1.4 ± 0.5).

As displayed in Fig. 28, the number of double stained neurons (positive for both c-Fos and CTb) is considerably lower than c-Fos positive neurons in all the considered nuclei, with values of a few units for all three experimental groups. Only in the DMH, a peak of double staining can be observed in the Torpor group (9.5 ± 3.00), which however is not statistically different from the two control groups.

4.1.4 TRIPLE STAINING IN LATERAL HYPOTHALAMUS

The analysis of samples in which triple staining for c-Fos, CTb and Orexin A has been performed at LH level and is still ongoing. An example of the results from an animal of the experimental group Torpor is shown in Fig. 29, highlighting the presence of at least one triple stained neuron (i.e. an orexinergic c-Fos positive neuron projecting to RPa).

4.2 EXPERIMENT II

4.2.1 EFFECTS OF SPONTANEOUS AND SYNTHETIC TORPOR ON CUTANEOUS AND HYPOTHALAMIC TEMPERATURE

In mice, cutaneous temperature was monitored during the experimental day by using a thermal camera, and measuring infrared emission of the lumbar region of the lower back of the animal (1 cm off the midline at upper lumbar level), a spot already used in other papers (Carrive *et al.*, 2007; Marks *et al.*, 2009; Vianna and Carrive, 2005). Cutaneous temperature in mice was calculated as mean value ±SEM of cutaneous temperature recorded every 10 minutes.

A shown in Fig. 30, in torpid animals (Mouse Torpor), the infrared emission significantly decreased shortly after the exposure to low ambient temperature in comparison with Mouse Control animals, reaching the mean value at the nadir of 16.43 ± 0.17°C.

In rats, hypothalamic temperature decreased significantly shortly after the administration of either muscimol (mean value at nadir 21.21 ± 0.49°C) (Fig. 31) or CHA (mean value at nadir 27.52 ± 0.92°C) (Fig. 32) in comparison with their respective control group.

4.2.2 EFFECTS OF SPONTANEOUS AND SYNTHETIC TORPOR ON LIVER MITOCHONDRIA

As shown in Fig. 33, no significant changes were observed in oxygen consumption rate in State 2, 3 and 4 between in the Rat RPa MUS compared to the Rat RPa ACSF. However, mostly due to a non-significant increase in State 4 levels, the respiratory control ratio (3/4 RCR) was significantly lower ($p<0.05$) in rats treated with muscimol (Rat RPa MUS, n=4, 7.82 ± 0.81 nmol/min/mg) in comparison with their control group (Rat RPa ACSF, n=5, 10.10 ± 0.51 nmol/min/mg). No significant changes in both State 2, 3 and 4 and in 3/4 RCR were observed between adenosine (CHA) treated rats (Rat ICV CHA, n=3) and their corresponding control group (Rat ICV ACSF, n=3). Since any effect on mitochondrial function during the occurrence

of deep hypothermia may be reasonably supposed to be due to tissue cooling, further analysis was made by pooling the data of the two experiments in order to assess the effects of synthetic torpor as a whole. The pooling of the two set of data (Rat Treatment: Rat RPa MUS + Rat ICV CHA, n=7; Rat Control: Rat RPa ACSF + Rat ICV ACSF, n=8) highlighted a significant increase in State 4 oxygen consumption rate in Rat Treatment (15.22 ± 1.89 nmol/min/mg) vs Rat Control (9.87 ± 0.82 nmol/min/mg), and a significant reduction in 3/4 RCR in Rat Treatment (7.01 ± 0.67 nmol/min/mg) vs Rat Control (9.87 ± 0.82 nmol/min/mg).

In mice, a significant reduction ($p<0.01$) in State 3 (Mouse Torpor, 78.75 ± 2.96 nmol/min/mg; Mouse Control, 72.49 ± 6.10 nmol/min/mg) and a significant increase ($p<0.05$) in State 4 (Mouse Torpor, 15.93 ± 1.94 nmol/min/mg; Mouse Control, 11.42 ± 1.20) nmol/min/mg) was observed in torpid compared to control animals. The 3/4 RCR was significantly ($p<0.01$) lower in torpid animals (Mouse Torpor 3.26 ± 0.32 nmol/min/mg vs Mouse Control 6.98 ± 0.98 nmol/min/mg) compared to control animal.

4.2.3 EFFECTS OF SPONTANEOUS AND SYNTHETIC TORPOR ON KIDNEY MITOCHONDRIA

As shown in Fig. 34, in both rats and mice the State 4 levels were apparently and paradoxically higher than those of the State 2 levels. This was not observed in liver and may be due to a possible frailness of the mitochondrial membranes after the isolation protocol occurring in both the kidney and, as shown later, the brain. Due to this, in both the kidney and the brain the RCR 3/2 was considered to be a more reliable index of respiratory coupling that RCR 3/4.

In the rat, a significant decrease ($p<0.05$) in State 4 (Rat RPa MUS 37.14 ± 2.63 nmol/min/mg vs Rat RPa ACSF 48.12 ± 2.27 nmol/min/mg), but non changes in both State 2 and State 3, and in RCR 3/2 were observed in muscimol treated rats compared to their controls. No changes were observed between CHA treated rats and their controls. A significant decrease ($p<0.05$) in State 4 mitochondrial oxygen consumption rate was observed after the pooling of the data in hypothermic animals compared to controls (Rat Treatment: Rat RPa MUS + Rat ICV CHA, 41.33 ± 3.16

nmol/min/mg; Rat Control: Rat RPa ACSF + Rat ICV ACSF, 49.89 ± 2.34 nmol/min/mg).

In mice, no changes were observed in State 2, 3, and 4 and in RCR 3/2 levels in Mouse Torpor compared to Mouse Control animals.

4.2.4 EFFECTS OF SPONTANEOUS AND SYNTHETIC TORPOR ON BRAIN MITOCHONDRIA

Brain was collected in CHA treated rats and corresponding controls, and in mice, but not in muscimol treated and control rats. As shown in Fig. 35, in CHA treated rats (Rat ICV CHA) there were no significant differences in State 2, 3, 4 or 3/2 RCR levels in comparison with controls (Rat ICV ACSF). In mice, a significant ($p<0.05$), reduction in State 4 (Mouse Torpor 28.95 ± 21.41 nmol/min/mg vs Mouse Control 36.29 ± 1.79 nmol/min/mg), and 3/2 RCR (Mouse Torpor 5.14 ± 0.24 nmol/min/mg vs Mouse Control 6.14 ± 0.39 nmol/min/mg) levels was observed in torpid animals vs controls.

4.2.5 EFFECTS OF SYNTHETIC TORPOR ON UNCOUPLING PROTEIN 2 EXPRESSION

Uncoupling protein 2 (UCP2) expression was also assessed in rats' mitochondria after the induction of synthetic torpor by means of the ICV administration of CHA or following the ICV injection of ACSF. As shown in Fig. 36, no significant differences in UCP2 expression were found in brain, liver, and kidney.

4.3 EXPERIMENT III

4.3.1 EFFECTS OF CENTRAL ACTIVATION AND INHIBITION OF THE RAPHE PALLIDUS IN THE PIG

As shown in Fig. 37, pigs were monitored throughout the experiment with a thermal camera, to detect changes in infrared emission of cutaneous temperature. After the injection of the GABA-A antagonist GABAzine, cutaneous temperature decreased (vasoconstriction), and following the injection of the GABA-A agonist muscimol

increased (vasodilation). Compared to baseline values, the microinjection of GABAzine induced a significant increase in heart rate (HR) (from 99 ± 7 to 174 ± 26 bpm; $p<0.01$), systolic arterial pressure SAP (from 87 ± 7 to 170 ± 20 mmHg; $p<0.05$), diastolic arterial pressure DAP (from 51 ± 3 to 98 ± 14 mmHg; $p<0.05$), and end-tidal CO_2 ($ETCO_2$)(from 49 ± 1 to 62 ± 3 mmHg; $p<0.01$). As seen in Fig. 38, shivering became evident shortly after the injection, affecting rapidly the entire body. The microinjection of the GABA-A agonist muscimol promptly arrested the shivering, and reversed the GABAzine-induced changes in HR, SAP, and DAP, restoring values similar to those of the baseline, whereas $ETCO_2$ levels (41 ± 1 mmHg) became even significantly lower ($p<0.05$) than those of the baseline. No significant changes were observed in central core temperature (Tcore) after the injection of either GABAzine or muscimol (Fig. 39).

The localization of the injection site was performed by collecting the brain at the end of the procedure. The brain was sliced coronally and observed under a microscope. An example of the collected brain is shown in Fig. 40.

5. DISCUSSION

5.1 Experiment I

The ability to induce a state of synthetic torpor is an ambitious goal pursued by many clinical studies and other applicative fields. The reduction in metabolic rate and body temperature would not only be beneficial in several clinical conditions, such as stroke, ischemia, sepsis, and many others, but would also be of use in other fields such as space exploration. Thus, it is understandable that many scientific efforts are put in the study of thermoregulation, hibernation, and torpor.

In fact, therapeutic hypothermia is currently used in some clinical conditions, but it has several drawbacks. Since it is induced exogenously, by external cooling, it does not impede the activation of all the autonomic responses evoked by cold defence: severe shivering, arrhythmia, kidney failure, and, most important, an increase in the very same metabolic rate that was attempted to be reduced. All those side effects limit the use of therapeutic hypothermia and, in fact, only a mild hypothermia can be safely induced (32-34°C).

Animals able to enter torpor can actively reduce their metabolism, which, concomitantly with the exposure to low ambient temperature, causes a severe decrease in core temperature, up to 2-5°C. However, the possible neural pathways and physiological mechanisms underlying this process are still unknown.

Thus, one of the aims of this study was to explore the neural pathways triggering torpor; the experiment was focused on understanding the role of several hypothalamic and extrahypothalamic structures in torpor induction in mice, a species that can enter daily torpor in situations where the metabolic demand cannot be fulfilled. Since the ability to enter torpor and hibernation is shared across different mammalian orders, it would be interesting to test the possibility to pharmacologically stimulate those areas in non-hibernators (such as the rat) to restore this lost ability. Among the possible neural targets, an interesting candidate is the Raphe Pallidus (RPa), a key structure within the brainstem that controls the homeostatic somatic and autonomic responses induced by exposure to low ambient temperature, and whose inhibition with local administration of a GABA-A agonist causes the appearance of a torpor like-state (synthetic torpor), in the rat (Cerri *et al.*, 2010). Considering the

key role of the RPa, all the projection to such area are possible new targets for the induction of a state of synthetic torpor.

The aim of experiment I was therefore to identify neuronal group specifically active at torpor onset and afference to RPa neurons that could initiate the entrance into torpor. Neuronal groups selectively activated at the beginning of torpor were identified by the expression of the neural activation marker c-Fos, in four hypothalamic and two extrahypothalamic nuclei known to be involved in food consumption and thermoregulation. Within those nuclei, neurons projecting directly to the RPa were also identified.

The expression of c-Fos in the Arcuate nucleus (ARC) has been shown to be high both in animals in torpor and in the fasted control group. The ARC is involved in food intake regulation and expresses c-Fos during fasting (Wang *et al.*, 2002). NPY central injections have been shown to induce hypothermia in mice (Esteban *et al.*, 1989), whereas NPY KO mice were reported to have a reduced ability to enter torpor (Gluck *et al.*, 2006). These last data could suggest that ARC neurons, and in particular NPY neurons, may play a role in the induction of torpor. Our data, though, suggest that the activation of such nucleus is not sufficient to induce torpor, although it appears to be necessary. In other words, ARC neurons may prime other areas to respond to cold exposure by entering torpor. NPY neurons are not the only neuronal population present in the ARC. POMC neurons are also present, but, at the moment, we have not phenotypized the two populations. C-Fos + neurons within the LPB were also high in two experimental groups: the torpor and the cold exposed control group. Within the LPB, neurons mediating the cold afference from the skin thermoceptors were found; these neurons projects to the thalamus and to the Median Preoptic nucleus (Morrison and Nakamura, 2011). The activation of LPB neurons in both the group cold-exposed is therefore not surprising. It is interesting to note that cold exposure acts as a torpor trigger in fasted animals. This suggests that the cold-induced activation of the LPB neurons can result in the induction of torpor by acting on a different neuronal population compared to the cold- exposed control group. Together with the data observed in the ARC nucleus, it can be hypothesized that fasting acts as a primer, by increasing the activity of NPY neurons within the ARC,

while cold exposure acts as a trigger, by means of the activation of the LPB neurons. ARC activated neurons in torpor would therefore act of a third group of neurons, priming them to respond to the LPB neurons input.

In a similar pattern, in the Lateral Hypothalamus (LH) no specific activation for torpor was found. LH is involved in food consumption regulation and thermoregulation (Sternson and Eiselt, 2017; Cerri and Morrison, 2005) and thus it is expectable to observe neural activation in all three experimental conditions. However, although unlikely, since the LH has a heterogeneous population, it cannot be ruled out that a different neuronal population is activated specifically in torpor. Some more detailed phenotipization of the LH neurons that may be involved in torpor triggering is still ongoing.

The nuclei that displayed the most interesting activation patterns are the Dorsomedial (DMH) and Paraventricular (PVH) Hypothalamic nuclei, since c-Fos expression in torpor is significantly higher in comparison with both control groups. Activation of PVH neurons in anaesthetized rats was shown to inhibit thermogenesis (Madden and Morrison, 2009), but the physiological function served by such inhibitory pathways was not identified. The specific increase in c-Fos positive neurons in the torpor group suggest that PVH neurons can be part of the torpor triggering pathways, even if the number of neurons positive for c-FOS and the retrograde tracer CTb is small.

The activation of DMH neurons was shown to activate thermogenesis (Cao and Morrison, 2006). It is therefore hard to interpret the increase in c-FOS positive neurons within such area. The cold-exposed control group showed a significantly reduced c-Fos positivity compared with the torpor group. Since DMH neurons are supposed to be excitatory to the RPa neurons (Morrison and Nakamura, 2011), such activation appears to be counterintuitive. It is possible that, in the torpor group, DMH neurons are activated by the central cooling, and are trying to drive thermogenesis, but their activity could be overwhelmed by a stronger inhibitory input to the same neuronal targets. Another possible explanation lays in a recently identified neuronal population within the DMH region positive for acetylcholine (Ach). DMH Ach positive neurons were shown to inhibit thermogenesis in both mice (Jeong *et al.*, 2015) and anaesthetized rats. In the latter, Ach positive neurons within DMH were

shown to be tonically active (Conceição *et al.*, 2017). Such tonic activation would not be compatible with the maintenance of euthermia, and therefore may be a side effect of anaesthesia. Double stained neurons for c-FOS and CTb within DMH were also present in higher number compared to all the other conditions, although not significantly different. All these data suggest that Ach neurons within DMH can indeed be a strong candidate to trigger torpor.

The protocol used in this study, based on the injection of a retrograde tracer in the RPa, unfortunately does not allow to verify the correct placement of the injection until the end of the experiment. Considering the procedural complexity of precise micro-injections in such a small brainstem structure in mice, the overall efficiency of correct micro-injection delivery was around 60%. Unfortunately, the majority of misplaced microinjections was within the Food Control animal group, in which only one animal in seven had a successful micro-injection. This affected the group numerosity and thus the statistical analysis did not allow to highlight any significant difference among experimental groups; however, it is interesting to note how the brain regions with most counted double stained neurons were DMH and PVH. In fact, statistical analysis on DMH between Torpor and Food and Control group, resulted in a p-value close to 0.05.

In conclusion, the results suggest the existence of a neural pathway regulating the entrance into torpor, and PVH and DMH are most likely candidates to be a crucial part of this pathway. Further work is necessary to identify the specific neurotransmitters involved.

5.2 Experiment II

These second group of experiments aimed at analysing the cellular mechanism underlying the reduction in metabolic rate in both spontaneous and synthetic torpor. To this aim, isolated mitochondrial activity was studied in three tissues in both conditions. The reduction in metabolic rate observed in torpor (Heldmaier *et al.*, 2004) suggests that cellular metabolism is reduced as well. The mechanism of such reduction are unknown, but it is reasonable to think that mitochondrial activity is involved. Mitochondrial activity can be reduced in multiple ways. A very direct one

is the presence of an inhibitor of the electron transport chain. If this was the mechanism underlying the torpor-induced metabolic reduction, a diminished activity in State 3 should be detectable in isolated mitochondria. For this aim, it is key to highlight that mitochondrial activity has to be measured at 37°C, to avoid the intrinsic reduction of activity induced by a low temperature. Among the tissues studied, only the liver mitochondria show a significant reduction in State 3 in mice, whereas such reduction was not observed in rats in synthetic torpor. A similar reduction was described in hamsters and squirrels (Brown *et al.*, 2007; Armstrong and Staples, 2010), State 4 was also shown to be significantly increased in liver mitochondrial of both mice and rats, suggesting that some degree of membrane damage may have been occurred or that an uncoupling protein was expressed. Expression of the UCP2 was negative, but it is possible that other proteins with uncoupling property were responsible of such observation. Fasting was shown not to change isolated mitochondrial activity.

The torpor specific changes in liver cells activity can also be exploited to investigate if a molecular fingerprint of torpor exist at cellular level. The identification of such fingerprints would consent to identify a specific marker of torpor at cellular level and discriminate which tissue are affected specifically by torpor compared to tissue simply responding to the hypothermia.

In conclusion, the state of synthetic torpor differs from spontaneous torpor in regard to the liver mitochondrial activity. This indicates that the changes in maximum mitochondrial activity observed in torpor are not the mere consequence of a decrease in body temperature, but are intrinsic to the activation of the processes leading to torpor occurrence. However, the degree of metabolic reduction that can be accounted to the reduced activity of liver mitochondria is not sufficient to justify the degree of metabolic reduction observed in torpor (Martin *et al.*, 1999). It is relevant to remember that the direct inhibition of the respiratory chain is only one of the ways in which mitochondrial activity can be reduced.

From a translational point of view, the absence of any reduction of State 3 in liver mitochondria in the hypothermic rat, suggests that synthetic torpor cannot be considered as being the mere reproduction of spontaneous torpor in a non-hibernator.

However, it can be seen as a positive outcome, since it shows that, apparently, mitochondrial function in the rat liver would not be reduced or impaired by the large lowering of body temperature, and mitochondria would be ready to express their full activity as soon as the rat starts the rewarming process.

5.3 Experiment III

The possibility to induce synthetic torpor in non-hibernating animals has been successfully explored in rats, where the central inhibition of the RPa led to reversible sharp decrease in central core temperature without any adverse effects observed. However, translating such procedure on humans has several issues: the brainstem has a complex surgical approach, the body size in hundreds of times bigger, it is unknown whether the central inhibition of the RPa would lead to similar effects on humans, and, since is a never tried-before procedure, it is unknown what consequences it would bring. Thus, the use of an intermediate animal model, more similar to humans, the swine, would be beneficial in the methodological and functional study of the procedure. In particular, pigs are glabrous and have a body size and central nervous system organization more similar to humans.

The main result of this study is the evidence that the activation of the RPa neurons in the pig induces effects very similar to those previously observed in rodents (Morrison, 1999; Cerri *et al.*, 2010). In particular, the increase in HR and in ETCO2 suggest an increase in metabolic rate driven by the activated neurons within the RPa. Core temperature did not rise significantly during the sympathetic activation, but that is most probably the consequence of the automatic management of the intraoperative thermal comfort.

The increase in both SAP and DAP appears to be larger than that commonly observed in anaesthetized rodents (Morrison, 1999). It is possible to interpret such findings hypothesizing that GABAzine diffused to the surrounding regions in the brainstem critically involved in the control or arterial pressure, such as the rostral ventromedial medulla (RVLM). In rodents, the activation of RVLM neurons was in fact shown to evoke a drastic increase in AP (Natarajan and Morrison, 1999). The large doses of the GABAzine used in the present study may sustain such interpretation, but, if this

was the case, a drastic drop in AP should have been expected after muscimol injection. Of course, another possible interpretation of this data is that of an interspecific variability.

The sympathetic activation which resulted from the disinhibition of RPa neurons was promptly reversed by the injection of the GABA-A agonist muscimol. ETCO2 levels drop to a value even significantly lower than that of the baseline. This effect suggests that the inhibition of RPa neurons may cause a reduction in metabolic rate. If this was the case, this observation would strengthen the possibility to induce synthetic torpor in the pig by inhibiting RPa neurons.

In conclusion, the role in modulating the sympathetic outflow described for RPa neurons in rodents was confirmed in pigs, supporting the possibility that the prolonged pharmacological inhibition of this region may induce a state of synthetic torpor in non-hibernators larger than small rodents. If this was the case, it would tangibly open the road to use this safe and effective procedure to induce synthetic torpor in humans to cope with many different clinical settings.

5.4 Conclusions

The induction of a state of synthetic torpor in clinical settings would be extremely beneficial in a variety of clinical conditions, but the mechanism underlying torpor are still largely unknown. In the present dissertation, new data regarding both the neural and cellular mechanism for torpor as well as the translational aspect relevant to the induction of synthetic torpor were presented. In particular, the neural pathways triggering torpor were begun being unravelled, pointing to at a few putative areas responsible for triggering torpor. The neural command to enter torpor was then showed to affect cell function specifically in the liver, an effect that was not replicated in synthetic torpor. As previously discussed, this can be seen as a positive outcome, since it indicates that mitochondrial activity would not be damaged by a condition of deep hypothermia in the rat. Finally, a preliminary study aimed at obtaining the proof of concept that synthetic torpor can be induced also in larger mammals showed promising results.

All these results strengths the possibility to develop an effective and safe procedure to induce synthetic torpor in humans.

6. FIGURES

Figure 1. Current proposed model of thermoregulatory circuitry in the rat.

Peripheral thermal information are conveyed by free nerve endings of sensory pseudounipolar neurons, whose cell body is located within dorsal root ganglia (DRG). The information are delivered to lamina I neurons of the dorsal horn (DH), whose ascending axons reach the external part of the Lateral Parabrachial nucleus (LPBel) in the pons. The LPBel is activated by skin cooling, whereas skin warming activates the dorsal part of the LPB (LPBd). When activated, LPBd sends glutamatergic excitatory projections to glutamatergic excitatory interneurons within the Median Preoptic Area (MnPO), which subsequently activate warm-sensitive neurons within the Medial Preoptic Area (MPO). On the other hand, LPBel transmits information to GABA-ergic (inhibitory) interneurons within the MnPO that finally inhibit the MPO warm-sensitive neurons. Warm-sensitive neurons are a heterogeneous population of inhibitory neurons; a subpopulation controls cutaneous vasomotion (CVC, Cutaneous Vasoconstriction) by modulating the activity of the rostral Raphe Pallidus (rRPa), which in turn modulates the activity of the intermediolateral column (IML). Efferent thermoregulatory signals about shivering and iBAT (interscapular brown adipose tissue) activity are delivered from the MPO to the Dorsomedial Hypothalamic nucleus (DMH), that in turn sends excitatory projections to the rRPa. In fact, rRPa contains premotoneurons that promote both iBAT activity and shivering.

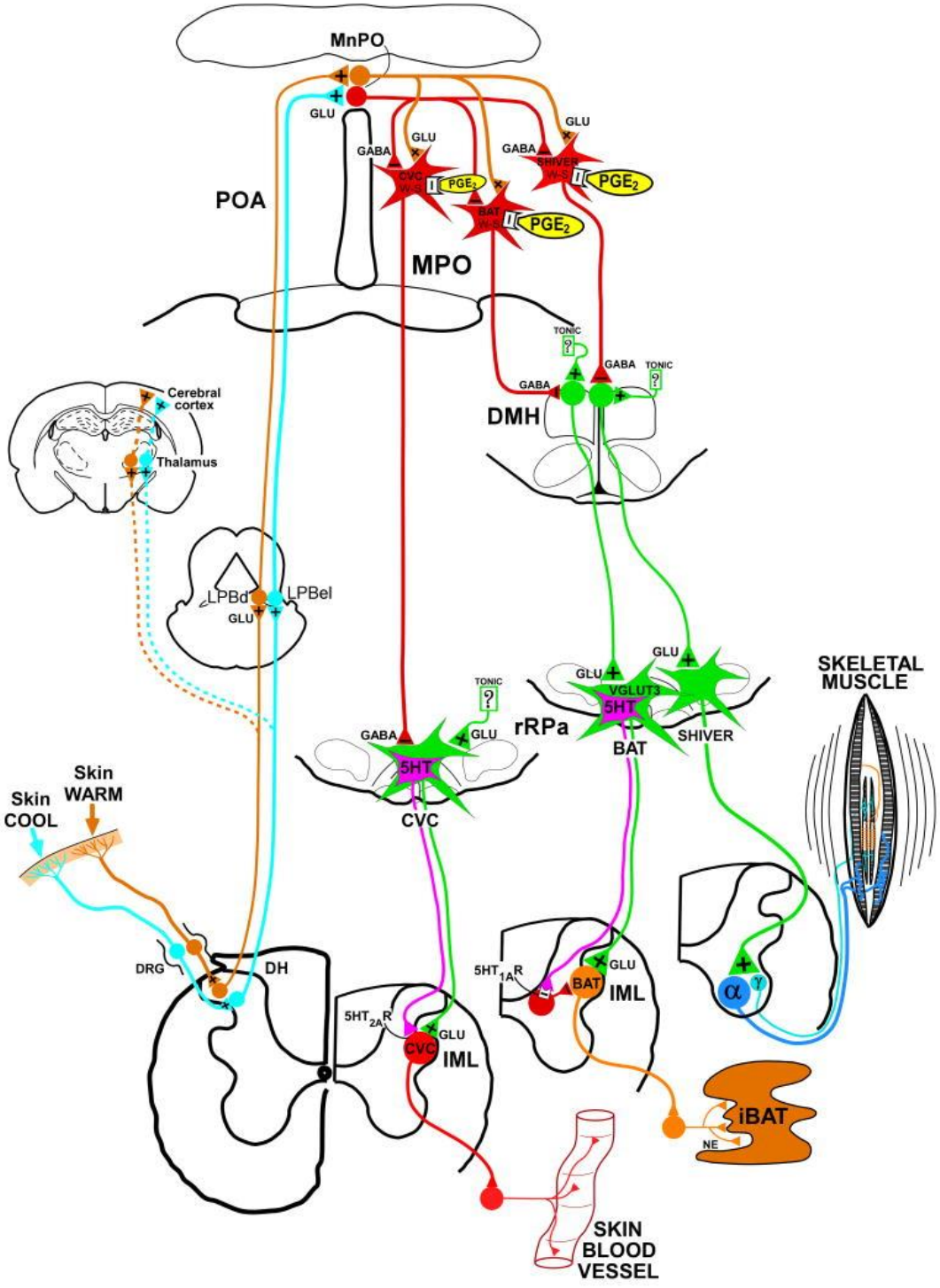

From: Morrison, S. F., & Nakamura, K. (2011). Frontiers in Bioscience (Landmark Edition), 16, 74–104.

Figure 2. Efferent pathways involved in thermoeffectors regulation.

The figure illustrates the efferent pathways involved in regulation of cutaneous vasomotion, non-shivering thermogenesis within the brown adipose tissue and shivering, in the rat. They all share a common modulatory region, the Raphe Pallidus (RPa), in the Rostral Ventromedial Medulla (RVMM), which regulates and controls the activity of thermogenic organs. DMH, Dorsomedial Hypothalamus; IML, Intermediolateral Column; PAG, Peraqueductal Gray; cPAG, Caudal PAG; rPAG, rostral PAG; PH, Posterior Hypothalamus; PVN, Paraventricular nucleus; RF, Reticular Formation; RPA, Raphe Pallidus; RRF, Retrorubral Field; VH, Ventral Horn; VMH, Ventromedial Hypothalamus; VTA, Ventral Tegmental Area.

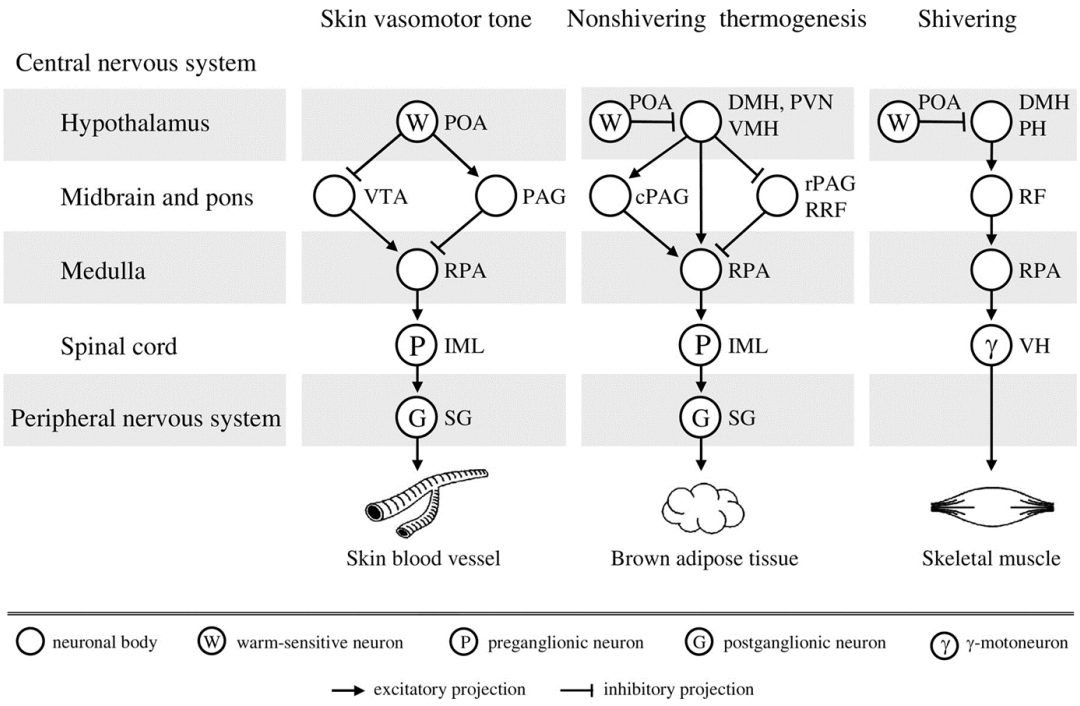

From: Romanovsky, A. A. (2006). AJP: Regulatory, Integrative and Comparative Physiology, 292(1), R37–R46.

Figure 3. Involvement of the Lateral Hypothalamus (LH) in the central circuits of hedonic control of food consumption.

The Lateral Hypothalamic Area (LHA) contains both inhibitory GABA-ergic and excitatory glutamatergic neurons. The GABA-ergic subpopulation inhibits the GABA-ergic neurons within the Ventral Tegmental Area (VTA), that when activated inhibit the shell of the Nucleus Accumbens (NAc). In the latter, neurons expressing D1 dopamine receptors are located that send inhibitory projections to the same GABA-ergic neurons within, to promote eating termination. Glutamatergic neurons within the LHA project to excitatory neurons of the Lateral Habenula (LHb), which stimulate GABA-ergic neurons of the VTA (the ones that inhibit dopaminergic neurons of the VTA). GABA-ergic neurons within the Bed Nucleus of Stria Terminalis (BNST) project mostly to glutamatergic LHA neurons.

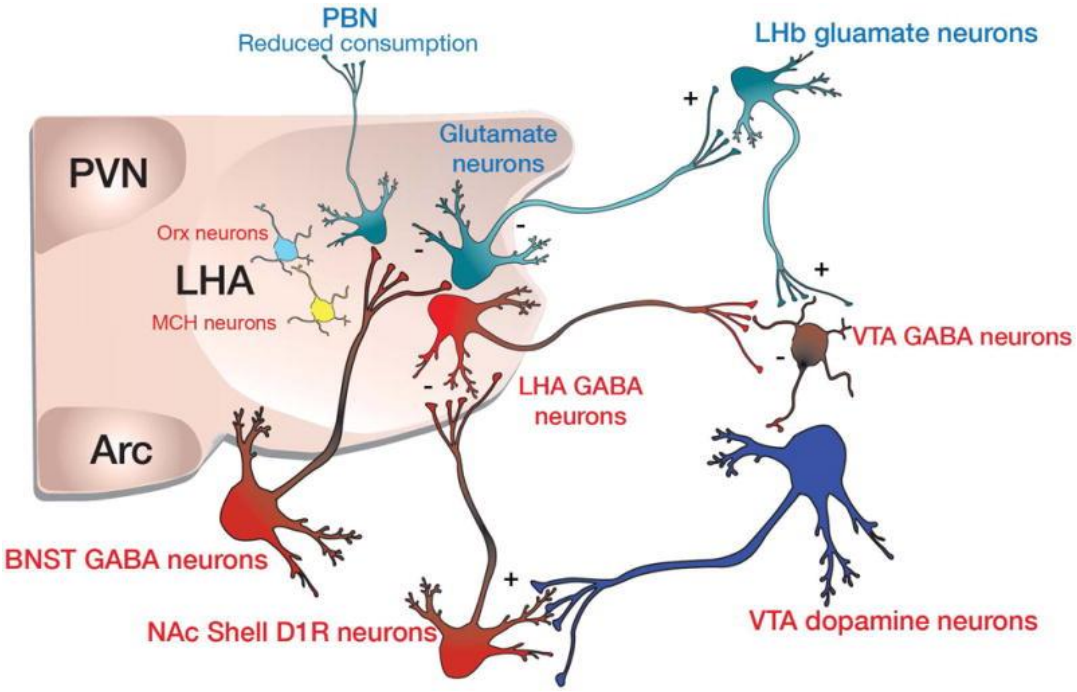

From: Stuber and Wise (2016). Nature Neuroscience, 19(2), 198–205.

Figure 4. Hypothalamic response to circulating leptin in the Arcuate nucleus.

Panel a. Schematization of the response evoked by circulating leptin on NPY/AGRP and POMC/CART neurons within the Arcuate nucleus (ARC) (NPY, neuropeptide Y; AGRP, agouti-related protein; POMC, proopiomelanocortin; CART, amphetamine-regulated transcript). Leptin inhibits NPY/AGRP I-order neurons (green) and stimulates POMC/CART neurons (red), which in turn project to the Paraventricular nucleus (PVN), and to II-order neurons involved in the regulation of energy expenditure and food consumption, located in the Lateral Hypothalamic Area (LHA) and in Perifornical Hypothalamic Area (PFA). NPY released in the PVN and LHA/PFA promotes eating, whilst α-MSH, released by POMC neurons in the PVN, promotes anorexia. *Panel b.* Region of the ARC marked with fluorescence in situ hybridization, showing mRNAs encoding for NPY (green) and POMC (red), near the third ventricle (3V).

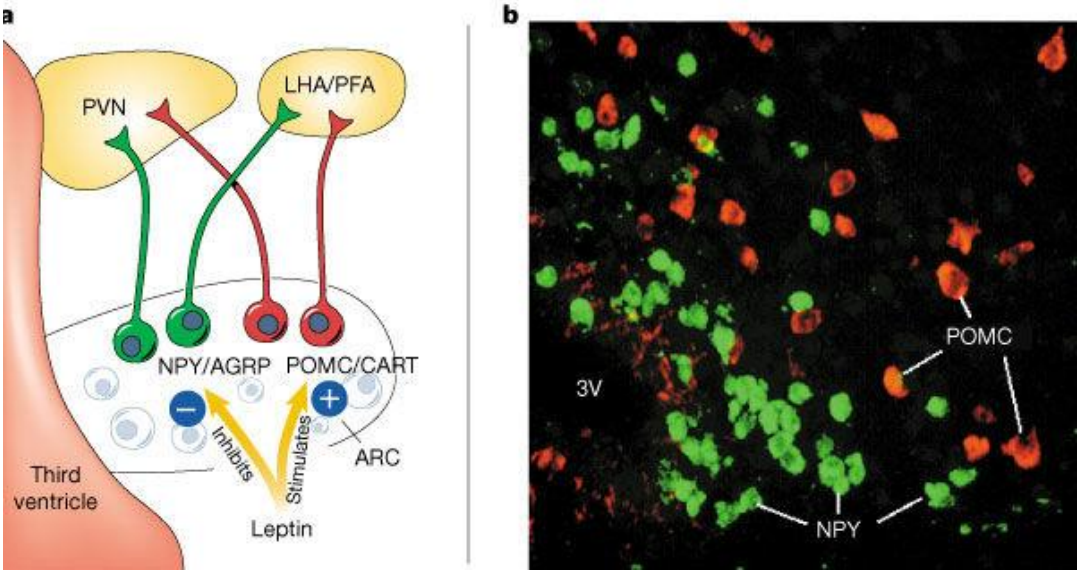

From: Schwartz et al. (2000). Nature, 404(6778), 661–671.

Figure 5. Metabolic rate (MR) and body temperature (Tb) during hibernating season in an Alpine marmot (Marmota marmota).

During entrance into hibernation, metabolic rate drops consistently, and body temperature decreases accordingly, leading to hypo-metabolism and hypothermia. Metabolic rate and body temperature recorded continuously throughout ten days show the progression of MR and Tb during entrance into hibernation (1), maintenance of hypo-metabolism and hypothermia during deep hibernation (2), increase of MR and Tb during rewarming (arousal) (3), regaining of constant high levels of metabolic rate and body temperature in the euthermic state (4).

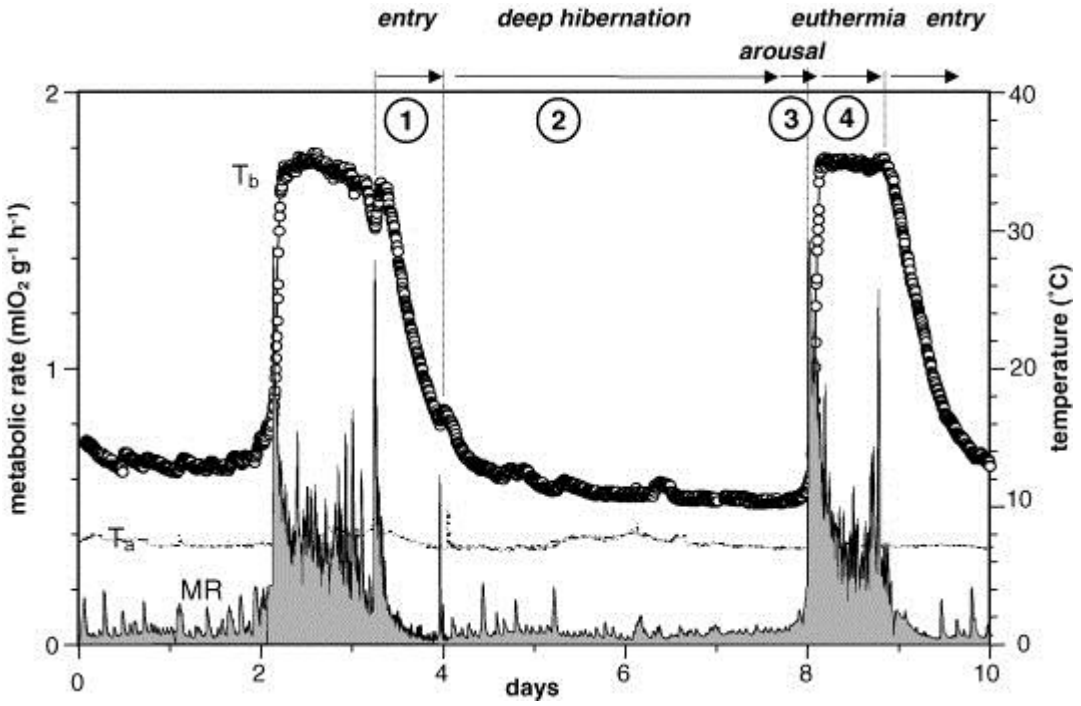

From: Heldmaier et al.(2004). Respiratory Physiology & Neurobiology, 141(3), 317–329.

Figure 6. Phylogenesis of hibernation.

The presence of hibernation (□) or daily torpor (△) in mammal orders in relation to their phylogenesys is shown. Orders are labelled when at least one species is known to enter torpor or hibernation. In marsupials, chiropterans and rodents several species are known to be able to enter one or both hypometabolic conditions. Since this feature is widespread across the animal kingdom (reported also in birds), hibernation and torpor likely rely on ancient genes in vertebrate physiology.

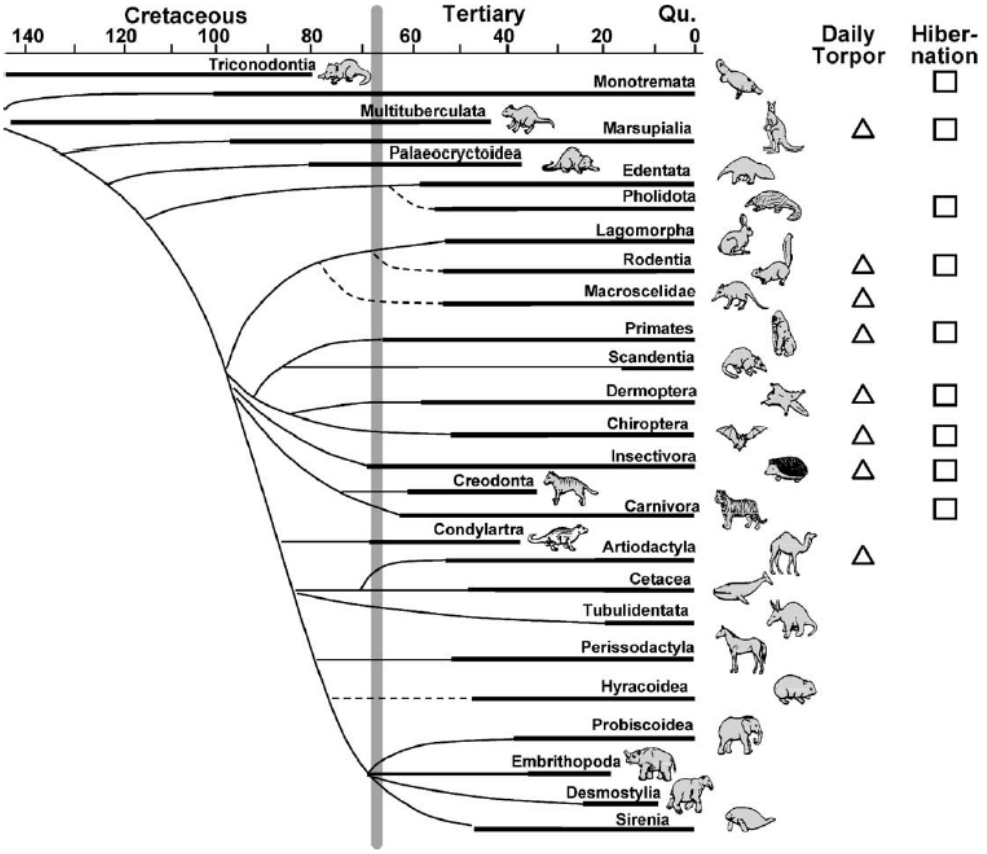

From: Heldmaier et al. (2004). Respiratory Physiology & Neurobiology, 141(3), 317–329.

Figure 7. Effects of central activation of adenosine A1 receptors (A1AR) in the rat.

Panel A. Single animal recording of physiological parameters (TBAT, brown adipose tissue temperature; TCORE, deep brain temperature; AP, arterial pressure; MAP, mean arterial pressure; HR, heart rate; EEG, electroencephalogram; L, Light; D, Dark) in three experimental conditions of 24 hours each: baseline, intracerebroventricular injection of N-6 Cyclohexyladenosine (CHA) (Inj), and intracerebroventricular injection of saline solution (Inj). Ambient temperature was kept at 25°C during the baseline day, whereas during treatment was lowered to 15°C and then increased to 28° at 6 h after the injection. *i–iv* representative fragments of recording of electromyogram (EMG) electrocardiogram (EKG), and arterial pressure (AP), which highlight the presence of bradycardic episodes associated with muscle contraction, during entrance, hypothermia, early and late recovery of euthermia. *Panel B.* 24-h time course of physiological parameters during baseline (light grey), intracerebroventricular injection of either CHA (black) or saline (SAL, dark grey). Red vertical bar shows the start of rewarming. *Panel C.* Normalized (to mean band amplitudes during the 24 h of the baseline day EEG) amplitudes of δ and θ EEG bands during the maximal effect of the intracerebroventricular CHA (1 hour), the same period is shown for the other days (SAL and baseline). The normalized root mean square amplitudes of the δ and θ bands after intracerebroventricular CHA were reduced compared to the baseline. All data are means ± SEM. *= $p < 0.05$.

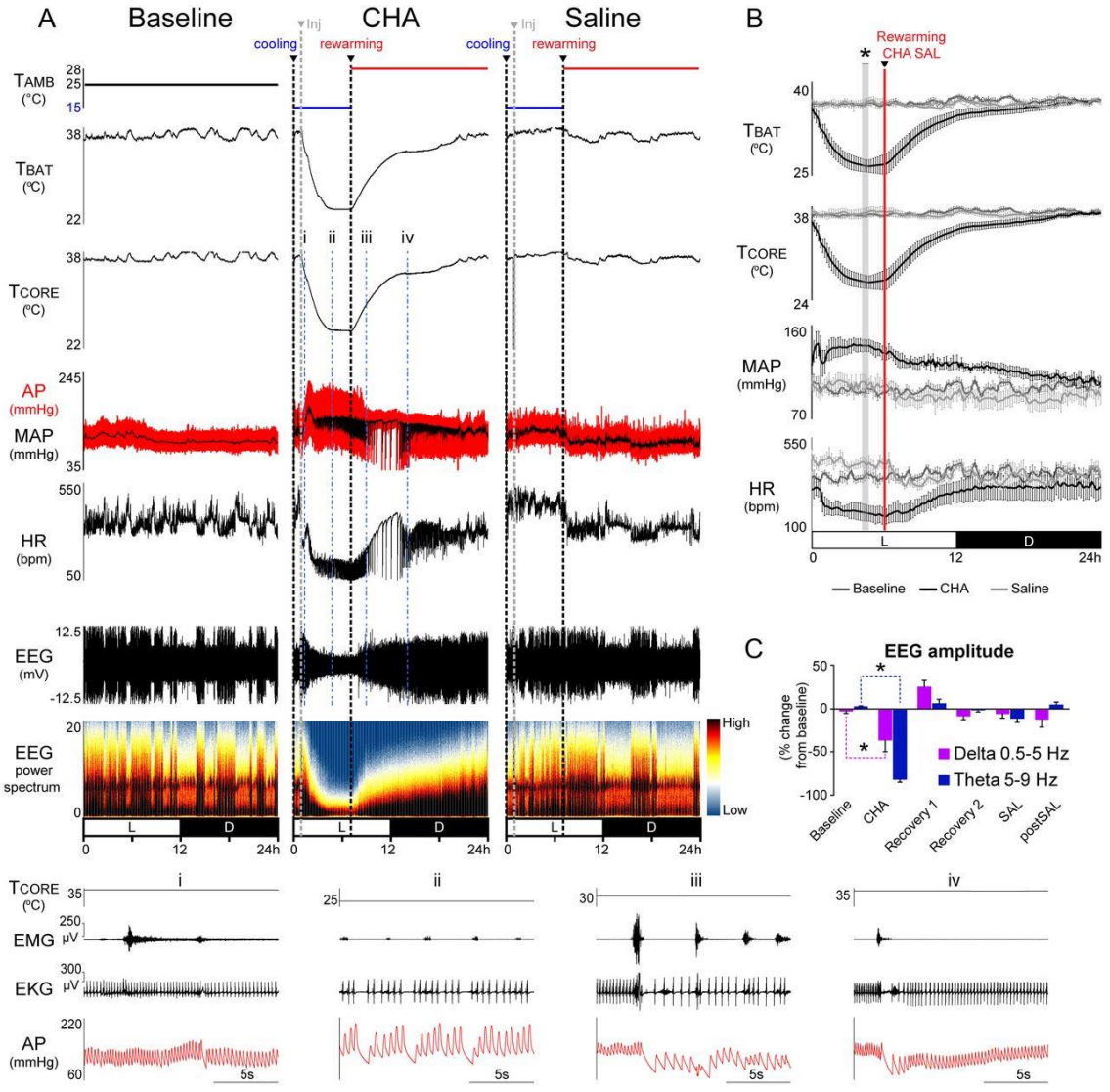

From: Tupone et al. (2013). Journal of Neuroscience, 33(36), 14512–14525.

Figure 8. Effects of the central inhibition of the Rostral Ventromedial Medulla (RVMM) in the rat.

Panel a. The inhibition of the RVMM neurons with multiple injections of a GABA-A agonist, muscimol (black arrows), causes consistent modifications in physiological parameters (HR, Heart Rate; AP, Arterial Pressure; Tbrain, deep brain temperature; Ta, ambient temperature; EEG, electroencephalogram). The inhibition of RVMM causes a reduction in Tbrain, HR and EEG, physiological values are regained after the return to normothermia. No significant changes are observed in AP. *Panel b.* Infrared images obtained by a thermal camera showing skin temperature and cutaneous vasomotion in the rat throughout the experiment: before the injection (B), after the first injection (C), and after the last injection (D).

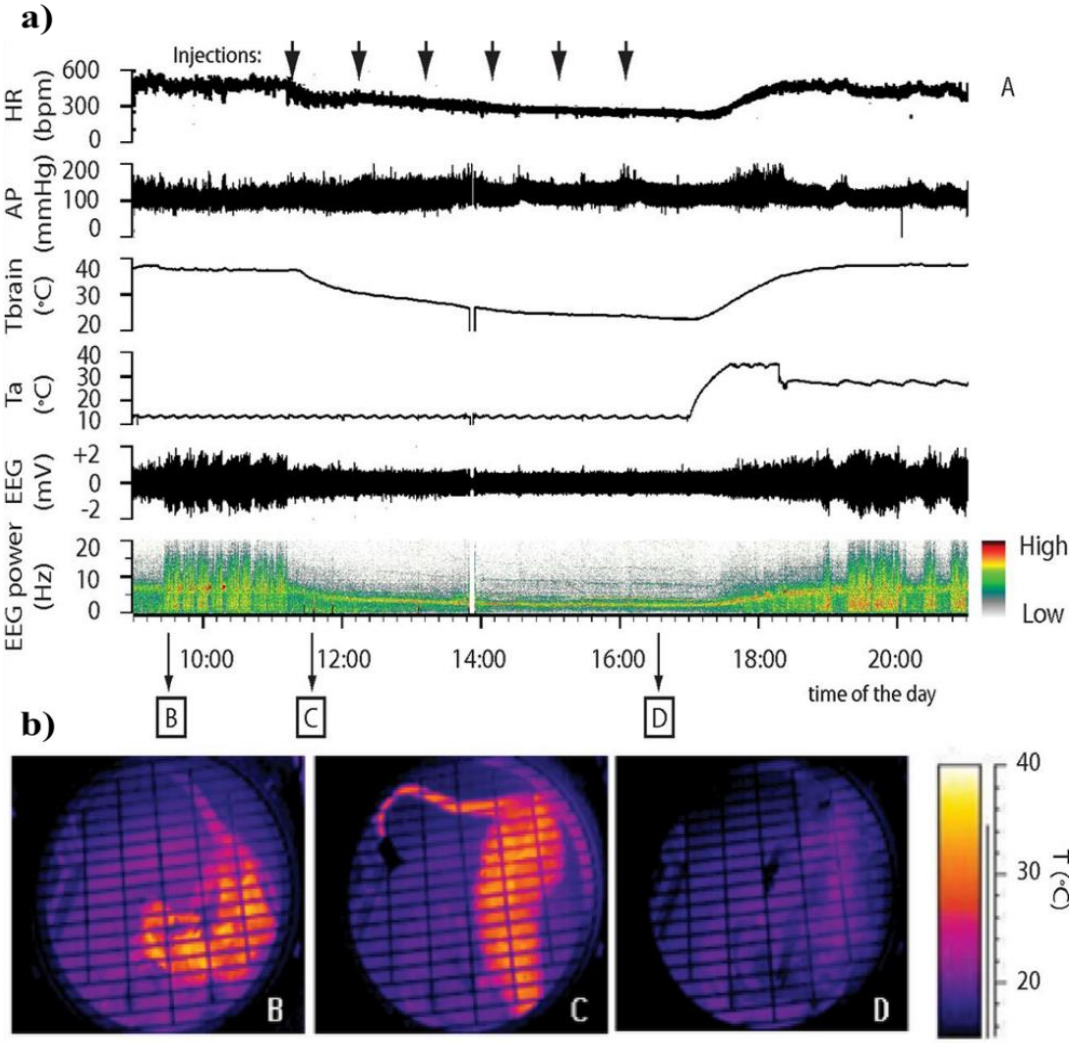

From: Cerri et al. (2013). Journal of Neuroscience, 33(7), 2984–2993

Figure 9. Experiment I: injection of the retrograde tracer Cholera Toxin b subunit (CTb) in the Raphe Pallidus in the mouse.

The upper figure is a representation of a mouse skull: the red dot on the interparietal bone is the superficial spot where the cannula was inserted during the surgery through a craniotomy. The coronal section underneath, obtained by "The Mouse Brain in Stereotaxic Coordinates" (Paxinos and Franklin, 2004) shows the target (Raphe Pallidus, red square) of the CTb injection, added with fluorescent microbeads to assess the correct placement of the tracer at the end of the experiment. *Panel a)* and *b)* show respectively an unsuccessful injection (located on the pyramidal tracts) and a successful one. Animals that did not display a correct injection site were excluded from the immunoistochemical detection of CTb+ neurons.

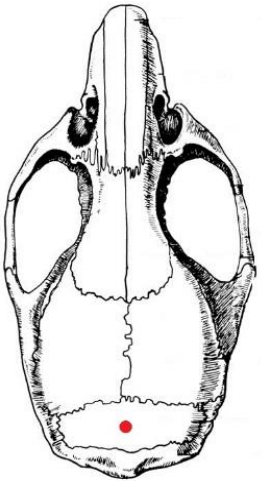

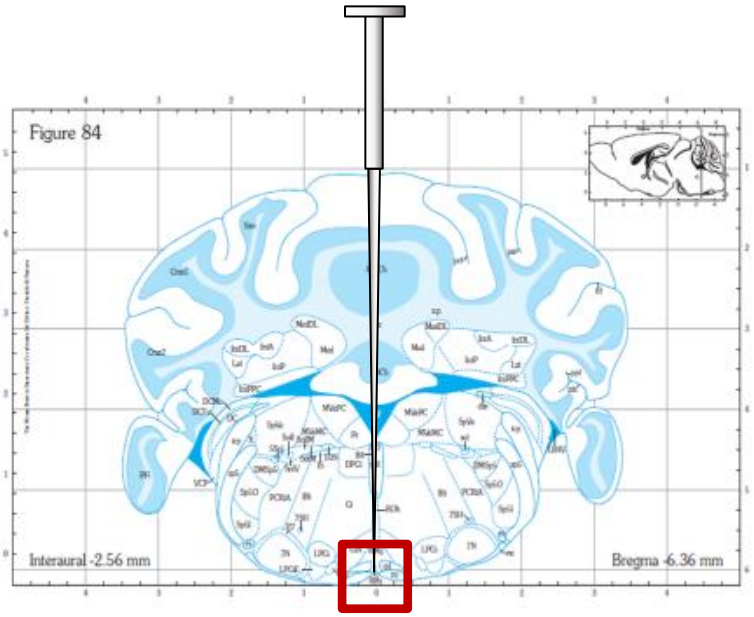
Figure 84
Interaural -2.56 mm
Bregma -6.36 mm

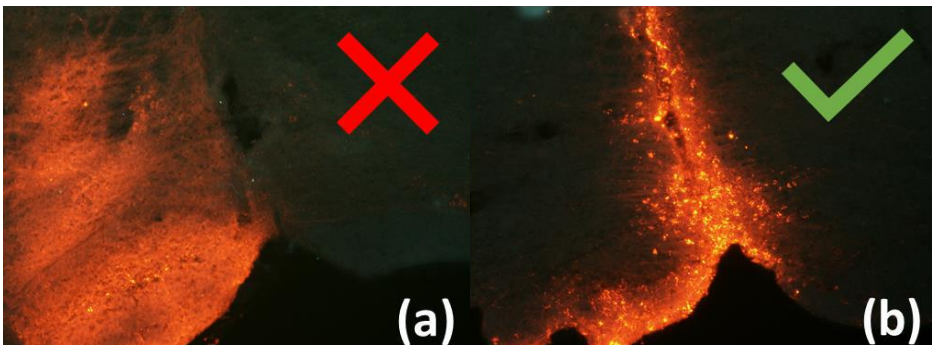
(a)
(b)

Figure 10. Experiment I: experimental protocol.

Schematization of the experimental protocol used in Experiment I. Upon their arrival, animals were kept in adaptation conditions (12h:12h Light-Dark (LD) Cycle, L: 9:00-21:00; ambient temperature (Ta) 24°C, food and water ad libitum) for one week. Animals were then moved to Torpor-inducing conditions for three weeks (12h:12h Light-Dark (LD) Cycle, L: 15:00-3:00; Ta 28°C, food and water ad libitum). At the end of the second week (Day 14), mice underwent surgery for the injection of the retrograde tracer CTb in the Raphe Pallidus. Animals were then randomly assigned to one of the experimental groups: Torpor group (n=4) was food deprived 36 hours prior to the experimental day. On the experimental day, at 9:00, animals were moved to a sub-thermoneutral temperature of 15°C leading to torpor onset around 10:30-11 am. Cold Control animals (n=5) were also moved to Ta 15°C but not food deprived, whereas Food Control mice (n=7) were food deprived but kept at Ta 28°C. At 13:00, all animals were perfused for subsequent immunohistochemistry analysis.

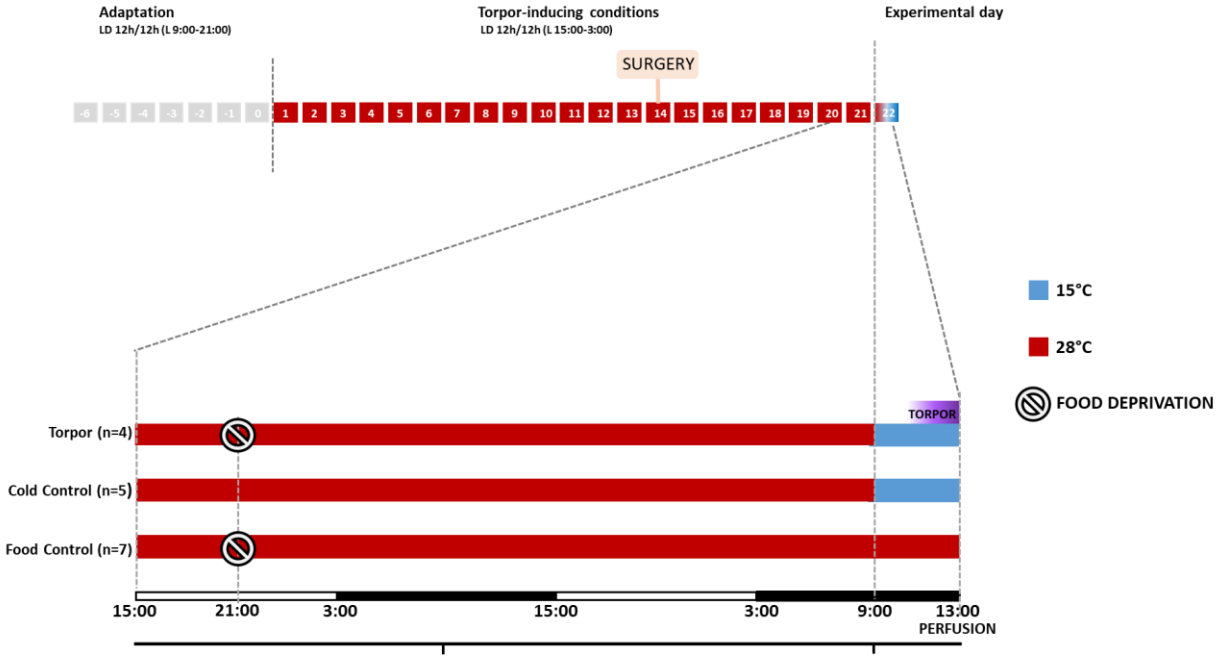
Adaptation
LD 12h/12h (L 9:00-21:00)
Torpor-inducing conditions
LD 12h/12h (L 15:00-3:00)
Experimental day
SURGERY
-6 -5 -4 -3 -2 -1 0 1 2 3 4 5 6 7 8 9 10 11 12 13 14 15 16 17 18 19 20 21 22
15°C
28°C
FOOD DEPRIVATION
TORPOR
Torpor (n=4)
Cold Control (n=5)
Food Control (n=7)
15:00 21:00 3:00 15:00 3:00 9:00 13:00
PERFUSION

Figure 11. Experiment I: infrared recording of cutaneous temperature (Tskin) in the mouse.

The upper figure is an example of the lower back cutaneous temperature recorded with a thermal camera positioned above the cage during the experimental day in two mice, one from the experimental group Torpor (red line), and one from the group Cold Control (blue line). At 09:00, the temperature was lowered to 15°C. While the Tskin remains pretty constant in Cold Control, the Torpor mouse starts to decrease around 10:30 and reaches the nadir at around 12:30.

Panels (a), (b) and *(c).* Screenshots of the infrared recording obtained by the thermal camera: the mouse from the Torpor group is in the upper part of the figure, Cold Control in the lower. (a) is at 09:00, (b) at 10:30, (c) 12:00.

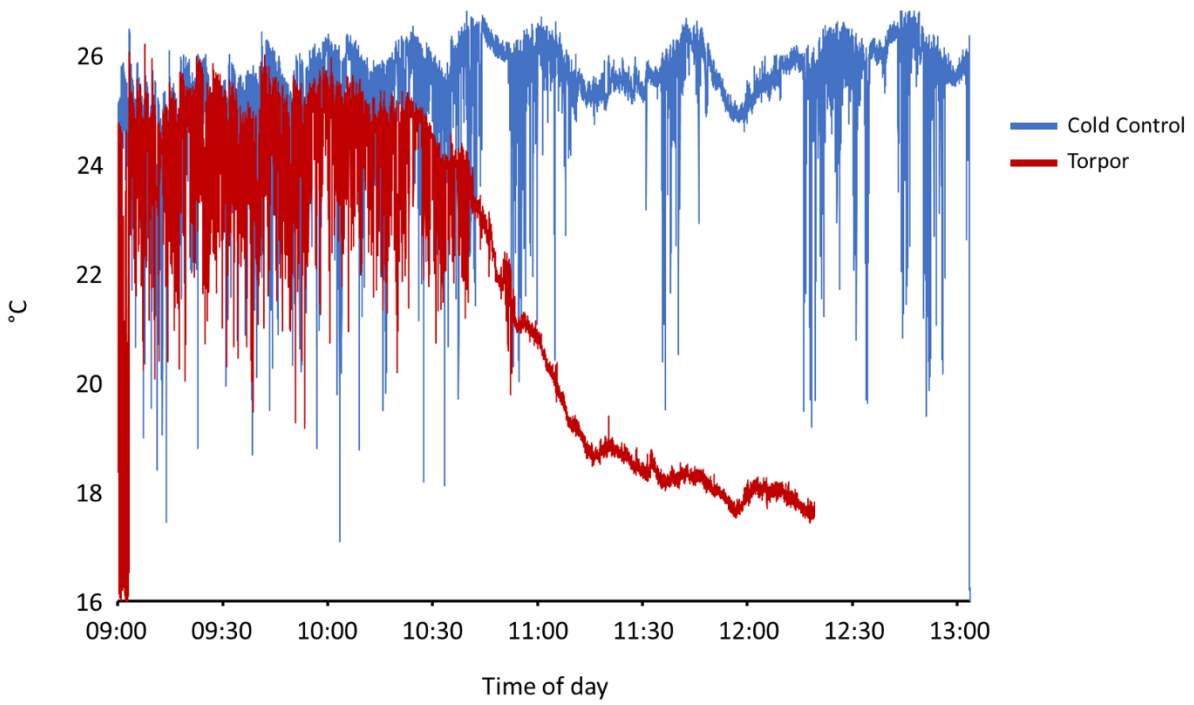
26
24
22
20
18
16
°C
09:00
09:30
10:00
10:30
11:00
11:30
12:00
12:30
13:00
Time of day
Cold Control
Torpor

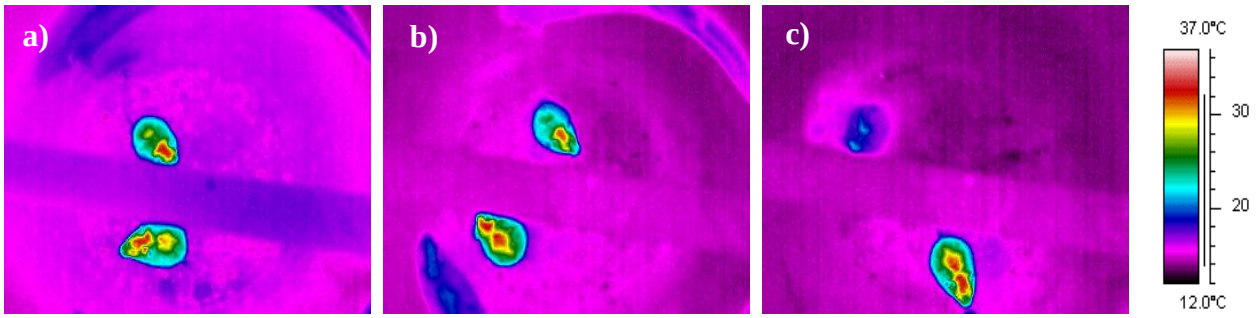
a)
b)
c)
37.0°C
30
20
12.0°C

Figure 12. Experiment II: surgical procedure for the chronic positioning of a microcannula in the Raphe Pallidus in the rat.

The upper figure is a representation of a rat skull: the green dot on the occipital bone is the superficial spot where the cannula was inserted during the surgery through a craniotomy, to deliver the GABA-A agonist muscimol. The four purple dots represent the sites of placement of the stainless steel screws to hold the resin, and the yellow dot indicates the placement of the hypothalamic thermistor. The coronal section underneath, obtained by "The Rat Brain in Stereotaxic Coordinates" (Paxinos and Watson, 2007), shows the target (Raphe Pallidus, red square) of the microcannula.

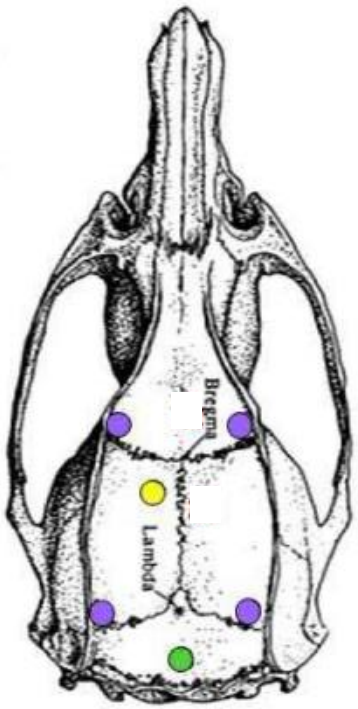
Bregma
Lambda

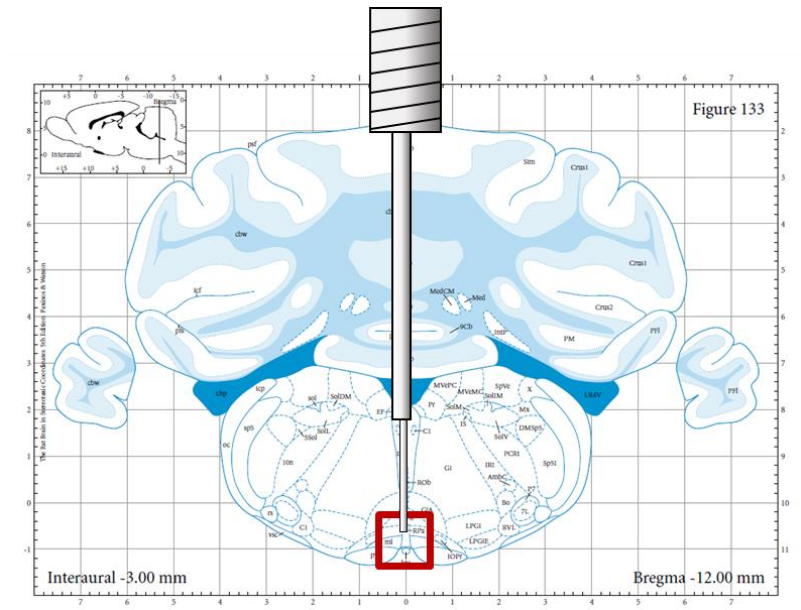
Figure 133
Interaural -3.00 mm
Bregma -12.00 mm

Figure 13. Experiment II: Surgical procedure for the chronic positioning an intracerebroventricular microcannula in the rat.

The upper figure is a representation of a rat skull: the orange dot on the right lateral parietal bone is the superficial spot where the cannula was inserted during the surgery through a craniotomy, to deliver N-6-Cyclohexyladenosine (CHA). The four purple dots represent the placement of the stainless steel screws to hold the resin, and the yellow dot indicates the placement of the hypothalamic thermistor. The coronal section underneath, obtained by "The Rat Brain in Stereotaxic Coordinates" (Paxinos and Watson, 2007), shows the target (right lateral ventricle, red square) of the microcannula.

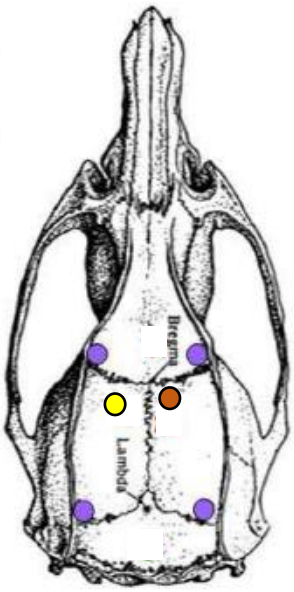
Bregma
Lambda

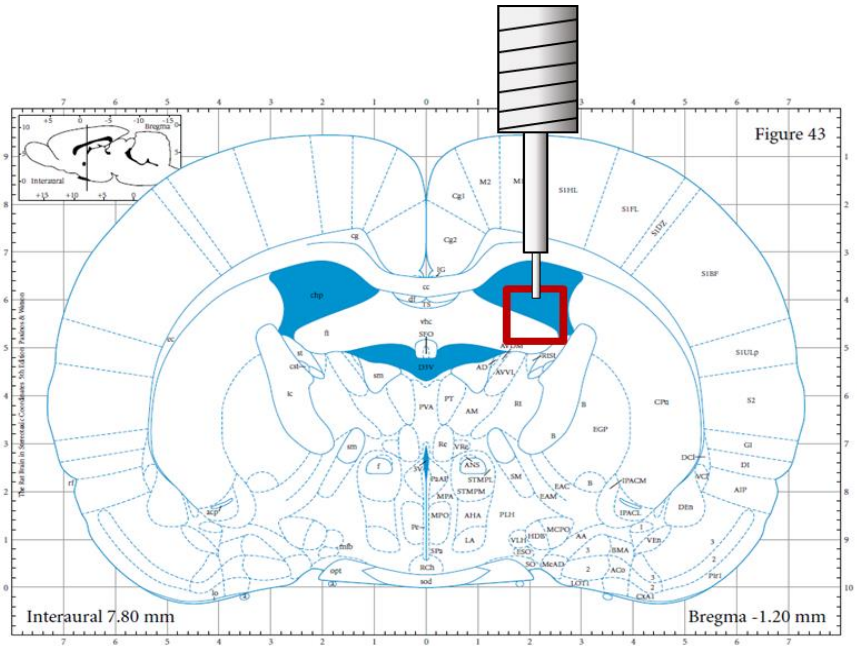
Figure 43
Interaural 7.80 mm
Bregma -1.20 mm

Figure 14. Experiment II: experimental protocol in mice.

Schematization of the experimental protocol used in Experiment II for mice. Upon their arrival, animals were kept in adaptation conditions (12h:12h Light-Dark (LD) Cycle, L: 9:00-21:00; ambient temperature (Ta) 24°C, food and water ad libitum) for one week. Animals were then moved to Torpor-inducing conditions for three weeks (12h:12h Light-Dark (LD) Cycle, L: 15:00-3:00; Ta 28°C, food and water ad libitum). Mice were then randomly assigned to one of the experimental groups: Mouse Torpor (n=8) group was food deprived 36 hours prior to the experimental day. On the experimental day, at 9:00, animals were moved to a sub-thermoneutral temperature of 15°C leading to torpor onset around 10:30-11 am. Mouse Control (n=8) animals were also moved to 15°C but were not food deprived. During the 13:30-15:00 time window, all animals were euthanized and organs were collected for mitochondrial analysis.

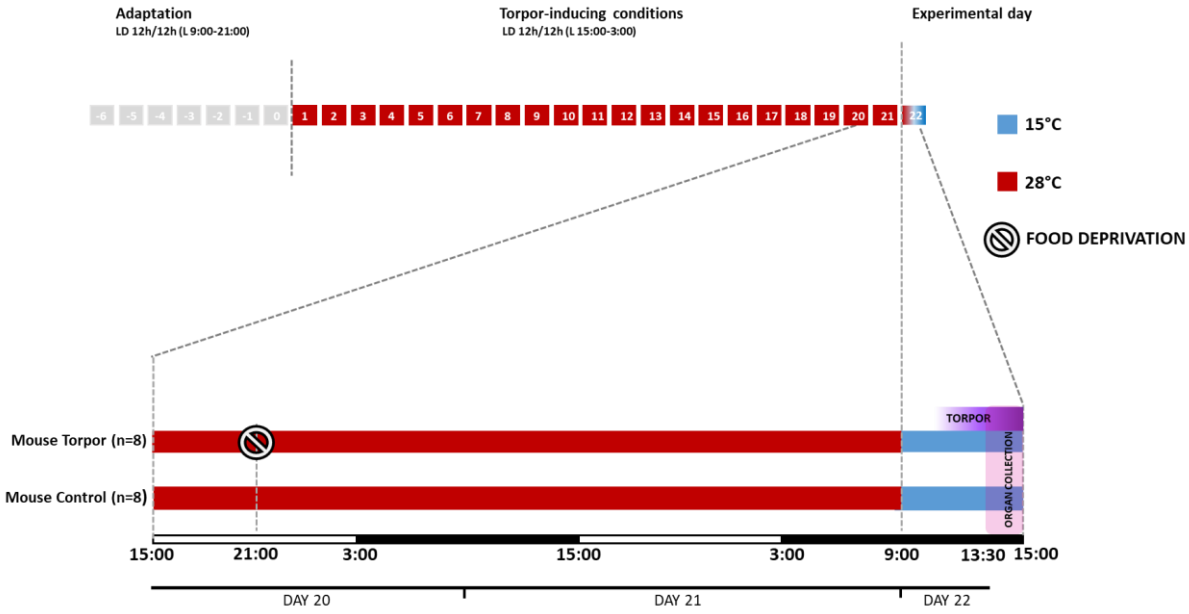
Adaptation
LD 12h/12h (L 9:00-21:00)
Torpor-inducing conditions
LD 12h/12h (L 15:00-3:00)
Experimental day
-6 -5 -4 -3 -2 -1 0 1 2 3 4 5 6 7 8 9 10 11 12 13 14 15 16 17 18 19 20 21 22
15°C
28°C
FOOD DEPRIVATION
Mouse Torpor (n=8)
Mouse Control (n=8)
TORPOR
ORGAN COLLECTION
15:00 21:00 3:00 15:00 3:00 9:00 13:30 15:00
DAY 20
DAY 21
DAY 22

Figure 15. Experiment II: experimental protocol in Rat-RPa-MUS

Schematization of the experimental protocol used for rats injected with the GABA-A agonist muscimol in Experiment II. Upon their arrival, animals were kept in adaptation conditions (12h:12h Light-Dark (LD) Cycle, L: 9:00-21:00; ambient temperature (Ta) 24°C, food and water ad libitum). On day 1, animals were surgically implanted with a microcannula within the Raphe Pallidus, and a hypothalamic thermistor. After a one-week recovery, rats were randomly assigned to one of the experimental groups: Rat RPa MUS (n=4) group underwent five (1/h) microinjections (100nl) of muscimol 1mM, whereas Rat RPa ACSF (n=5) where injected with artificial cerebrospinal fluid (ACSF, 100nl, 1/h), starting from 09:00. At the end of the experiment, during the 13:30-15:00 time window, all animals were euthanized and organs were collected for mitochondrial analysis.

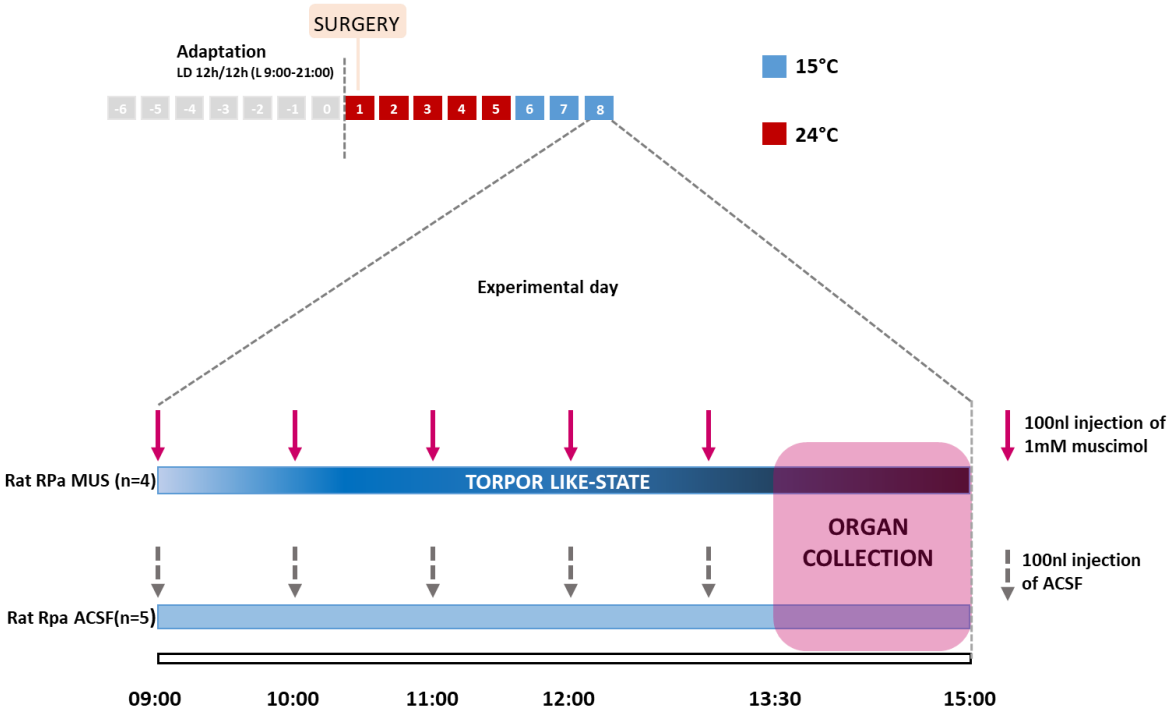
SURGERY
Adaptation
LD 12h/12h (L 9:00-21:00)
-6
-5
-4
-3
-2
-1
0
1
2
3
4
5
6
7
8
15°C
24°C
Experimental day
100nl injection of
1mM muscimol
Rat RPa MUS (n=4)
TORPOR LIKE-STATE
ORGAN
COLLECTION
100nl injection
of ACSF
Rat Rpa ACSF(n=5)
09:00
10:00
11:00
12:00
13:30
15:00

Figure 16. Experiment II: experimental protocol in Rat-ICV-CHA

Schematization of the experimental protocol used for rats injected with the A1 adenosine receptor agonist N-6-cyclohexyladenosine (CHA) in Experiment II. Upon their arrival, animals were kept in adaptation conditions (12h:12h Light-Dark (LD) Cycle, L: 9:00-21:00; ambient temperature (Ta) 24°C, food and water ad libitum). On day 1, animals were surgically implanted with an intracerebroventricular microcannula, and a hypothalamic thermistor. After a one-week recovery, rats were randomly assigned to one of the experimental groups: Rat ICV CHA (n=3) group underwent an intracerebroventricular microinjection (5µl) of CHA 1mM, whereas Rat ICV ACSF (n=3) where injected with artificial cerebrospinal fluid (ACSF, 5µl), AT 09:00. At the end of the experiment, during the 13:30-15:00 time window, all animals were euthanized and organs were collected for mitochondrial analysis.

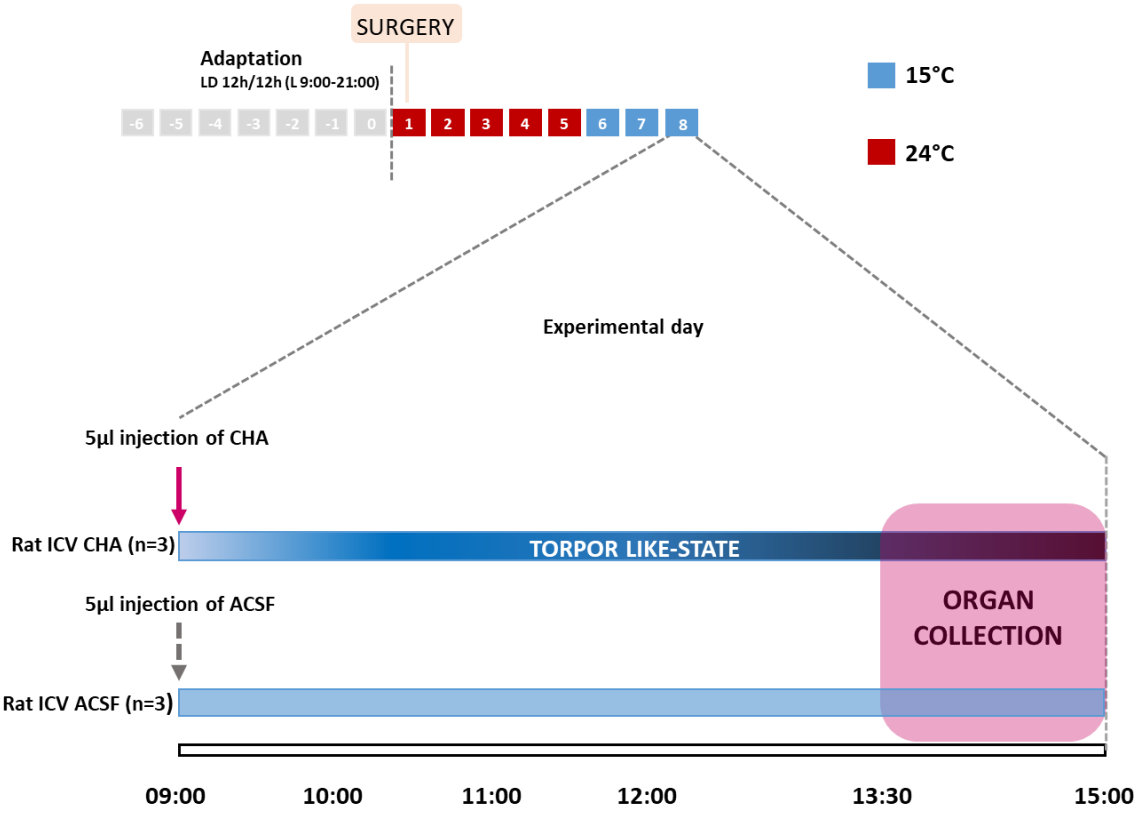
SURGERY
Adaptation
LD 12h/12h (L 9:00-21:00)
-6
-5
-4
-3
-2
-1
0
1
2
3
4
5
6
7
8
15°C
24°C
Experimental day
5µl injection of CHA
Rat ICV CHA (n=3)
TORPOR LIKE-STATE
ORGAN COLLECTION
5µl injection of ACSF
Rat ICV ACSF (n=3)
09:00
10:00
11:00
12:00
13:30
15:00

Figure 17. Experiment II: Set up for microinjections in the free-behaving rat.

Schematic representation of the experimental set-up for microinjections in the free-behaving rat. Animals are positioned in a sound-attenuated thermoregulated experimental box. A microinjection pump located outside the chamber holds the syringe filled with the drug, connected with a 1-m Teflon tube, with a constant diameter (0.2 mm). After cannulating the animal, the operator closed the box and started the microinjection procedure, evaluating the correct drug delivery by observing the oil-liquid interface (pushing the drug) moving under the microscope. This system permits to perform microinjections without disturbing the rat, as explained in more detail in the Material and Methods section.

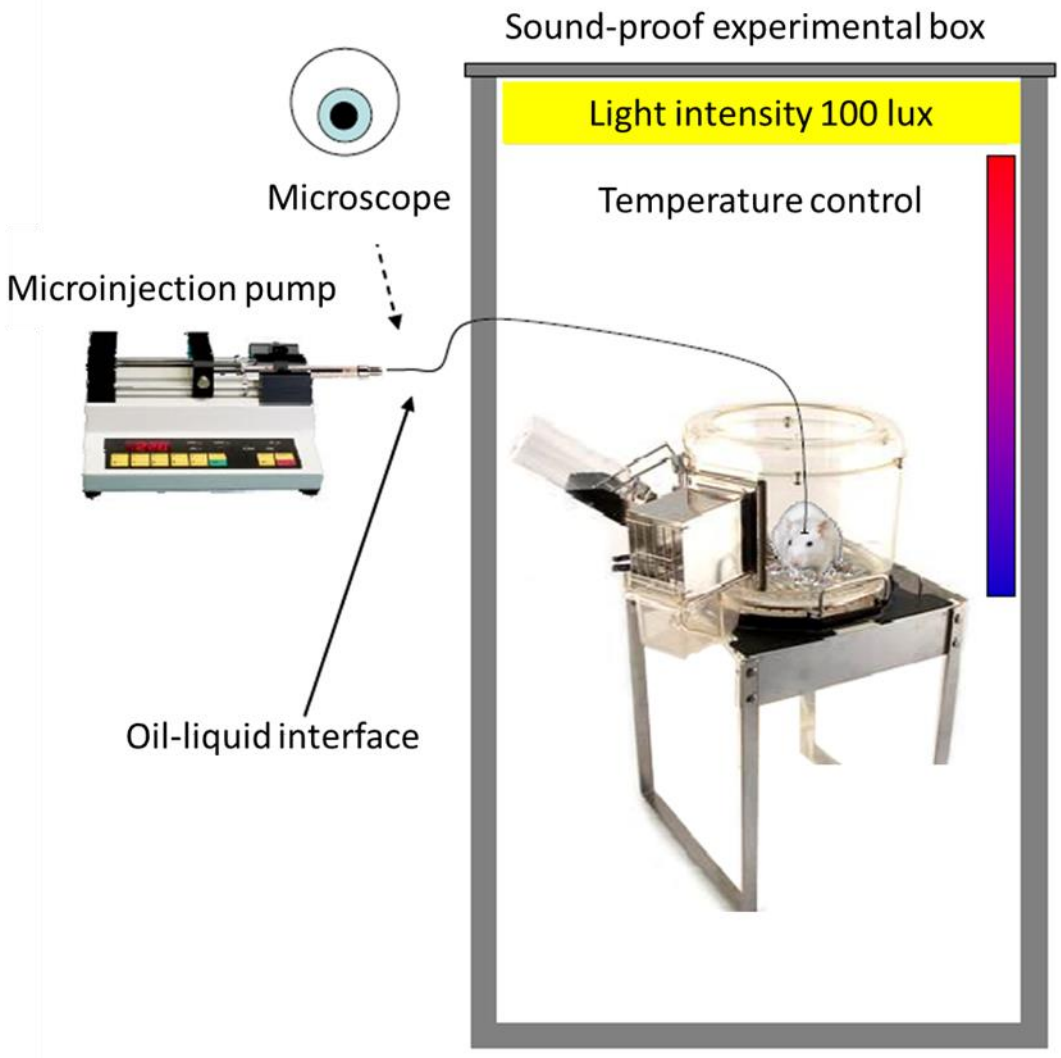
Sound-proof experimental box
Light intensity 100 lux
Temperature control
Microscope
Microinjection pump
Oil-liquid interface

Figure 18. Experiment II: in vitro measurement of mitochondrial oxygen consumption.

When a 10 mM glutamate/malate substrate is added to tissue mitochondrial homogenate, mitochondria respires at a relatively high rate; this condition goes under the name of State 2 respiration. If adenosine diphosphate (ADP) is added to the solution, oxygen is consumed at a higher rate and coupled to phosphorylation of ADP to adenosine triphosphate (ATP), which is driven by the energy obtained from the electron transfer chain; this state of fully coupled respiration is called State 3 phosphorylation. When ADP is exhausted (because all ADP has been phosphorylated to ATP), mitochondria continue respiration at a much lower rate, the so-called State 4 respiration ("resting state"). Energy obtained by the electron transport chain is no more coupled to oxidative phosphorylation (since ADP is absent), thus respiration becomes uncoupled.

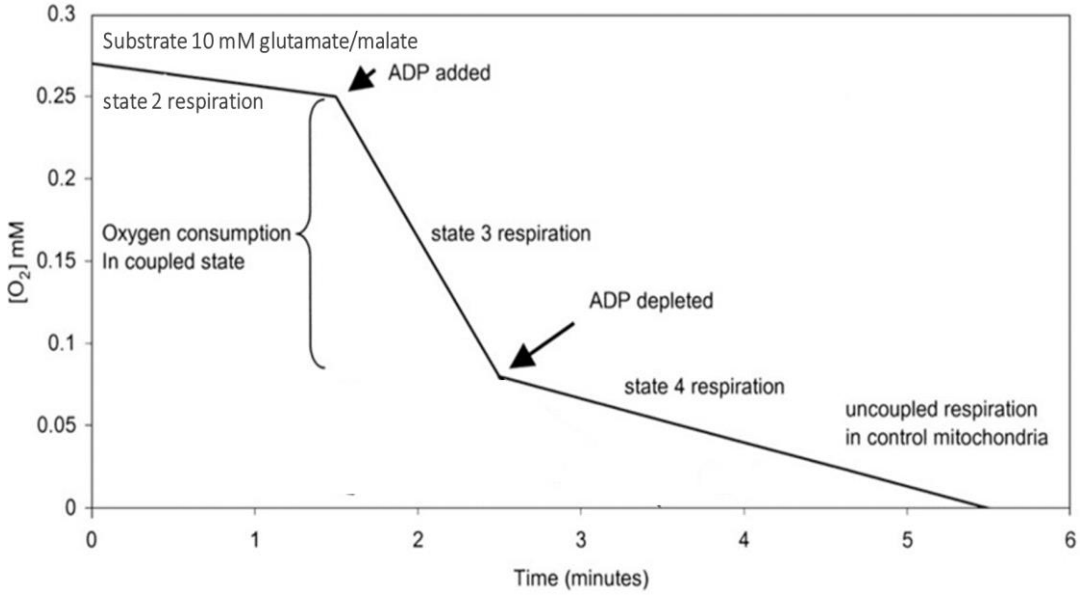

Modified from: Hesselink et al. (2003).Obesity Research, 11(12), 1429–1443.

Figure 19. Experiment III: surgical procedures in swine.

Some pictures from surgery procedures used in Experiment III are shown. Piglets underwent surgery under general anaesthesia, to implant a cannula within the Raphe Pallidus, with the help of a neuronavigator (middle left). During surgery, either a GABA-A agonist (muscimol) or antagonist (GABAzine), were administered in the Raphe Pallidus, and vital parameters were monitored.

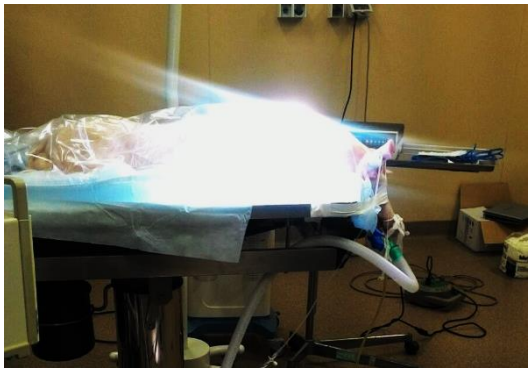

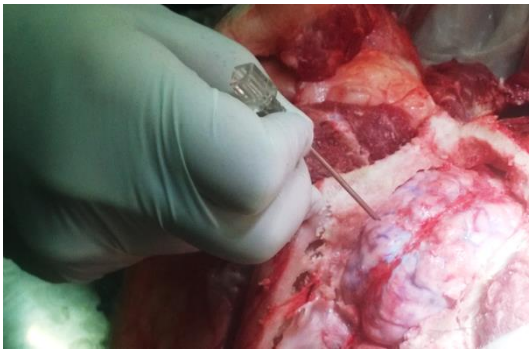

Figure 20. Experiment I: time course of cutaneous temperature during the experimental day in mice

Cutaneous temperature was monitored during the experimental day with a thermal camera placed above the cage. The graph shows the mean value ±SEM of cutaneous temperature recorded every 10 minutes on the cutaneous surface of the lower back in all three experimental groups. Cutaneous temperature was rather stable around 32-34°C in the Food Control mice (pink), which were exposed to Ta 28°C. Cutaneous temperature was significantly lower (not shown in the graph) in the two groups exposed to Ta 15°C. In particular, in cold-exposed groups, it shows significantly lower levels in Torpor group (purple) in comparison with Cold Control group (light blue) (*=$p<0.05$, **=$p<0.01$).

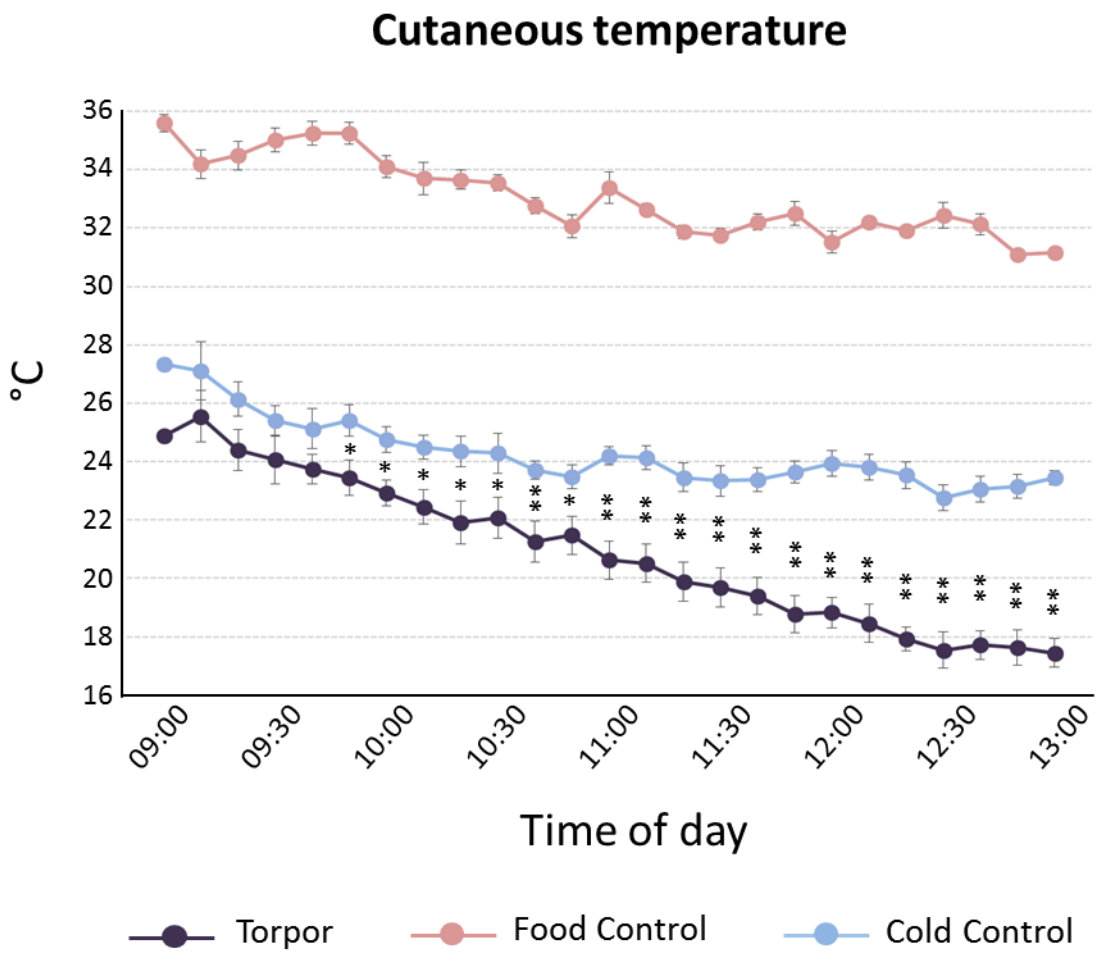
Cutaneous temperature
°C
36
34
32
30
28
26
24
22
20
18
16
09:00
09:30
10:00
10:30
11:00
11:30
12:00
12:30
13:00
Time of day
Torpor
Food Control
Cold Control

Figure 21. Experiment I: immunoistochemical study of the Lateral Parabrachial nucleus (LPB).

The right panel shows the atlas positioning in a coronal section of the LPB, obtained from "The Mouse Brain in Stereotaxic Coordinates" (Paxinos and Franklin, 2004). Images obtained from a fluorescence microscope can be observed on the left. A sample of the immunoistochemical staining of the LPB is shown for an animal from the Torpor group (first column, from left), the Cold Control group (second column), and the Food Control group (third column). For each column, in the first row, positive c-Fos neurons are shown (green), while the second row displays positive immunoreaction for tracer CTb (yellow), and the third row is a merge of the upper two, to highlight double-stained neurons (c-Fos+/CTb+)

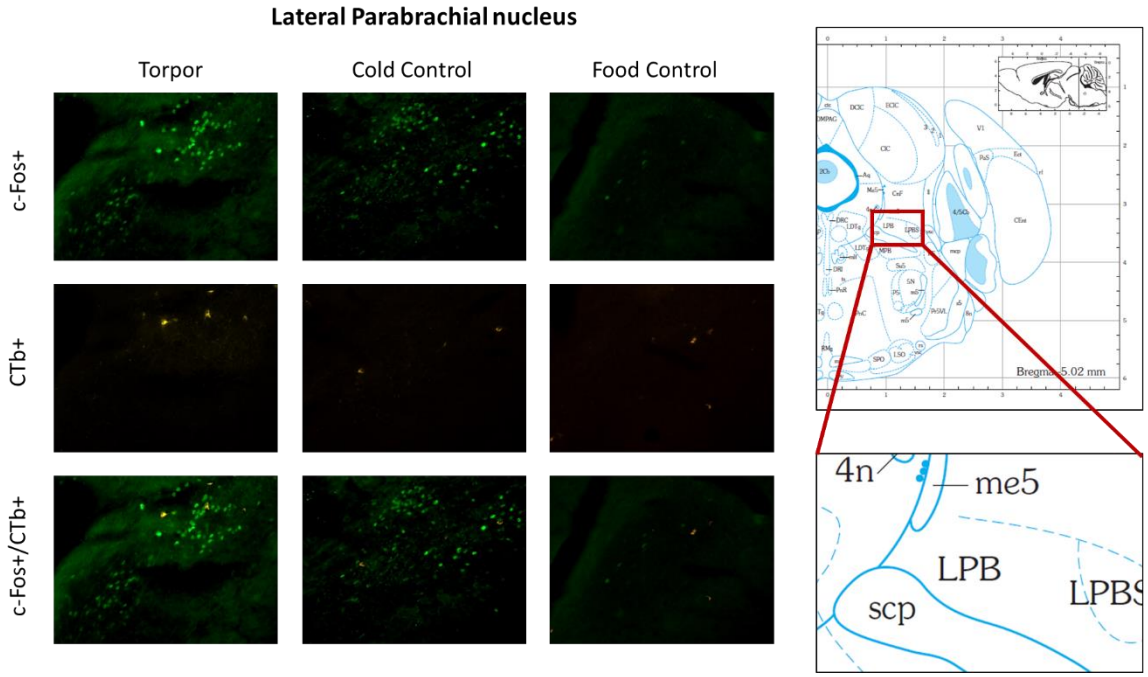
Lateral Parabrachial nucleus
Torpor
Cold Control
Food Control
c-Fos+
CTb+
c-Fos+/CTb+
Bregma -5.02 mm
4n
me5
LPB
scp
LPBS

Figure 22. Experiment I: immunoistochemical study of the Ventrolateral Periaqueductal Gray (VLPAG).

The right panel shows the atlas positioning in a coronal section of the VLPAG, obtained from "The Mouse Brain in Stereotaxic Coordinates" (Paxinos and Franklin, 2004). Images obtained from a fluorescence microscope can be observed on the left. A sample of the immunoistochemical staining of the VLPAG is shown for an animal from the Torpor group (first column, from left), the Cold Control group (second column), and the Food Control group (third column). For each column, in the first row, positive c-Fos neurons are shown (green), while the second row displays positive immunoreaction for tracer CTb (yellow), and the third row is a merge of the upper two, to highlight double-stained neurons (c-Fos+/CTb+).

Ventrolateral Peraqueductal Gray

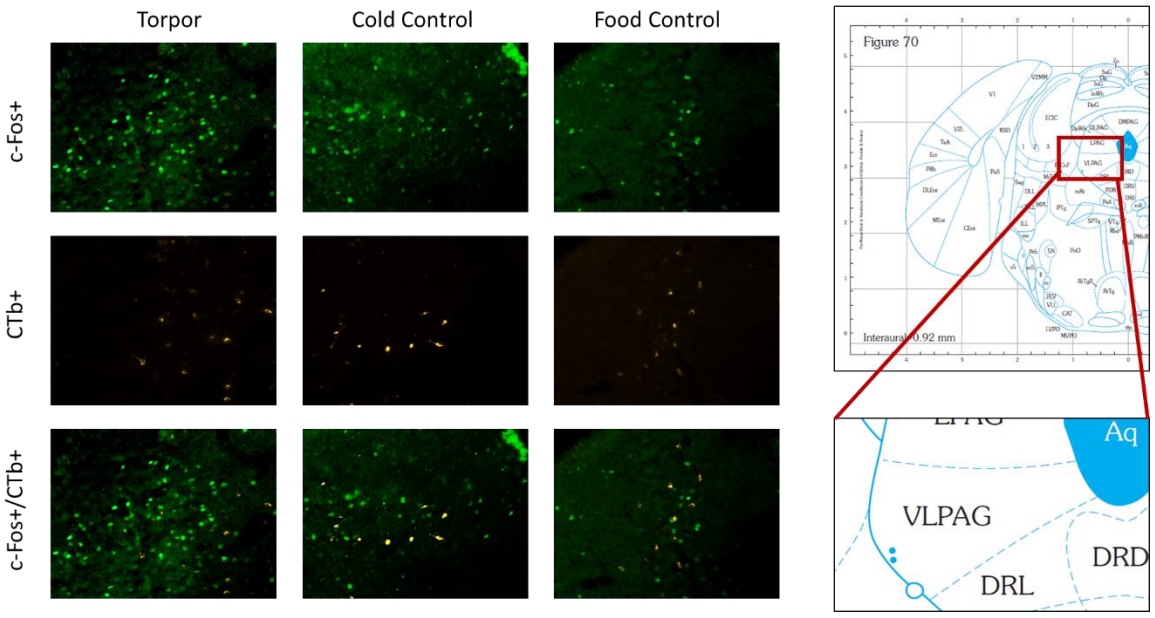

Figure 23. Experiment I: immunoistochemical study of the Dorsomedial Hypothalamic nucleus (DMH).

The right panel shows the atlas positioning in a coronal section of the DMH, obtained from "The Mouse Brain in Stereotaxic Coordinates" (Paxinos and Franklin, 2004). Images obtained from a fluorescence microscope can be observed on the left. A sample of the immunoistochemical staining of the DMH is shown for an animal from the Torpor group (first column, from left), the Cold Control group (second column), and the Food Control group (third column). For each column, in the first row, positive c-Fos neurons are shown (green), while the second row displays positive immunoreaction for tracer CTb (yellow), and the third row is a merge of the upper two, to highlight double-stained neurons (c-Fos+/CTb+).

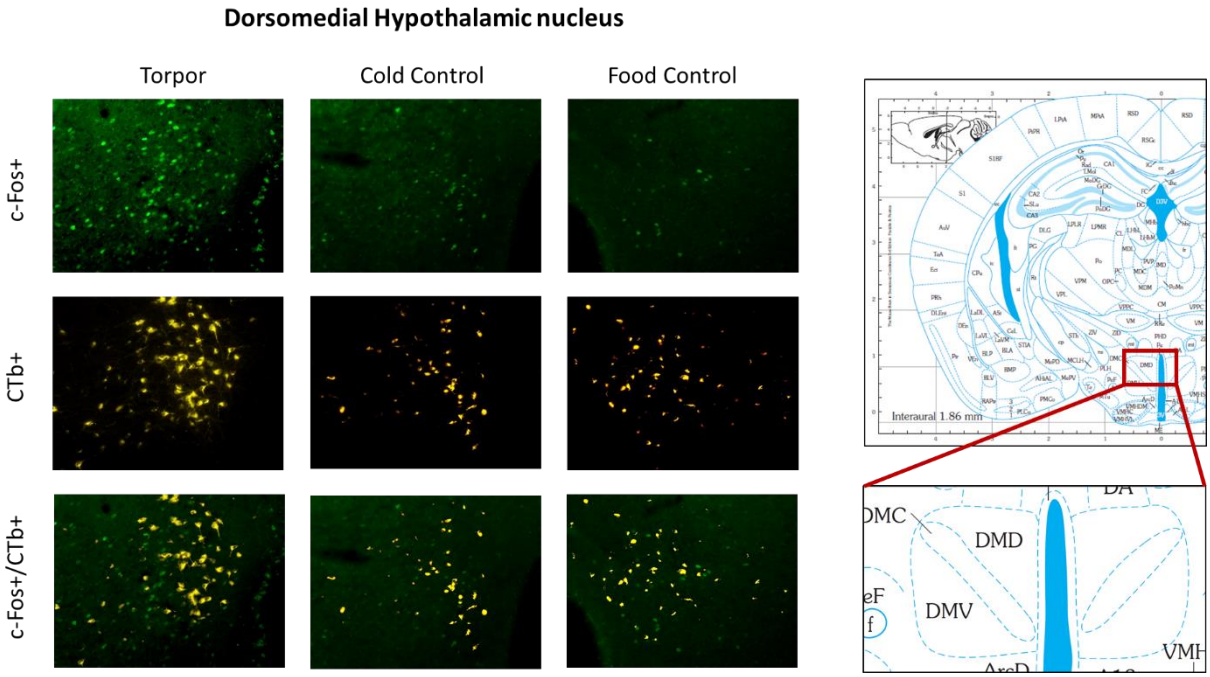
Dorsomedial Hypothalamic nucleus
Torpor
Cold Control
Food Control
c-Fos+
CTb+
c-Fos+/CTb+
Interaural 1.86 mm
DMC
DMD
DMV
VMH

Figure 24. Experiment I: immunoistochemical study of the Arcuate nucleus (ARC).

The right panel shows the atlas positioning in a coronal section of the ARC, obtained from "The Mouse Brain in Stereotaxic Coordinates" (Paxinos and Franklin, 2004). Images obtained from a fluorescence microscope can be observed on the left. A sample of the immunoistochemical staining of the ARC is shown for an animal from the Torpor group (first column, from left), the Cold Control group (second column), and the Food Control group (third column). For each column, in the first row, positive c-Fos neurons are shown (green), while the second row displays positive immunoreaction for tracer CTb (yellow), and the third row is a merge of the upper two, to highlight double-stained neurons (c-Fos+/CTb+).

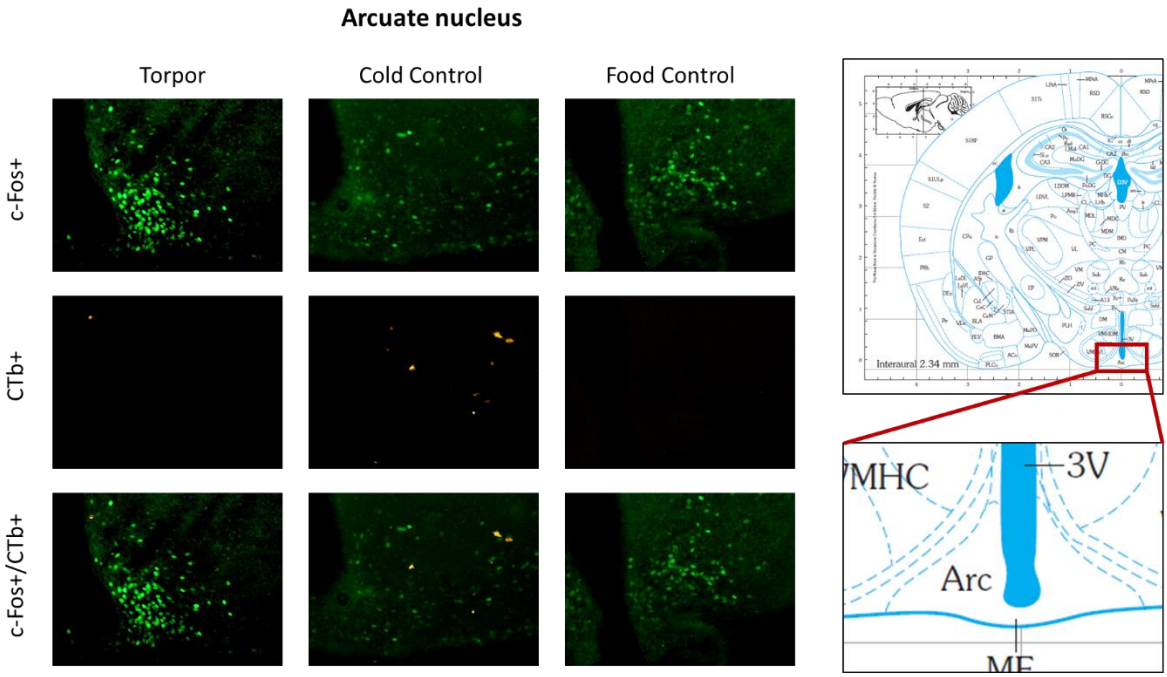
Arcuate nucleus
Torpor
Cold Control
Food Control
c-Fos+
CTb+
c-Fos+/CTb+
Interaural 2.34 mm
3V
Arc
ME

Figure 25. Experiment I: immunoistochemical study of the Lateral Hypothalamus (LH).

The right panel shows the atlas positioning in a coronal section of the LH, obtained from "The Mouse Brain in Stereotaxic Coordinates" (Paxinos and Franklin, 2004). Images obtained from a fluorescence microscope can be observed on the left. A sample of the immunoistochemical staining of the LH is shown for an animal from the Torpor group (first column, from left), the Cold Control group (second column), and the Food Control group (third column). For each column, in the first row, positive c-Fos neurons are shown (green), while the second row displays positive immunoreaction for tracer CTb (yellow), and the third row is a merge of the upper two, to highlight double-stained neurons (c-Fos+/CTb+).

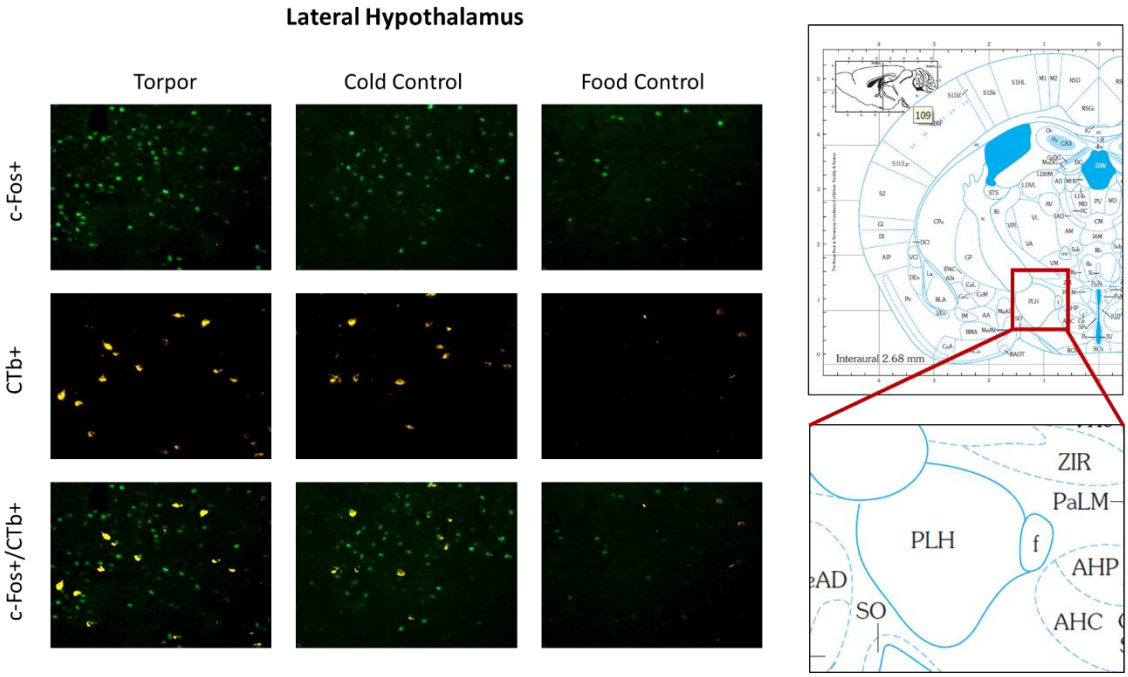
Lateral Hypothalamus
Torpor
Cold Control
Food Control
c-Fos+
CTb+
c-Fos+/CTb+
Interaural 2.68 mm
ZIR
PaLM
PLH
f
AHP
AHC
SO

Figure 26. Experiment I: immunoistochemical study of the Paraventricular Hypothalamic nucleus (PVH).

The right panel shows the atlas positioning in a coronal section of the PVH, obtained from "The Mouse Brain in Stereotaxic Coordinates" (Paxinos and Franklin, 2004). Images obtained from a fluorescence microscope can be observed on the left. A sample of the immunoistochemical staining of the PVH is shown for an animal from the Torpor group (first column, from left), the Cold Control group (second column), and the Food Control group (third column). For each column, in the first row, positive c-Fos neurons are shown (green), while the second row displays positive immunoreaction for tracer CTb (yellow), and the third row is a merge of the upper two, to highlight double-stained neurons (c-Fos+/CTb+).

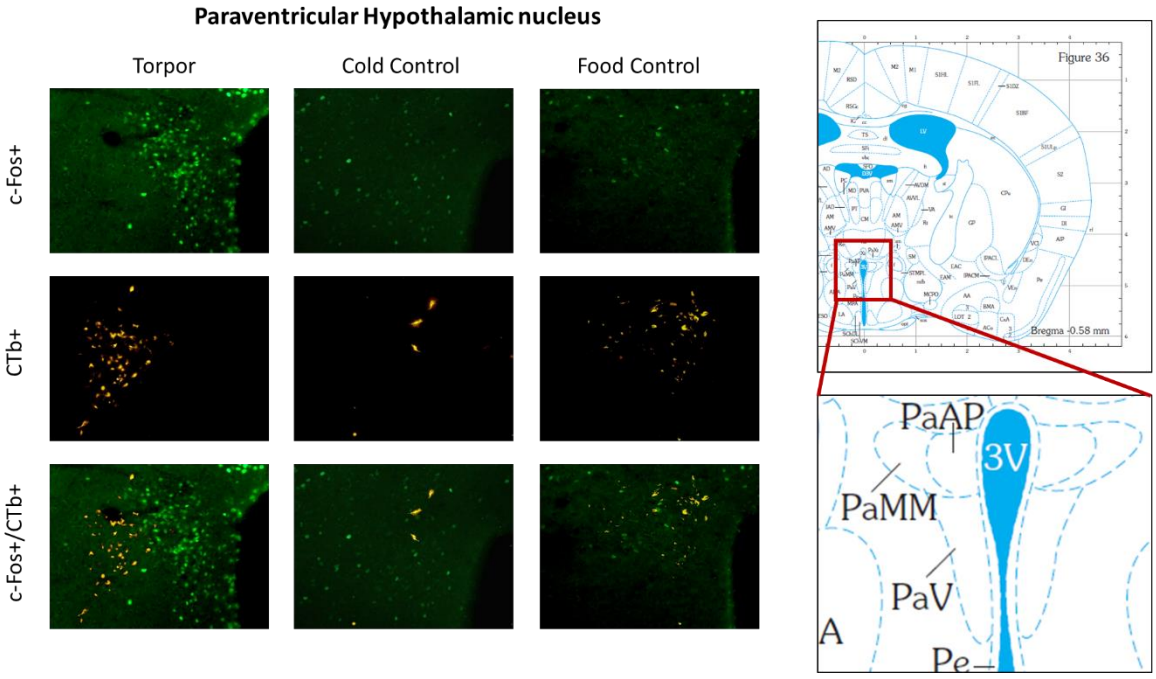
Paraventricular Hypothalamic nucleus
Torpor
Cold Control
Food Control
c-Fos+
CTb+
c-Fos+/CTb+
Figure 36
Bregma -0.58 mm
PaAP
3V
PaMM
PaV
A
Pe

Figure 27. Experiment I: number of c-Fos positive neurons in different brain regions.

The number (mean ± SEM) of positive c-Fos neurons in each of the nuclei studied, for each of the three experimental groups is shown: Cold Control, light blue; Food Control, pink; Torpor group, purple. The number was calculated as the average of the counted neurons on different slides for each nucleus (*=$p<0.05$ Torpor vs Cold Control, #=$p<0.05$ Torpor vs Food Control) (LPB, Lateral Parabrachial nucleus; VLPAG, Ventrolateral Periaqueductal Gray, DMH, Dorsomedial Hypothalamic nucleus, ARC, Arcuate nucleus; LH, Lateral Hypothalamus; PVH, Paraventricular Hypothalamic nucleus).

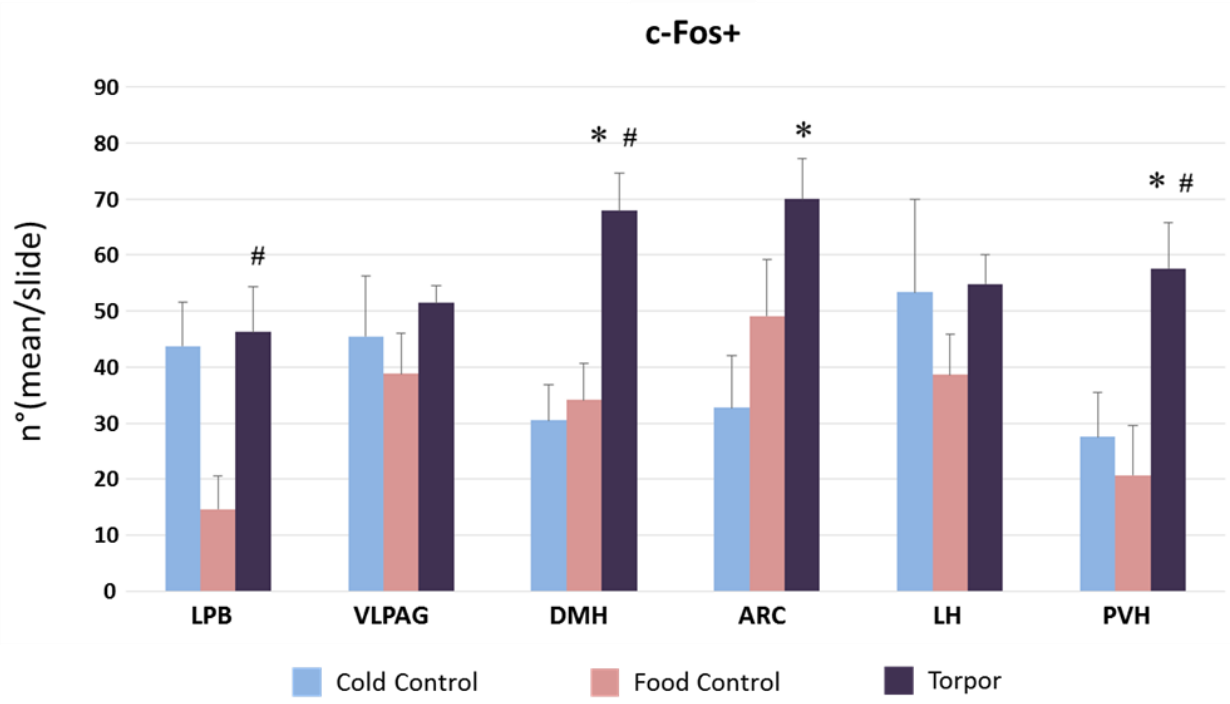
c-Fos+
n°(mean/slide)
90
80
70
60
50
40
30
20
10
0
#
* #
*
* #
LPB
VLPAG
DMH
ARC
LH
PVH
Cold Control
Food Control
Torpor

Figure 28. Experiment I: number of double stained (CTb+/c-Fos+) neurons in different brain regions.

The number (mean ± SEM) of double stained neurons in each of the nuclei studied, for each of the three experimental groups is shown: Cold Control, light blue; Food Control, pink; Torpor group, purple. The number was calculated as the average of the counted neurons on different slides for each nucleus (LPB, Lateral Parabrachial nucleus; VLPAG, Ventrolateral Periaqueductal Gray, DMH, Dorsomedial Hypothalamic nucleus, ARC, Arcuate nucleus; LH, Lateral Hypothalamus; PVH, Paraventricular Hypothalamic nucleus).

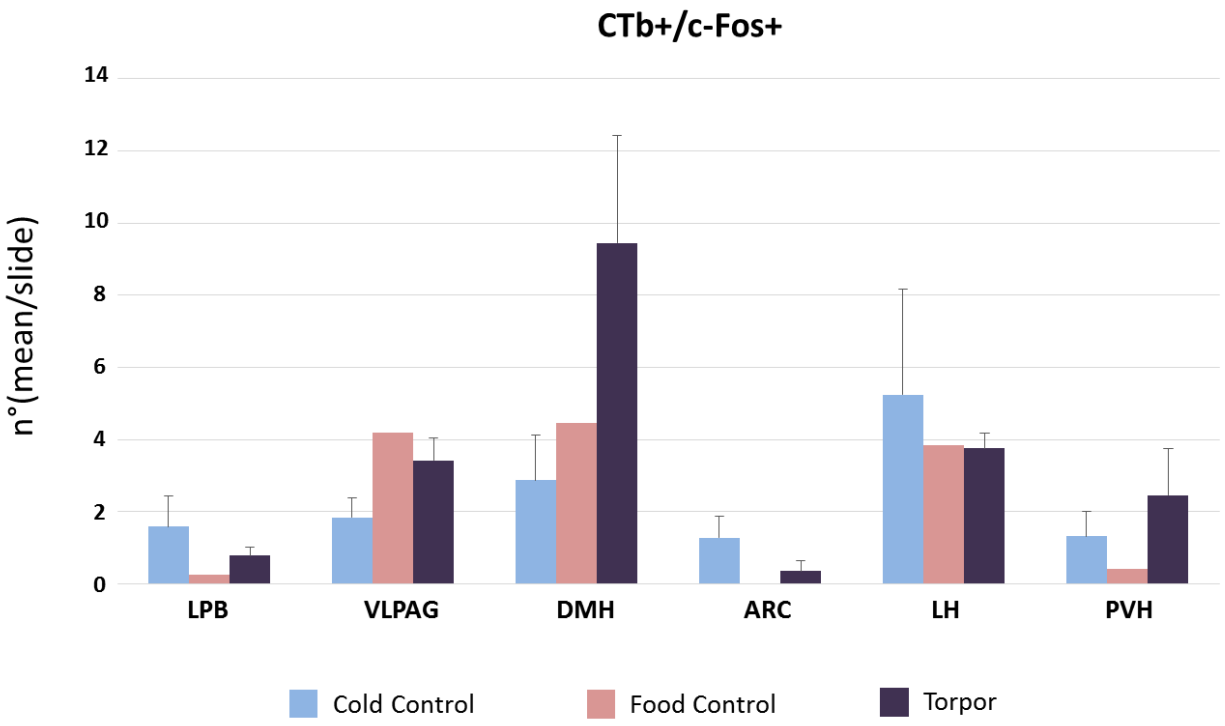
CTb+/c-Fos+
n°(mean/slide)
14
12
10
8
6
4
2
0
LPB
VLPAG
DMH
ARC
LH
PVH
Cold Control
Food Control
Torpor

Figure 29. Experiment I: example of triple staining (CTb, c-Fos, and OrxA) in the Lateral Hypothalamus.

An example of triple staining in the Lateral Hypothalamus area of a torpid mouse is shown in the figure. Neurons are labelled for c-Fos expression (green), the presence of the retrograde tracer CTb (yellow), and the presence of orexin A (OrxA, red). As shown in the figure, several neurons (green nucleus and red cell body) are double stained for c-Fos and OrxA, whilst the neuron in the red circle is triple stained (for CTb, c-Fos and OrxA), therefore showing the activation of an orexinergic neuron projecting to the Raphe Pallidus.

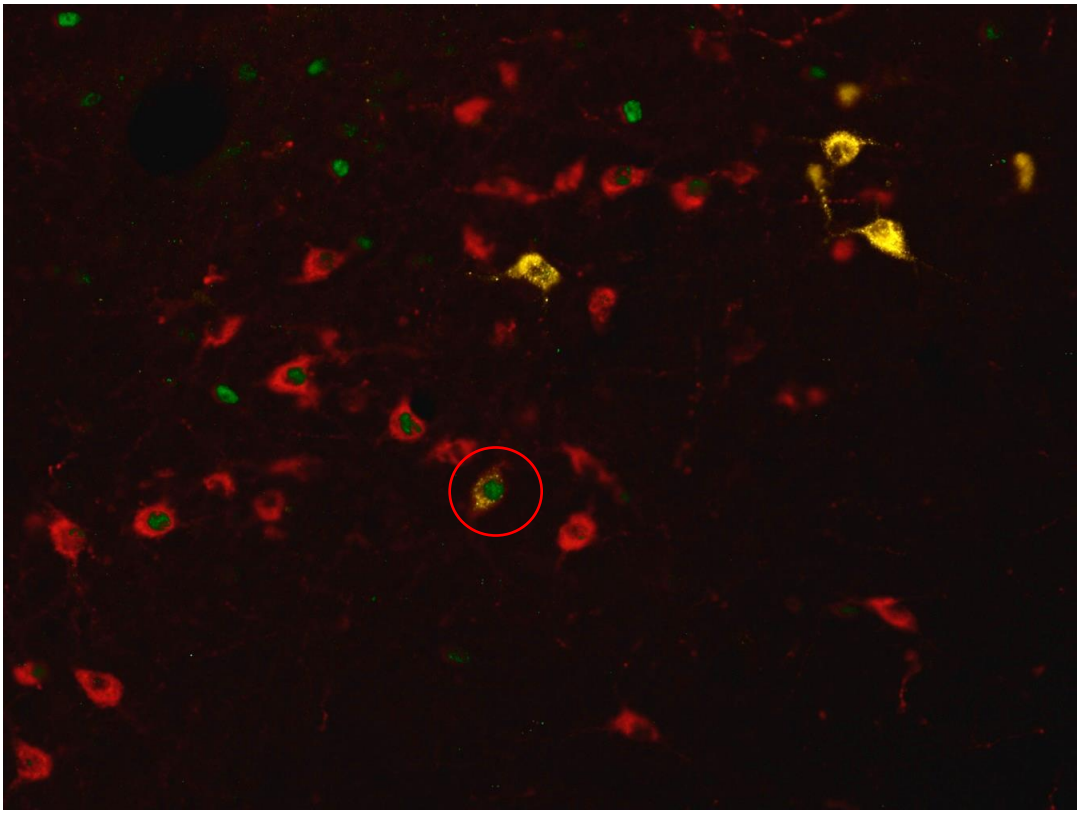

Figure 30. Experiment II: time course of cutaneous temperature during the experimental day in mice.

Cutaneous temperature was monitored during the experimental day with a thermal camera placed above the cage. The graph shows the mean value ±SEM of cutaneous temperature recorded every 10 minutes on the cutaneous surface of the lower back in all three experimental groups. Cutaneous temperature was significantly lower levels in Torpor group (purple) in comparison with Cold Control group (light blue), (*=$p<0.05$, **=$p<0.01$).

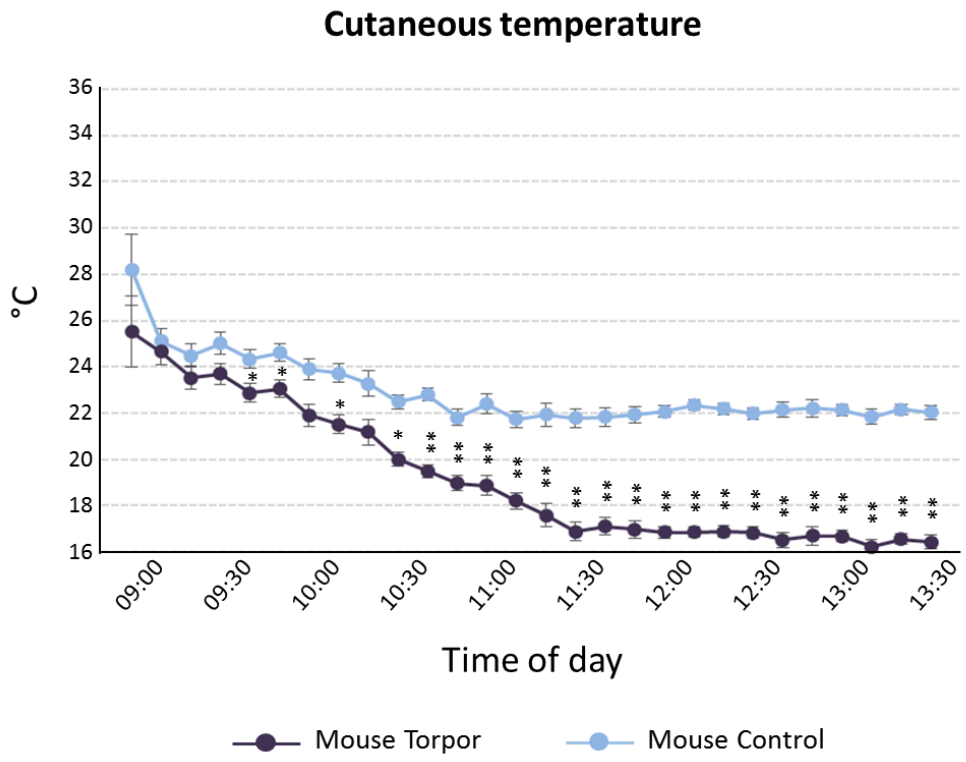
Cutaneous temperature
°C
36
34
32
30
28
26
24
22
20
18
16
09:00
09:30
10:00
10:30
11:00
11:30
12:00
12:30
13:00
13:30
Time of day
Mouse Torpor
Mouse Control

Figure 31. Experiment II: time course of hypothalamic temperature in Rat-RPa-MUS.

The graph represents the mean value ±SEM of every 30 minutes of hypothalamic temperature (Thy) in the experimental day in rats injected with the GABA-A agonist muscimol (purple) of ACSF in the Raphe Pallidus (RPa) (light blue). Shortly after the first injection (9:00), rats with central inhibition of the RPa lower their core temperature considerably, reaching around 22°C, with a significant difference with animals treated with ACSF (*=$p<0.05$, **=$p<0.01$).

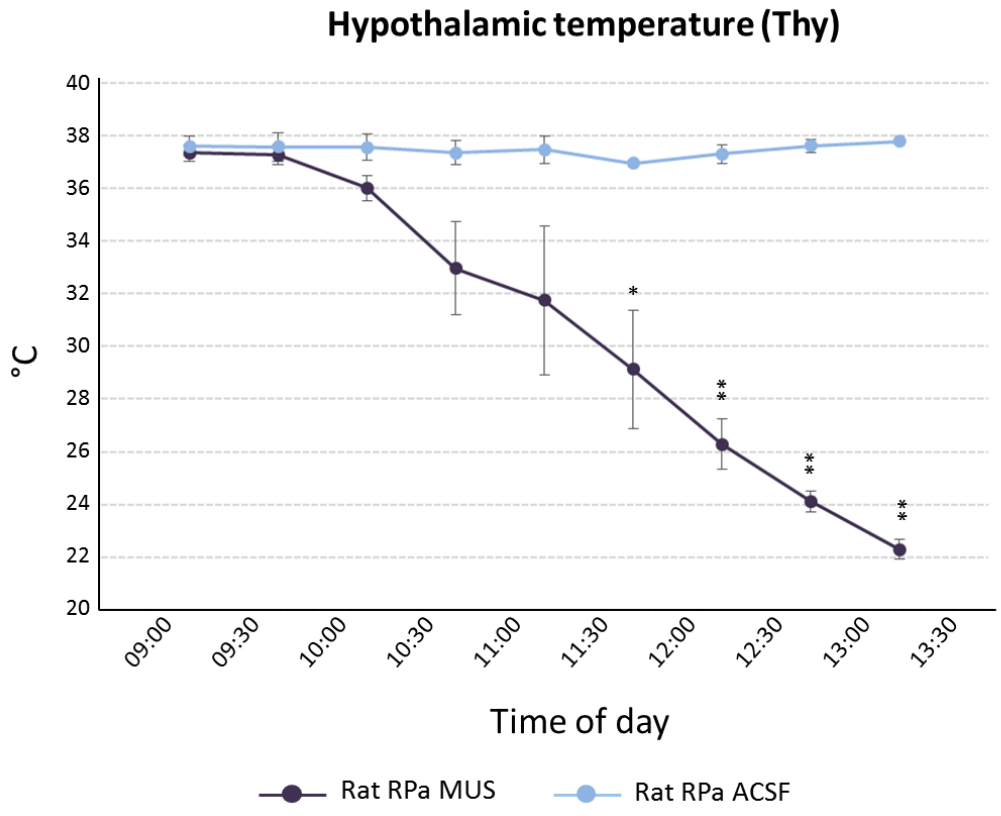
Hypothalamic temperature (Thy)
°C
40
38
36
34
32
30
28
26
24
22
20
09:00
09:30
10:00
10:30
11:00
11:30
12:00
12:30
13:00
13:30
Time of day
Rat RPa MUS
Rat RPa ACSF

Figure 32. Experiment II: time course of hypothalamic temperature in Rat-ICV-CHA.

The graph represents the mean value ±SEM of every 30 minutes of hypothalamic temperature (Thy) in the experimental day in rats injected with the A1AR receptor agonist N-6-cyclohexyladenosine (CHA) (purple) or ACSF (light blue) intracerebroventricularly. Shortly after the injection (9:00), rats injected with CHA lower their core temperature considerably, reaching around 28°C, with a significant difference with animals treated with ACSF (*=$p<0.05$, **=$p<0.01$).

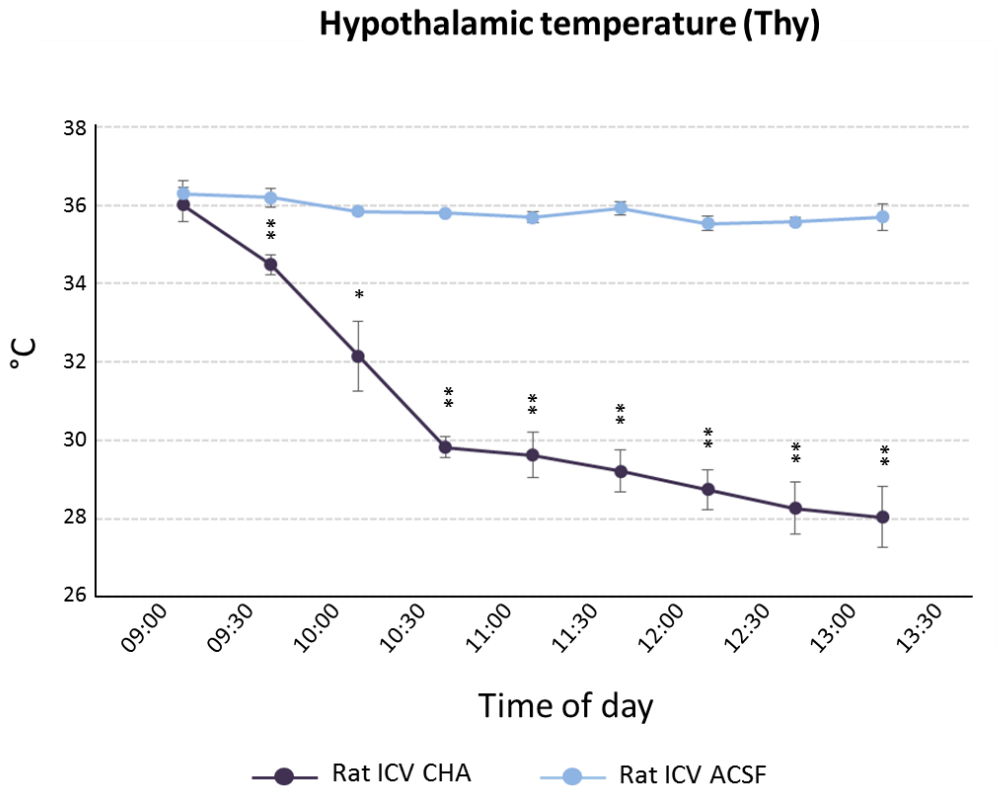
Hypothalamic temperature (Thy)
°C
38
36
34
32
30
28
26
09:00
09:30
10:00
10:30
11:00
11:30
12:00
12:30
13:00
13:30
Time of day
Rat ICV CHA
Rat ICV ACSF

Figure 33. Experiment II: mitochondrial respiration in liver during either spontaneous (mouse) or synthetic (rats) torpor.

Oxygen consumption rate (nmol/min/mg; mean±SEM) of State 2, 3 and 4, and respiratory control ratio (RCR 3/4) is shown for isolated liver mitochondria of rats and mice. For all histogram, treated animals are shown in purple and control animals are shown in light blue. In the first row, the results for rats in a condition of synthetic torpor induced through the central inhibition of the Raphe Pallidus by the local delivery of the GABA-A agonist .muscimol (Rat RPa MUS) are shown in comparison with controls treated with artificial cerebrospinal fluid (Rat RPa ACSF). In the second row, the results for rats in a condition of synthetic torpor induced by central activation of A1AR receptor (Rat ICV CHA) are shown in comparison with controls treated with artificial cerebrospinal fluid (Rat ICV ACSF). In the third row data from the previous experiment were pooled (Rat treatment; Rat Control). In the fourth row the results for mice in spontaneous torpor (Mouse Torpor) in comparison with euthermic controls (Mouse Control) (**=$p<0.01$, *=$p<0.05$).

LIVER

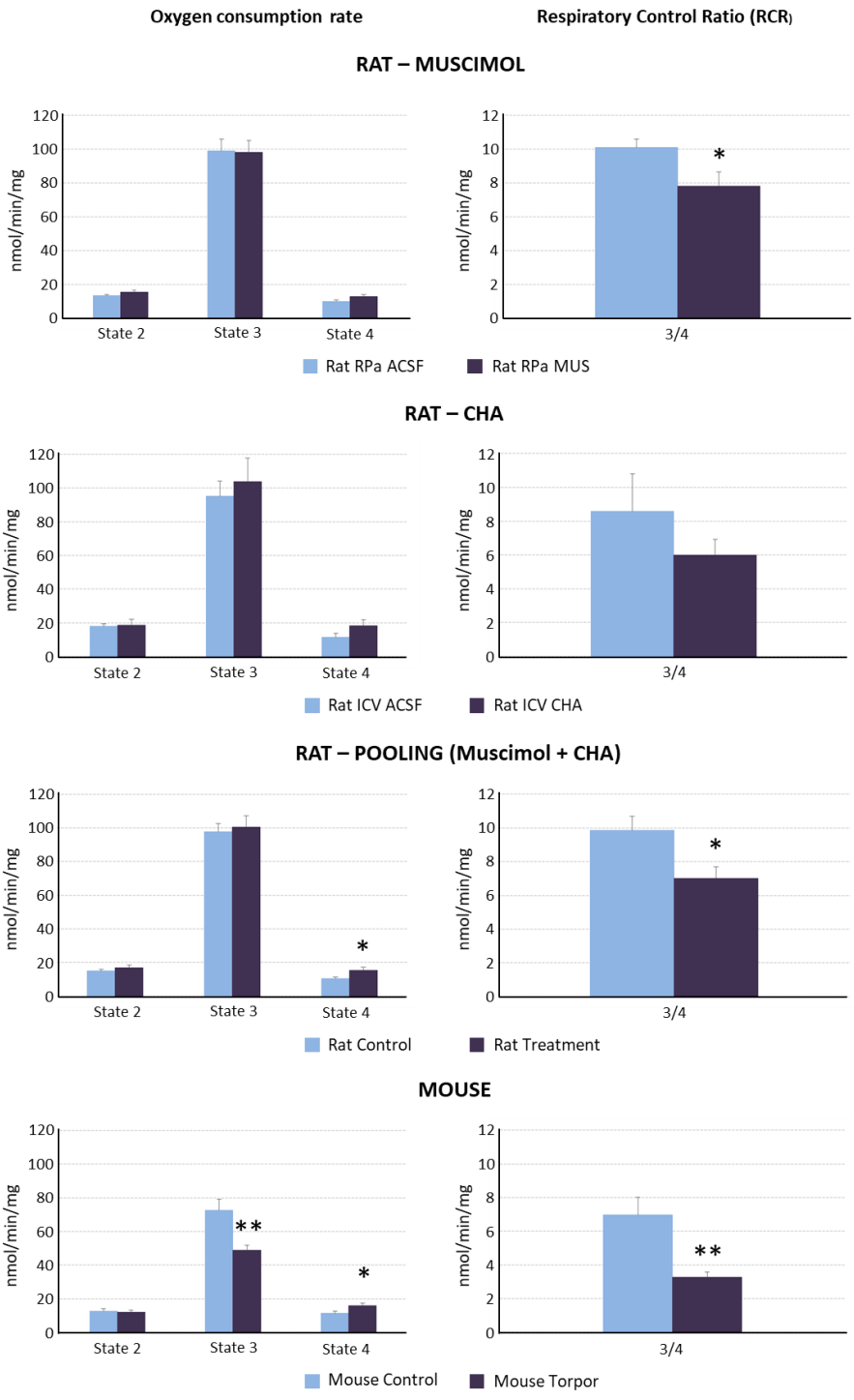
Oxygen consumption rate
Respiratory Control Ratio (RCR)
RAT – MUSCIMOL
nmol/min/mg
State 2
State 3
State 4
3/4
Rat RPa ACSF
Rat RPa MUS
RAT – CHA
Rat ICV ACSF
Rat ICV CHA
RAT – POOLING (Muscimol + CHA)
Rat Control
Rat Treatment
MOUSE
Mouse Control
Mouse Torpor

Figure 34. Experiment II: mitochondrial respiration in kidney during either spontaneous (mouse) or synthetic (rats) torpor.

Oxygen consumption rate (nmol/min/mg; mean±SEM) of State 2, 3 and 4, and respiratory control ratio (RCR 3/4) is shown for isolated kidney mitochondria of rats and mice. For all histogram, treated animals are shown in purple and control animals are shown in light blue. In the first row, the results for rats in a condition of synthetic torpor induced through the central inhibition of the Raphe Pallidus by the local delivery of the GABA-A agonist muscimol (Rat RPa MUS) are shown in comparison with controls treated with artificial cerebrospinal fluid (Rat RPa ACSF). In the second row, the results for rats in a condition of synthetic torpor induced by central activation of A1AR receptor (Rat ICV CHA) are shown in comparison with controls treated with artificial cerebrospinal fluid (Rat ICV ACSF). In the third row, data from the previous experiment were pooled (Rat treatment; Rat Control). In the fourth row the results for mice in spontaneous torpor (Mouse Torpor) in comparison with euthermic controls (Mouse Control) (*=$p<0.05$).

KIDNEY

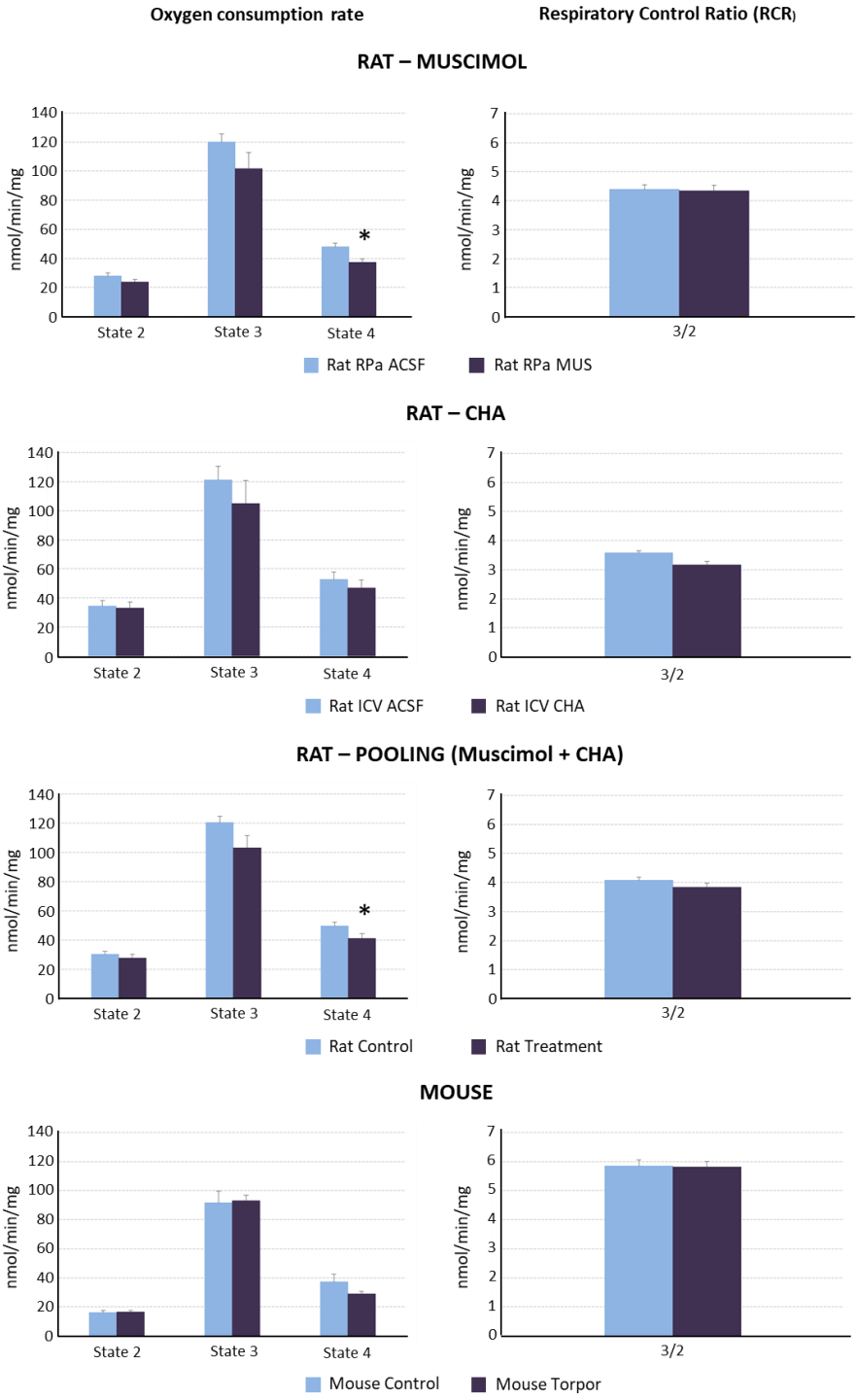
Oxygen consumption rate
Respiratory Control Ratio (RCR)
RAT – MUSCIMOL
nmol/min/mg
State 2
State 3
State 4
3/2
*
Rat RPa ACSF
Rat RPa MUS
RAT – CHA
Rat ICV ACSF
Rat ICV CHA
RAT – POOLING (Muscimol + CHA)
Rat Control
Rat Treatment
MOUSE
Mouse Control
Mouse Torpor

Figure 35. Experiment II: mitochondrial respiration in brain during either spontaneous (mouse) or synthetic (rats) torpor.

Oxygen consumption rate (nmol/min/mg; mean±SEM) of State 2, 3 and 4, and respiratory control ratio (RCR 3/4) is shown for isolated brain mitochondria of rats and mice. For all histogram, treated animals are shown in purple and control animals are shown in light blue. In the first row, the results for rats in a condition of synthetic torpor induced by central activation of A1AR receptor (Rat ICV CHA) are shown in comparison with controls treated with artificial cerebrospinal fluid (Rat ICV ACSF). In the second row, data from the previous experiment were pooled (Rat treatment; Rat Control). In the fourth row the results for mice in spontaneous torpor (Mouse Torpor) in comparison with euthermic controls (Mouse Control) (*=$p<0.05$).

BRAIN

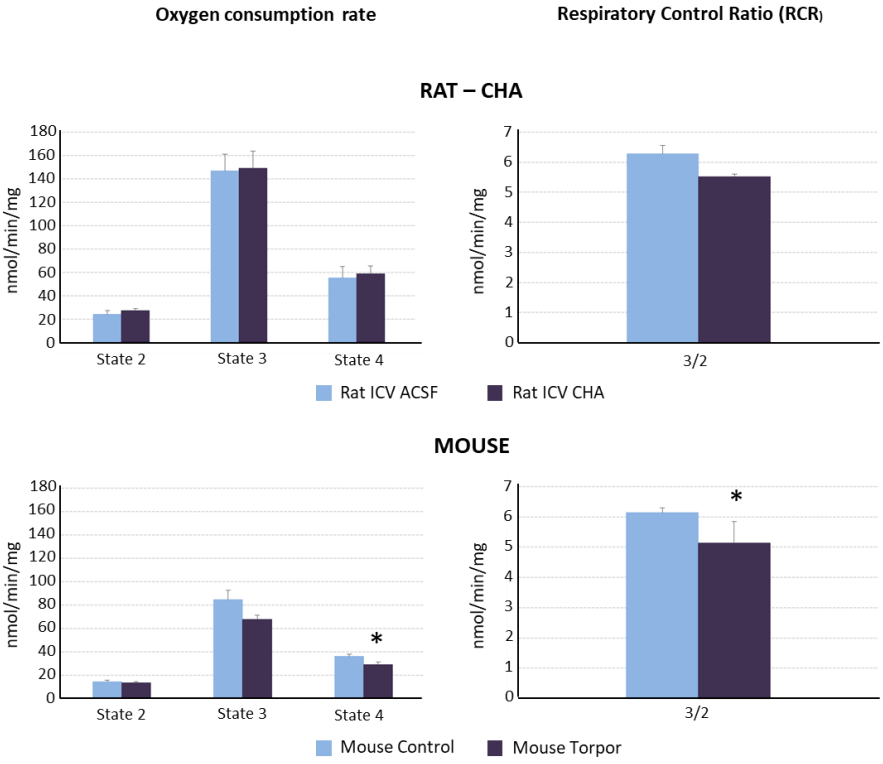
Oxygen consumption rate
Respiratory Control Ratio (RCR)
RAT – CHA
nmol/min/mg
180
160
140
120
100
80
60
40
20
0
State 2
State 3
State 4
7
6
5
4
3
2
1
0
3/2
Rat ICV ACSF
Rat ICV CHA
MOUSE
*
Mouse Control
Mouse Torpor

Figure 36. Experiment II: uncoupling protein 2 (UCP2) mitochondrial expression in synthetic torpor

UCP2 expression in brain, liver, and kidney mitochondria in rats after the induction of synthetic torpor by means of the ICV administration of the A1 receptor agonist N-6-Cyclohexyladenosine (CHA) or following the ICV injection of artificial cerebrospinal fluid (ACSF) is shown. The expression was evaluated by electrophoresis followed by a western blot analysis. The red arrow indicates the position in gel of the UCP2 protein (30 kDa).

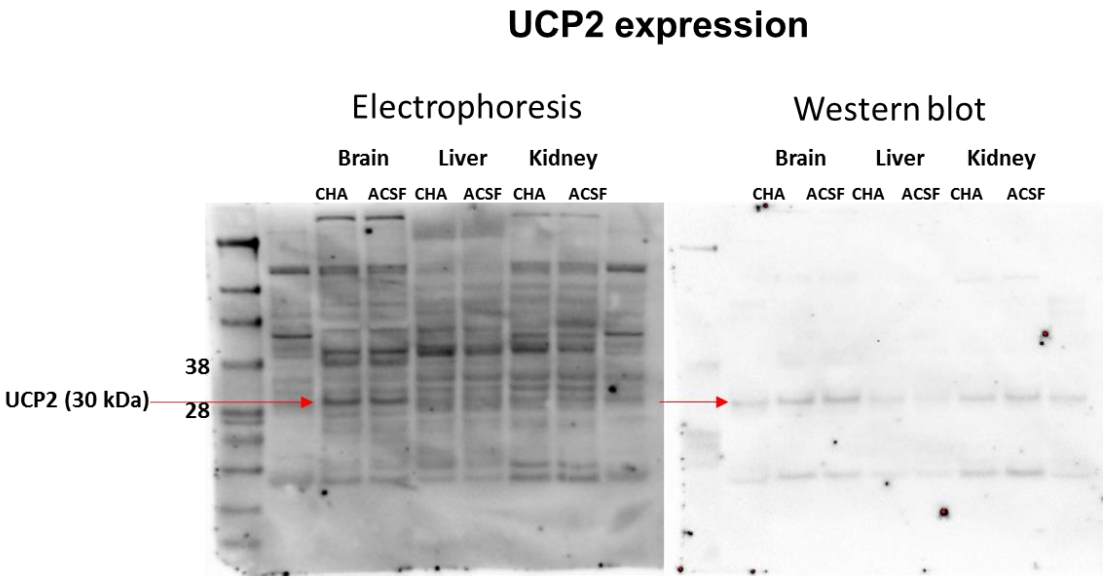
UCP2 expression
Electrophoresis
Western blot
Brain
Liver
Kidney
CHA
ACSF
38
28
UCP2 (30 kDa)

Figure 37. Experiment III: infrared images of a pig during surgery

Infrared images of a pig, recorded with a thermal camera during surgery. The upper image shows the animal after the injection of the GABA-A antagonist GABAzine, whereas the bottom one represents the infrared image of the pig after the injection of the GABA-A agonist muscimol. A consistent cutaneous vasodilation can be observed following muscimol injection.

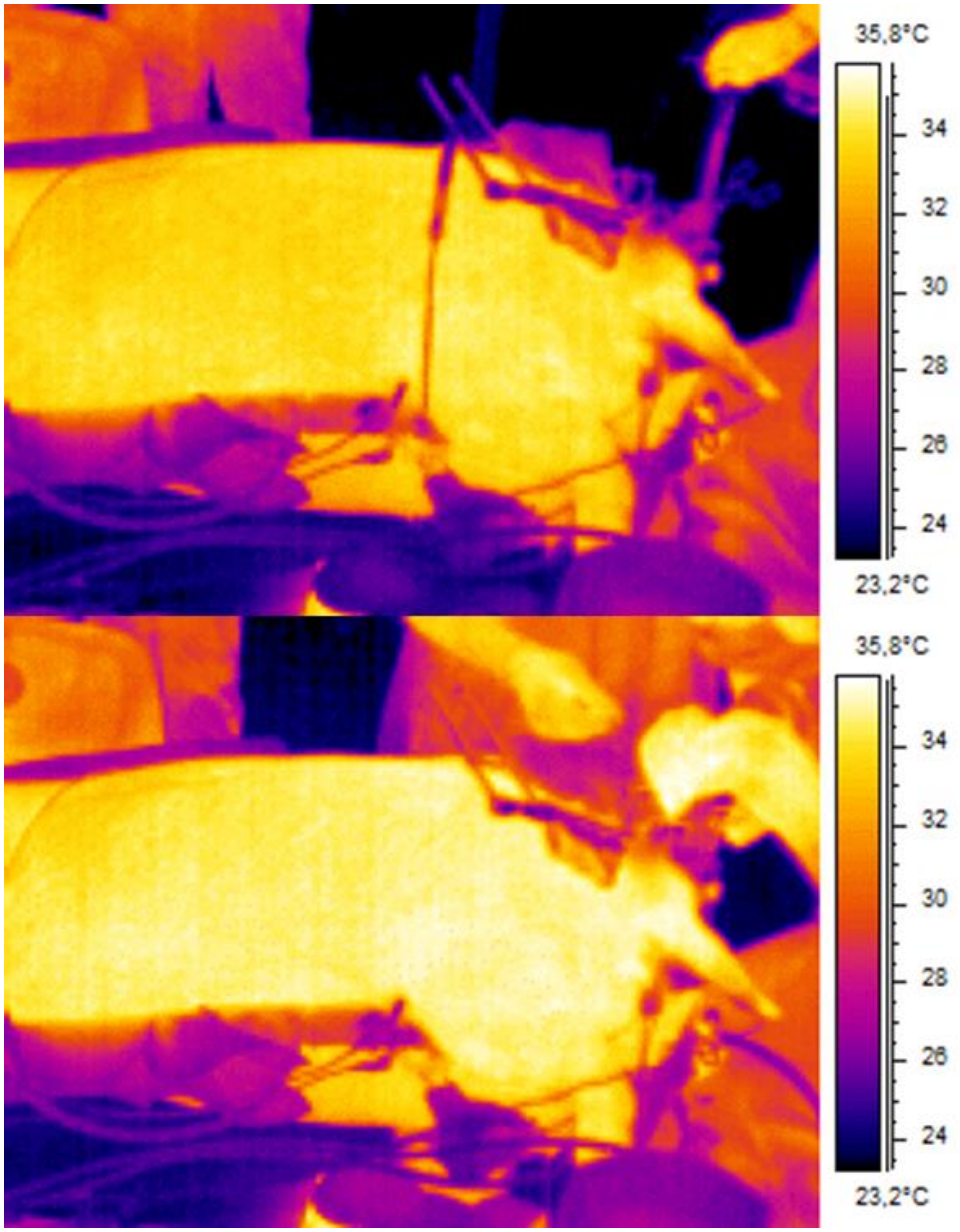
35,8°C
34
32
30
28
26
24
23,2°C
35,8°C
34
32
30
28
26
24
23,2°C

Figure 38. Experiment III: effects of the central manipulation of the Raphe Pallidus on physiological parameters in swine.

Graphic representation of several physiological variables parameters (HR, heart rate; AP, arterial pressure; ETCO2, end-tidal CO2; Tcore, central core temperature) measured in a pig during surgery, after injection of the GABA-A antagonist GABAzine (G) followed by the injection of the GABA-A agonist muscimol (M) in the Raphe Pallidus region. Shivering was visually assessed by an operator and its intensity evaluated on an arbitrary unit scale (0= absence of shivering, 10=modest shivering, 20=moderate shivering, 30=severe shivering).

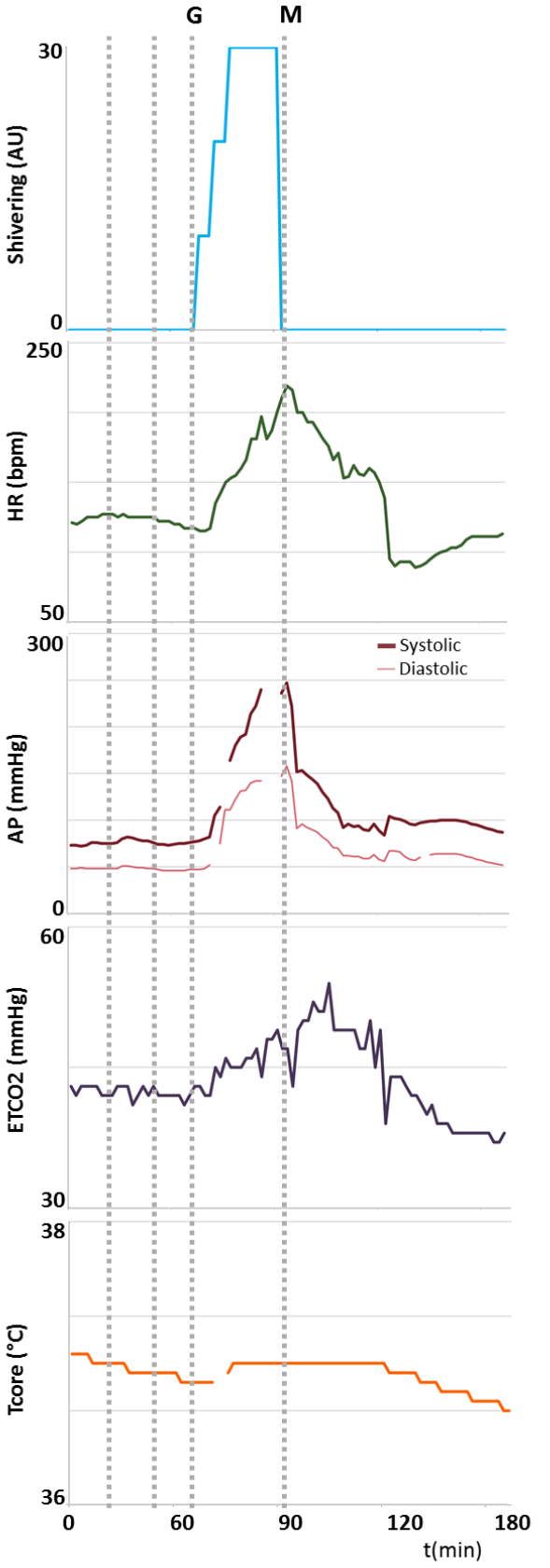

G = GABAzine injection M = Muscimol injection

Figure 39. Experiment III: effects of the central manipulation of the Raphe Pallidus on physiological parameters in swine.

Physiological parameters (HR, heart rate; SAP, systolic arterial pressure; DAP, diastolic arterial pressure; ETCO2, end-tidal CO2; Tcore, central core temperature; mean ± SEM) which were determined in anaesthetized pigs are shown in the histogram for the three different experimental conditions: i) baseline (yellow); ii) after the central administration of the GABA-A antagonist GABAzine in the Raphe Pallidus (red); iii) after the subsequent administration of the GABA-A agonist muscimol in the same region (blue). (**=$p<0.01$, *=$p<0.05$ GABAzine vs baseline; #=$p<0.05$ muscimol vs GABAzine).

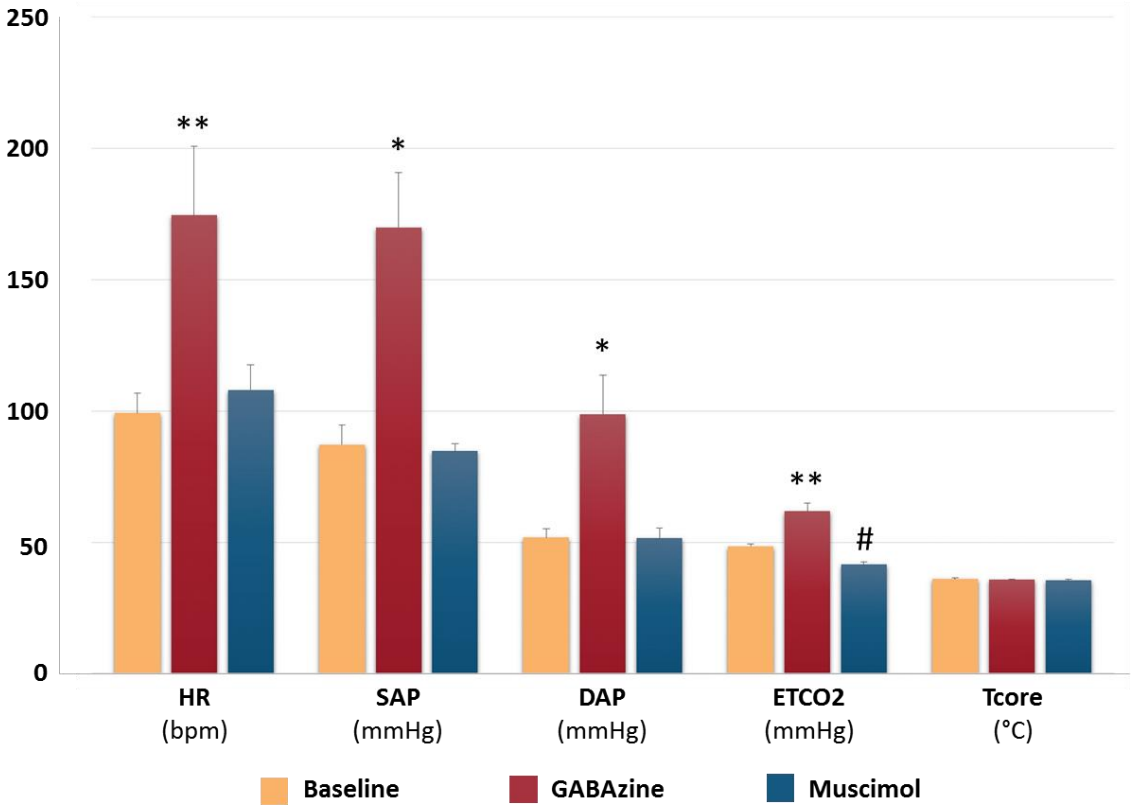
250
200
150
100
50
0
**
*
*
**
#
HR
(bpm)
SAP
(mmHg)
DAP
(mmHg)
ETCO2
(mmHg)
Tcore
(°C)
Baseline
GABAzine
Muscimol

Figure 40. Experiment III: example of injection site in the brainstem of a pig.

Example of a coronal section of a pig brain collected at the end of the experimental procedure. The red square represents the injection site, marked with fluorescent microbeads, in correspondence of the Raphe Pallidus (RPa).

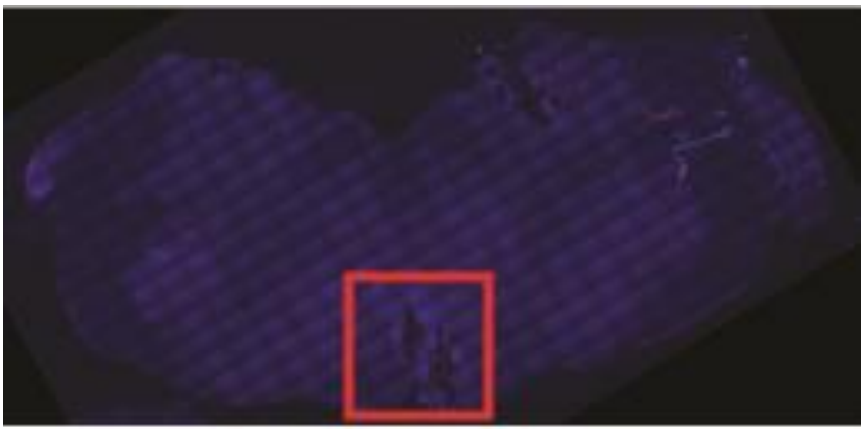

7. REFERENCES

Adamantidis, A.R., Zhang, F., Aravanis, A.M., Deisseroth, K., de Lecea, L. (2007) Neural substrates of awakening probed with optogenetic control of hypocretin neurons. *Nature*. **450**(7168), 420–424.

Aleardi, A.M., Benard, G., Augereau, O., Malgat, M., Talbot, J.C., Mazat, J.P., Letellier, T., Dachary-Prigent, J., Solaini, G.C., Rossignol, R. (2005) Gradual alteration of mitochondrial structure and function by beta-amyloids: importance of membrane viscosity changes, energy deprivation, reactive oxygen species production, and cytochrome c release. *Journal of bioenergetics and biomembranes*. **37**(4), 207–25.

Alhadeff, A.L., Hayes, M.R., Grill, H.J. (2014) Leptin receptor signaling in the lateral parabrachial nucleus contributes to the control of food intake. *AJP: Regulatory, Integrative and Comparative Physiology*. **307**(11), R1338–R1344.

Anderson, R., Sheehan, M.J., Strong, P. (1994) Characterization of the adenosine receptors mediating hypothermia in the conscious mouse. *British journal of pharmacology*. **113**(4), 1386–90.

Aponte, Y., Atasoy, D., Sternson, S.M. (2011) AGRP neurons are sufficient to orchestrate feeding behavior rapidly and without training. *Nature Neuroscience*. **14**(3), 351–355.

Armstrong, C., Staples, J.F. (2010) The role of succinate dehydrogenase and oxaloacetate in metabolic suppression during hibernation and arousal. *Journal of Comparative Physiology B*. **180**(5), 775–783.

Arnold, W., Heldmaier, G., Ortmann, S., Pohl, H., Ruf, T., Steinlechner, S. (1991) Ambient temperatures in hibernacula and their energetic consequences for alpine marmots Marmota marmota. *Journal of Thermal Biology*. **16**(4), 223–226.

Baird, B.J., Dickey, J.S., Nakamura, A.J., Redon, C.E., Parekh, P., Griko, Y. V., Aziz, K., Georgakilas, A.G., Bonner, W.M., Martin, O.A. (2011) Hypothermia postpones DNA damage repair in irradiated cells and protects against cell killing. *Mutation Research/Fundamental and Molecular Mechanisms of*

Mutagenesis. **711**(1–2), 142–149.

Barnes, B.M. (1989) Freeze avoidance in a mammal: body temperatures below 0 degree C in an Arctic hibernator. *Science (New York, N.Y.)*. **244**(4912), 1593–5.

Barros, R.C.H., Branco, L.G.S., Cárnio, E.C. (2006) Respiratory and body temperature modulation by adenosine A1 receptors in the anteroventral preoptic region during normoxia and hypoxia. *Respiratory physiology & neurobiology*. **153**(2), 115–25.

Betley, J.N., Cao, Z.F.H., Ritola, K.D., Sternson, S.M. (2013) Parallel, Redundant Circuit Organization for Homeostatic Control of Feeding Behavior. *Cell*. **155**(6), 1337–1350.

Bicego, K.C., Barros, R.C.H., Branco, L.G.S. (2007) Physiology of temperature regulation: Comparative aspects. *Comparative Biochemistry and Physiology Part A: Molecular & Integrative Physiology*. **147**(3), 616–639.

Blackstone, E., Morrison, M., Roth, M.B. (2005) H2S Induces a Suspended Animation-Like State in Mice. *Science*. **308**(5721), 518–518.

Blessing, W.W., Nalivaiko, E. (2001) Raphe magnus/pallidus neurons regulate tail but not mesenteric arterial blood flow in rats. *Neuroscience*. **105**(4), 923–9.

Boulant, J.A. (2005) Neuronal basis of Hammel's model for set-point thermoregulation. *Journal of Applied Physiology*. **100**(4), 1347–1354.

Boulant, J.A., Hardy, J.D. (1974) The effect of spinal and skin temperatures on the firing rate and thermosensitivity of preoptic neurones. *The Journal of physiology*. **240**(3), 639–60.

Bouma, H.R., Verhaag, E.M., Otis, J.P., Heldmaier, G., Swoap, S.J., Strijkstra, A.M., Henning, R.H., Carey, H. V. (2012) Induction of torpor: Mimicking natural metabolic suppression for biomedical applications. *Journal of Cellular Physiology*. **227**(4), 1285–1290.

Boyer, B.B., Barnes, B.M., Lowell, B.B., Grujic, D. (1998) Differential regulation

of uncoupling protein gene homologues in multiple tissues of hibernating ground squirrels. *The American journal of physiology*. **275**(4 Pt 2), R1232-8.

Boyles, J.G., Thompson, A.B., McKechnie, A.E., Malan, E., Humphries, M.M., Careau, V. (2013) A global heterothermic continuum in mammals. *Global Ecology and Biogeography*. **22**(9), 1029–1039.

Braulke, L.J., Klingenspor, M., DeBarber, A., Tobias, S.C., Grandy, D.K., Scanlan, T.S., Heldmaier, G. (2008) 3-Iodothyronamine: a novel hormone controlling the balance between glucose and lipid utilisation. *Journal of Comparative Physiology B*. **178**(2), 167–177.

Brown, J.C.L., Gerson, A.R., Staples, J.F. (2007) Mitochondrial metabolism during daily torpor in the dwarf Siberian hamster: role of active regulated changes and passive thermal effects. *American journal of physiology. Regulatory, integrative and comparative physiology*. **293**(5), R1833-45.

Brown, J.C.L., Staples, J.F. (2014) Substrate-specific changes in mitochondrial respiration in skeletal and cardiac muscle of hibernating thirteen-lined ground squirrels. *Journal of Comparative Physiology B*. **184**(3), 401–414.

Brown, J.W., Sirlin, E.A., Benoit, A.M., Hoffman, J.M., Darnall, R.A. (2008) Activation of 5-HT1A receptors in medullary raphé disrupts sleep and decreases shivering during cooling in the conscious piglet. *American journal of physiology. Regulatory, integrative and comparative physiology*. **294**(3), R884-94.

Buck, C.L., Barnes, B.M. (2000) Effects of ambient temperature on metabolic rate, respiratory quotient, and torpor in an arctic hibernator. *American journal of physiology. Regulatory, integrative and comparative physiology*. **279**(1), R255-62.

Calvert, J.W., Coetzee, W.A., Lefer, D.J. (2010) Novel Insights Into Hydrogen Sulfide–Mediated Cytoprotection. *Antioxidants & Redox Signaling*. **12**(10), 1203–1217.

Campos, C.A., Bowen, A.J., Schwartz, M.W., Palmiter, R.D. (2016) Parabrachial

CGRP Neurons Control Meal Termination. *Cell Metabolism*. **23**(5), 811–820.

Cannon, B., Nedergaard, J. (2004) Brown Adipose Tissue: Function and Physiological Significance. *Physiological Reviews*. **84**(1), 277–359.

Cano, G., Passerin, A.M., Schiltz, J.C., Card, J.P., Morrison, S.F., Sved, A.F. (2003) Anatomical substrates for the central control of sympathetic outflow to interscapular adipose tissue during cold exposure. *The Journal of Comparative Neurology*. **460**(3), 303–326.

Cao, W.-H., Morrison, S.F. (2006) Glutamate receptors in the raphe pallidus mediate brown adipose tissue thermogenesis evoked by activation of dorsomedial hypothalamic neurons. *Neuropharmacology*. **51**(3), 426–437.

Carey, H. V., Andrews, M.T., Martin, S.L. (2003) Mammalian Hibernation: Cellular and Molecular Responses to Depressed Metabolism and Low Temperature. *Physiological Reviews*. **83**(4), 1153–1181.

Carpenter, F.L., Hixon, M.A. (1988) A New Function for Torpor: Fat Conservation in a Wild Migrant Hummingbird. *The Condor*. **90**(2), 373–378.

Carrettiero, D.C., Fior-Chadi, D.R. (2008) Age-dependent changes in adenosine A1 receptor distribution and density within the nucleus tractus solitarii of normotensive and hypertensive rats. *Journal of Neural Transmission*. **115**(8), 1109–1118.

Carrive, P., Marks, A., Vianna, D.M. (2007) What causes conditioned fear induced hyperthermia in the rat? An infrared thermographic study. *Autonomic Neuroscience*. **135**(1–2), 65.

Carter, M.E., Soden, M.E., Zweifel, L.S., Palmiter, R.D. (2013) Genetic identification of a neural circuit that suppresses appetite. *Nature*. **503**(7474), 111–114.

Cerri, M. (2017) The Central Control of Energy Expenditure: Exploiting Torpor for Medical Applications. *Annual Review of Physiology*. **79**(1), 167–186.

Cerri, M., Mastrotto, M., Tupone, D., Martelli, D., Luppi, M., Perez, E., Zamboni,

G., Amici, R. (2013) The Inhibition of Neurons in the Central Nervous Pathways for Thermoregulatory Cold Defense Induces a Suspended Animation State in the Rat. *Journal of Neuroscience*. **33**(7), 2984–2993.

Cerri, M., Morrison, S.F. (2005) Activation of lateral hypothalamic neurons stimulates brown adipose tissue thermogenesis. *Neuroscience*. **135**(2), 627–638.

Cerri, M., Zamboni, G., Tupone, D., Dentico, D., Luppi, M., Martelli, D., Perez, E., Amici, R. (2010) Cutaneous vasodilation elicited by disinhibition of the caudal portion of the rostral ventromedial medulla of the free-behaving rat. *Neuroscience*. **165**(3), 984–995.

Conceição, E.P.S., Madden, C.J., Morrison, S.F. (2017) Tonic inhibition of brown adipose tissue sympathetic nerve activity via muscarinic acetylcholine receptors in the rostral raphe pallidus. *The Journal of Physiology*. **000.00**, 1–14.

Cowley, M.A., Smart, J.L., Rubinstein, M., Cerdán, M.G., Diano, S., Horvath, T.L., Cone, R.D., Low, M.J. (2001) Leptin activates anorexigenic POMC neurons through a neural network in the arcuate nucleus. *Nature*. **411**(6836), 480–484.

Cowley, M.A., Smith, R.G., Diano, S., Tschöp, M., Pronchuk, N., Grove, K.L., Strasburger, C.J., Bidlingmaier, M., Esterman, M., Heiman, M.L., Garcia-Segura, L.M., Nillni, E.A., Mendez, P., Low, M.J., Sotonyi, P., Friedman, J.M., Liu, H., Pinto, S., Colmers, W.F., Cone, R.D., Horvath, T.L. (2003) The distribution and mechanism of action of ghrelin in the CNS demonstrates a novel hypothalamic circuit regulating energy homeostasis. *Neuron*. **37**(4), 649–61.

Craig, A.D. (2000) The functional anatomy of lamina I and its role in post-stroke central pain. In *Progress in brain research*. pp. 137–151.

Csifáry, A., Görcs, T.J., Palkovits, M. (1990) Neuropeptide Y innervation of ACTH-immunoreactive neurons in the arcuate nucleus of rats: a correlated light and electron microscopic double immunolabeling study. *Brain research*. **506**(2), 215–22.

Dark, J., Miller, D.R., Zucker, I. (1994) Reduced glucose availability induces torpor in Siberian hamsters. *The American journal of physiology*. **267**(2 Pt 2), R496-501.

Darnall, R.A., Harris, M.B., Gill, W.H., Hoffman, J.M., Brown, J.W., Niblock, M.M. (2005) Inhibition of serotonergic neurons in the nucleus paragigantocellularis lateralis fragments sleep and decreases rapid eye movement sleep in the piglet: implications for sudden infant death syndrome. *The Journal of neuroscience : the official journal of the Society for Neuroscience*. **25**(36), 8322–32.

Dausmann, K.H., Glos, J., Ganzhorn, J.U., Heldmaier, G. (2004) Hibernation in a tropical primate. *Nature*. **429**(6994), 825–826.

Delgado, J.M.R., Anand, B.K. (1953) Increase of food intake induced by electrical stimulation of the lateral hypothalamus. *The American journal of physiology*. **172**(1), 162–8.

Derwall, M., Francis, R.C., Kida, K., Bougaki, M., Crimi, E., Adrie, C., Zapol, W.M., Ichinose, F. (2011) Administration of hydrogen sulfide via extracorporeal membrane lung ventilation in sheep with partial cardiopulmonary bypass perfusion: a proof of concept study on metabolic and vasomotor effects. *Critical Care*. **15**(1), R51.

Drabek, T., Kochanek, P.M., Stezoski, J., Wu, X., Bayr, H., Morhard, R.C., Stezoski, S.W., Tisherman, S.A. (2011) Intravenous Hydrogen Sulfide Does Not Induce Hypothermia or Improve Survival from Hemorrhagic Shock in Pigs. *Shock*. **35**(1), 67–73.

Drew, K.L., Buck, C.L., Barnes, B.M., Christian, S.L., Rasley, B.T., Harris, M.B. (2007) Central nervous system regulation of mammalian hibernation: implications for metabolic suppression and ischemia tolerance. *Journal of Neurochemistry*. **102**(6), 1713–1726.

Dugbartey, G.J., Talaei, F., Houwertjes, M.C., Goris, M., Epema, A.H., Bouma, H.R., Henning, R.H. (2015) Dopamine treatment attenuates acute kidney injury in a rat model of deep hypothermia and rewarming – The role of renal H2S-

producing enzymes. *European Journal of Pharmacology*. **769**, 225–233.

Dulloo, A.G., Samec, S. (2001) Uncoupling proteins: their roles in adaptive thermogenesis and substrate metabolism reconsidered. *The British journal of nutrition*. **86**(2), 123–39.

Dunwiddie, T. V., Masino, S.A. (2001) The Role and Regulation of Adenosine in the Central Nervous System. *Annual Review of Neuroscience*. **24**(1), 31–55.

Esteban, J., Chover, A.J., Sánchez, P.A., Micó, J.A., Gibert-Rahola, J. (1989) Central administration of neuropeptide y induces hypothermia in mice. Possible interaction with central noradrenergic systems. *Life Sciences*. **45**(25), 2395–2400.

Florant, G.L., Heller, H.C. (1977) CNS regulation of body temperature in euthermic and hibernating marmots (Marmota flaviventris). *The American journal of physiology*. **232**(5), R203-8.

Forster, R.E., Ferguson, T.B. (1952) Relationship between hypothalamic temperature and thermo-regulatory effectors in unanesthetized cat. *The American journal of physiology*. **169**(2), 255–69.

Foster-Schubert, K.E., Overduin, J., Prudom, C.E., Liu, J., Callahan, H.S., Gaylinn, B.D., Thorner, M.O., Cummings, D.E. (2008) Acyl and Total Ghrelin Are Suppressed Strongly by Ingested Proteins, Weakly by Lipids, and Biphasically by Carbohydrates. *The Journal of Clinical Endocrinology & Metabolism*. **93**(5), 1971–1979.

Frank, S.M., Satitpunwaycha, P., Bruce, S.R., Herscovitch, P., Goldstein, D.S. (2003) Increased myocardial perfusion and sympathoadrenal activation during mild core hypothermia in awake humans. *Clinical Science*. **104**(5), 503–508.

Fredholm, B.B., Lindström, K. (1999) Autoradiographic comparison of the potency of several structurally unrelated adenosine receptor antagonists at adenosine A1 and A(2A) receptors. *European journal of pharmacology*. **380**(2–3), 197–202.

French, A.R. (1985) Allometries of the durations of torpid and euthermic intervals

during mammalian hibernation: A test of the theory of metabolic control of the timing of changes in body temperature. *Journal of Comparative Physiology B*. **156**(1), 13–19.

Fuhrman, F.A., Fuhrman, G.J., Farr, D.A., Fail, J.H. (1961) Relationship between tissue respiration and total metabolic rate in hypo- and normothermic rats. *The American journal of physiology*. **201**, 231–4.

Fuxe, K., Tinner, B., Caberlotto, L., Bunnemann, B., Agnati, L.F. (1997) NPY Y1 receptor like immunoreactivity exists in a subpopulation of beta-endorphin immunoreactive nerve cells in the arcuate nucleus: a double immunolabelling analysis in the rat. *Neuroscience letters*. **225**(1), 49–52.

Gallagher, K., Staples, J.F. (2013) Metabolism of Brain Cortex and Cardiac Muscle Mitochondria in Hibernating 13-Lined Ground Squirrels *Ictidomys tridecemlineatus*. *Physiological and Biochemical Zoology*. **86**(1), 1–8.

Geiser, F. (2004) Metabolic Rate and Body Temperature Reduction During Hibernation and Daily Torpor. *Annual Review of Physiology*. **66**(1), 239–274.

Geiser, F., Brigham, R.M. (2012) The Other Functions of Torpor. In *Living in a Seasonal World*. Berlin, Heidelberg: Springer Berlin Heidelberg, pp. 109–121.

Gluck, E.F., Stephens, N., Swoap, S.J. (2006) Peripheral ghrelin deepens torpor bouts in mice through the arcuate nucleus neuropeptide Y signaling pathway. *AJP: Regulatory, Integrative and Comparative Physiology*. **291**(5), R1303–R1309.

Gordon, C.J. (1990) Thermal biology of the laboratory rat. *Physiology & behavior*. **47**(5), 963–91.

Gornall, A.G., Bardawill, C.J., David, M.M. (1949) Determination of serum proteins by means of the biuret reaction. *The Journal of biological chemistry*. **177**(2), 751–66.

Grill, H.J., Hayes, M.R. (2012) Hindbrain Neurons as an Essential Hub in the Neuroanatomically Distributed Control of Energy Balance. *Cell Metabolism*.

16(3), 296–309.

Hammel, H.T., Hardy, J.D., Fusco, M.M. (1960) Thermoregulatory responses to hypothalamic cooling in unanesthetized dogs. *The American journal of physiology*. **198**, 481–6.

Harris, G.C., Wimmer, M., Aston-Jones, G. (2005) A role for lateral hypothalamic orexin neurons in reward seeking. *Nature*. **437**(7058), 556–559.

Heinricher, M.M., Neubert, M.J., Martenson, M.E., Gonçalves, L. (2004) Prostaglandin E2 in the medial preoptic area produces hyperalgesia and activates pain-modulating circuitry in the rostral ventromedial medulla. *Neuroscience*. **128**(2), 389–398.

Heldmaier, G., Ortmann, S., Elvert, R. (2004) Natural hypometabolism during hibernation and daily torpor in mammals. *Respiratory Physiology & Neurobiology*. **141**(3), 317–329.

Heller, H., Colliver, G.W., Beard, J. (1977) Thermoregulation during entrance into hibernation. *Pfl*  *gers Archiv European Journal of Physiology*. **369**(1), 55–59.

Hellstrom, B., Hammel, H.T. (1967) Some characteristics of temperature regulation in the unanesthetized dog. *The American journal of physiology*. **213**(2), 547–56.

Hoffman, J.M., Brown, J.W., Sirlin, E.A., Benoit, A.M., Gill, W.H., Harris, M.B., Darnall, R.A. (2007) Activation of 5-HT1A receptors in the paragigantocellularis lateralis decreases shivering during cooling in the conscious piglet. *AJP: Regulatory, Integrative and Comparative Physiology*. **293**(1), R518–R527.

Ter Horst, G.J., Hautvast, R.W., De Jongste, M.J., Korf, J. (1996) Neuroanatomy of cardiac activity-regulating circuitry: a transneuronal retrograde viral labelling study in the rat. *The European journal of neuroscience*. **8**(10), 2029–41.

Hosoi, T., Kawagishi, T., Okuma, Y., Tanaka, J., Nomura, Y. (2002) Brain Stem Is a Direct Target for Leptin's Action in the Central Nervous System.

Endocrinology. **143**(9), 3498–3504.

Huang, Z.G., Xue, D., Preston, E., Karbalai, H., Buchan, A.M. (1999) Biphasic opening of the blood-brain barrier following transient focal ischemia: effects of hypothermia. *The Canadian journal of neurological sciences. Le journal canadien des sciences neurologiques*. **26**(4), 298–304.

Hudson, J.W., Scott, I.M. (1979) Daily Torpor in the Laboratory Mouse, Mus musculus Var. Albino. *Physiological Zoology*. **52**(2), 205–218.

Iliff, B.W., Swoap, S.J. (2012) Central adenosine receptor signaling is necessary for daily torpor in mice. *American journal of physiology. Regulatory, integrative and comparative physiology*. **303**(5), R477-84.

Imai-Matsumura, K., Matsumura, K., Nakayama, T. (1984) Involvement of ventromedial hypothalamus in brown adipose tissue thermogenesis induced by preoptic cooling in rats. *The Japanese journal of physiology*. **34**(5), 939–43.

Ingalls, A.M., Dickie, M.M., Snell, G.D. (1950) Obese, a new mutation in the house mouse. *The Journal of heredity*. **41**(12), 317–8.

Jego, S., Glasgow, S.D., Herrera, C.G., Ekstrand, M., Reed, S.J., Boyce, R., Friedman, J., Burdakov, D., Adamantidis, A.R. (2013) Optogenetic identification of a rapid eye movement sleep modulatory circuit in the hypothalamus. *Nature Neuroscience*. **16**(11), 1637–1643.

Jennings, J.H., Ung, R.L., Resendez, S.L., Stamatakis, A.M., Taylor, J.G., Huang, J., Veleta, K., Kantak, P.A., Aita, M., Shilling-Scrivo, K., Ramakrishnan, C., Deisseroth, K., Otte, S., Stuber, G.D. (2015) Visualizing Hypothalamic Network Dynamics for Appetitive and Consummatory Behaviors. *Cell*. **160**(3), 516–527.

Jeong, J.H., Lee, D.K., Blouet, C., Ruiz, H.H., Buettner, C., Chua, S., Schwartz, G.J., Jo, Y.-H. (2015) Cholinergic neurons in the dorsomedial hypothalamus regulate mouse brown adipose tissue metabolism. *Molecular Metabolism*. **4**(6), 483–492.

Ju, H., So, H., Ha, K., Park, K., Lee, J.-W., Chung, C.-M., Choi, I. (2011) Sustained torpidity following multi-dose administration of 3-iodothyronamine in mice. *Journal of Cellular Physiology*. **226**(4), 853–858.

Jurkovich, G.J., Pitt, R.M., Curreri, P.W., Granger, D.N. (1988) Hypothermia prevents increased capillary permeability following ischemia-reperfusion injury. *The Journal of surgical research*. **44**(5), 514–21.

Karnatovskaia, L. V., Wartenberg, K.E., Freeman, W.D. (2014) Therapeutic Hypothermia for Neuroprotection. *The Neurohospitalist*. **4**(3), 153–163.

Kerman, I.A., Akil, H., Watson, S.J. (2006) Rostral Elements of Sympatho-motor Circuitry: A Virally Mediated Transsynaptic Tracing Study. *Journal of Neuroscience*. **26**(13), 3423–3433.

Klok, M.D., Jakobsdottir, S., Drent, M.L. (2007) The role of leptin and ghrelin in the regulation of food intake and body weight in humans: a review. *Obesity Reviews*. **8**(1), 21–34.

Komelina, N.P., Polskaya, A.I., Amerkhanov, Z.G. (2015) Artificial hypothermia in rats, unlike natural hibernation in ground squirrels Spermophilus undulatus, is not accompanied by the inhibition of respiration in liver mitochondria. *Biochemistry (Moscow) Supplement Series A: Membrane and Cell Biology*. **9**(4), 293–302.

Körtner, G., Geiser, F. (2000) The temporal organization of daily torpor and hibernation: circadian and circannual rhythms. *Chronobiology international*. **17**(2), 103–28.

Kovács, K.J. (2008) Measurement of Immediate-Early Gene Activation- *c-fos* and Beyond. *Journal of Neuroendocrinology*. **20**(6), 665–672.

Krashes, M.J., Koda, S., Ye, C., Rogan, S.C., Adams, A.C., Cusher, D.S., Maratos-Flier, E., Roth, B.L., Lowell, B.B. (2011) Rapid, reversible activation of AgRP neurons drives feeding behavior in mice. *Journal of Clinical Investigation*. **121**(4), 1424–1428.

Krashes, M.J., Shah, B.P., Koda, S., Lowell, B.B. (2013) Rapid versus Delayed Stimulation of Feeding by the Endogenously Released AgRP Neuron Mediators GABA, NPY, and AgRP. *Cell Metabolism*. **18**(4), 588–595.

Krilowicz, B.L., Szymusiak, R., McGinty, D. (1994) Regulation of posterior lateral hypothalamic arousal related neuronal discharge by preoptic anterior hypothalamic warming. *Brain research*. **668**(1–2), 30–8.

Kuskin, S.M., Wang, S.C., Rugh, R. (1959) Protective effect of artificially induced hibernation against lethal doses of whole body x-irradiation in CF male mice. *The American journal of physiology*. **196**(6), 1211–3.

Kutschke, M., Grimpo, K., Kastl, A., Schneider, S., Heldmaier, G., Exner, C., Jastroch, M. (2013) Depression of mitochondrial respiration during daily torpor of the Djungarian hamster, Phodopus sungorus, is specific for liver and correlates with body temperature. *Comparative Biochemistry and Physiology Part A: Molecular & Integrative Physiology*. **164**(4), 584–589.

Latini, S., Pedata, F. (2001) Adenosine in the central nervous system: release mechanisms and extracellular concentrations. *Journal of neurochemistry*. **79**(3), 463–84.

Lee, C.C. (2008) Is Human Hibernation Possible? *Annual Review of Medicine*. **59**(1), 177–186.

Leinninger, G.M., Opland, D.M., Jo, Y.-H., Faouzi, M., Christensen, L., Cappellucci, L.A., Rhodes, C.J., Gnegy, M.E., Becker, J.B., Pothos, E.N., Seasholtz, A.F., Thompson, R.C., Myers, M.G. (2011) Leptin Action via Neurotensin Neurons Controls Orexin, the Mesolimbic Dopamine System and Energy Balance. *Cell Metabolism*. **14**(3), 313–323.

Levine, A.S., Kneip, J., Grace, M., Morley, J.E. (1983) Effect of centrally administered neurotensin on multiple feeding paradigms. *Pharmacology, biochemistry, and behavior*. **18**(1), 19–23.

Lomax, P., Malveaux, E., Smith, R.E. (1964) Brain temperatures in the rat during exposure to low environmental temperatures. *The American journal of*

physiology. **207**, 736–9.

Lynch, G.R., White, S.E., Grundel, R., Berger, M.S. (1978) Effects of photoperiod, melatonin administration and thyroid block on spontaneous daily torpor and temperature regulation in the white-footed mouse,Peromyscus leucopus. *Journal of Comparative Physiology B*. **125**(2), 157–163.

MacLaren, R., Gallagher, J., Shin, J., Varnado, S., Nguyen, L. (2014) Assessment of adverse events and predictors of neurological recovery after therapeutic hypothermia. *The Annals of pharmacotherapy*. **48**(1), 17–25.

Madden, C.J., Morrison, S.F. (2009) Neurons in the paraventricular nucleus of the hypothalamus inhibit sympathetic outflow to brown adipose tissue. *American journal of physiology. Regulatory, integrative and comparative physiology*. **296**(3), R831-43.

Margules, D.L., Goldman, B., Finck, A. (1979) Hibernation: an opioid-dependent state? *Brain research bulletin*. **4**(6), 721–4.

Marks, A., Vianna, D.M.L., Carrive, P. (2009) Nonshivering thermogenesis without interscapular brown adipose tissue involvement during conditioned fear in the rat. *AJP: Regulatory, Integrative and Comparative Physiology*. **296**(4), R1239–R1247.

Martin, S.L., Maniero, G.D., Carey, C., Hand, S.C. (1999) Reversible Depression of Oxygen Consumption in Isolated Liver Mitochondria during Hibernation. *Physiological and Biochemical Zoology*. **72**(3), 255–264.

Mattiasson, G., Shamloo, M., Gido, G., Mathi, K., Tomasevic, G., Yi, S., Warden, C.H., Castilho, R.F., Melcher, T., Gonzalez-Zulueta, M., Nikolich, K., Wieloch, T. (2003) Uncoupling protein-2 prevents neuronal death and diminishes brain dysfunction after stroke and brain trauma. *Nature Medicine*. **9**(8), 1062–1068.

McAllen, R.M. (1986) Action and specificity of ventral medullary vasopressor neurones in the cat. *Neuroscience*. **18**(1), 51–9.

McAllen, R.M., Farrell, M., Johnson, J.M., Trevaks, D., Cole, L., McKinley, M.J.,

Jackson, G., Denton, D.A., Egan, G.F. (2006) Human medullary responses to cooling and rewarming the skin: A functional MRI study. *Proceedings of the National Academy of Sciences*. **103**(3), 809–813.

McAllen, R.M., Neil, J.J., Loewy, A.D. (1982) Effects of kainic acid applied to the ventral surface of the medulla oblongata on vasomotor tone, the baroreceptor reflex and hypothalamic autonomic responses. *Brain research*. **238**(1), 65–76.

Messier, M.L., Li, A., Nattie, E.E. (2004) Inhibition of medullary raphe serotonergic neurons has age-dependent effects on the CO2 response in newborn piglets. *Journal of applied physiology (Bethesda, Md. : 1985)*. **96**(5), 1909–19.

Miller, L.P., Hsu, C. (1992) Therapeutic potential for adenosine receptor activation in ischemic brain injury. *Journal of neurotrauma*. **9 Suppl 2**, S563-77.

Milsom, W.K., Zimmer, M.B., Harris, M.B. (1999) Regulation of cardiac rhythm in hibernating mammals. *Comparative biochemistry and physiology. Part A, Molecular & integrative physiology*. **124**(4), 383–91.

Morrison, S.F. (2003) Raphe pallidus neurons mediate prostaglandin E2-evoked increases in brown adipose tissue thermogenesis. *Neuroscience*. **121**(1), 17–24.

Morrison, S.F. (1999) RVLM and raphe differentially regulate sympathetic outflows to splanchnic and brown adipose tissue. *The American journal of physiology*. **276**(4 Pt 2), R962-73.

Morrison, S.F., Nakamura, K. (2011) Central neural pathways for thermoregulation. *Frontiers in bioscience (Landmark edition)*. **16**, 74–104.

Morrison, S.F., Nakamura, K., Madden, C.J. (2008) Central control of thermogenesis in mammals. *Experimental physiology*. **93**(7), 773–97.

Nakamura, K., Matsumura, K., Hübschle, T., Nakamura, Y., Hioki, H., Fujiyama, F., Boldogköi, Z., König, M., Thiel, H.-J., Gerstberger, R., Kobayashi, S., Kaneko, T. (2004) Identification of Sympathetic Premotor Neurons in Medullary Raphe Regions Mediating Fever and Other Thermoregulatory Functions. *Journal of Neuroscience*. **24**(23), 5370–5380.

Nakamura, K., Matsumura, K., Kobayashi, S., Kaneko, T. (2005) Sympathetic premotor neurons mediating thermoregulatory functions. *Neuroscience Research*. **51**(1), 1–8.

Nakamura, K., Morrison, S.F. (2010) A thermosensory pathway mediating heat-defense responses. *Proceedings of the National Academy of Sciences*. **107**(19), 8848–8853.

Nakayama, T., Hammel, H.T., Hardy, J.D., Eisenman, J.S. (1963) *American journal of physiology*. American Physiological Society.

Natarajan, M., Morrison, S.F. (1999) Adrenal epinephrine secretion is not regulated by sympathoinhibitory neurons in the caudal ventrolateral medulla. *Brain research*. **827**(1–2), 169–75.

Oelkrug, R., Heldmaier, G., Meyer, C.W. (2011) Torpor patterns, arousal rates, and temporal organization of torpor entry in wildtype and UCP1-ablated mice. *Journal of Comparative Physiology B*. **181**(1), 137–145.

Olson, J.M., Jinka, T.R., Larson, L.K., Danielson, J.J., Moore, J.T., Carpluck, J., Drew, K.L. (2013) Circannual Rhythm in Body Temperature, Torpor, and Sensitivity to A_1 Adenosine Receptor Agonist in Arctic Ground Squirrels. *Journal of Biological Rhythms*. **28**(3), 201–207.

Ootsuka, Y., Blessing, W.W. (2005) Inhibition of medullary raphé/parapyramidal neurons prevents cutaneous vasoconstriction elicited by alerting stimuli and by cold exposure in conscious rabbits. *Brain Research*. **1051**(1–2), 189–193.

Ootsuka, Y., Blessing, W.W., McAllen, R.M. (2004) Inhibition of rostral medullary raphé neurons prevents cold-induced activity in sympathetic nerves to rat tail and rabbit ear arteries. *Neuroscience Letters*. **357**(1), 58–62.

Paul, M.J., Freeman, D.A., Park, J.H., Dark, J. (2005) Neuropeptide Y induces torpor-like hypothermia in Siberian hamsters. *Brain Research*. **1055**(1–2), 83–92.

Paxinos, G., Franklin, K.B.J. (2004) *The mouse brain in stereotaxic coordinates*.

Elsevier Academic Press.

Paxinos, G., Watson, C. (2007) *The rat brain in stereotaxic coordinates*. Elsevier.

Polderman, K.H. (2004) Keeping a cool head: How to induce and maintain hypothermia. *Critical care medicine*. **32**(12), 2558–60.

Puente-Maestu, L., Pérez-Parra, J., Godoy, R., Moreno, N., Tejedor, A., González-Aragoneses, F., Bravo, J.-L., Alvarez, F.V., Camaño, S., Agustí, A. (2009) Abnormal mitochondrial function in locomotor and respiratory muscles of COPD patients. *The European respiratory journal*. **33**(5), 1045–52.

Qu, D., Ludwig, D.S., Gammeltoft, S., Piper, M., Pelleymounter, M.A., Cullen, M.J., Mathes, W.F., Przypek, J., Kanarek, R., Maratos-Flier, E. (1996) A role for melanin-concentrating hormone in the central regulation of feeding behaviour. *Nature*. **380**(6571), 243–247.

Quinones, Q.J., Ma, Q., Zhang, Z., Barnes, B.M., Podgoreanu, M. V (2014) Organ protective mechanisms common to extremes of physiology: a window through hibernation biology. *Integrative and comparative biology*. **54**(3), 497–515.

Raimbault, S., Dridi, S., Denjean, F., Lachuer, J., Couplan, E., Bouillaud, F., Bordas, A., Duchamp, C., Taouis, M., Ricquier, D. (2001) An uncoupling protein homologue putatively involved in facultative muscle thermogenesis in birds. *The Biochemical journal*. **353**(Pt 3), 441–4.

Roberts, J.C., Chaffee, R.R. (1973) Effects of cold acclimation, hibernation and temperature on succinoxidase activity of heart homogenates from hamster, rat and squirrel monkey. *Comparative biochemistry and physiology. B, Comparative biochemistry*. **44**(1), 137–44.

Romanovsky, A.A. (2006) Thermoregulation: some concepts have changed. Functional architecture of the thermoregulatory system. *AJP: Regulatory, Integrative and Comparative Physiology*. **292**(1), R37–R46.

Ruf, T., Geiser, F. (2015) Daily torpor and hibernation in birds and mammals. *Biological Reviews*. **90**(3), 891–926.

Ruf, T., Stieglitz, A., Steinlechner, S., Blank, J.L., Heldmaier, G. (1993) Cold exposure and food restriction facilitate physiological responses to short photoperiod in Djungarian hamsters (Phodopus sungorus). *Journal of Experimental Zoology*. **267**(2), 104–112.

Saito, M., Okamatsu-Ogura, Y., Matsushita, M., Watanabe, K., Yoneshiro, T., Nio-Kobayashi, J., Iwanaga, T., Miyagawa, M., Kameya, T., Nakada, K., Kawai, Y., Tsujisaki, M. (2009) High Incidence of Metabolically Active Brown Adipose Tissue in Healthy Adult Humans: Effects of Cold Exposure and Adiposity. *Diabetes*. **58**(7), 1526–1531.

Sakurai, T. (2014) Roles of orexins in the regulation of body weight homeostasis. *Obesity Research & Clinical Practice*. **8**(5), e414–e420.

Sakurai, T., Amemiya, A., Ishii, M., Matsuzaki, I., Chemelli, R.M., Tanaka, H., Williams, S.C., Richardson, J.A., Kozlowski, G.P., Wilson, S., Arch, J.R., Buckingham, R.E., Haynes, A.C., Carr, S.A., Annan, R.S., McNulty, D.E., Liu, W.S., Terrett, J.A., Elshourbagy, N.A., Bergsma, D.J., Yanagisawa, M. (1998) Orexins and orexin receptors: a family of hypothalamic neuropeptides and G protein-coupled receptors that regulate feeding behavior. *Cell*. **92**(4), 573–85.

Saper, C.B. (2002) The Central Autonomic Nervous System: Conscious Visceral Perception and Autonomic Pattern Generation. *Annual Review of Neuroscience*. **25**(1), 433–469.

Saper, C.B., Lu, J., Chou, T.C., Gooley, J. (2005) The hypothalamic integrator for circadian rhythms. *Trends in Neurosciences*. **28**(3), 152–157.

Scanlan, T.S., Suchland, K.L., Hart, M.E., Chiellini, G., Huang, Y., Kruzich, P.J., Frascarelli, S., Crossley, D.A., Bunzow, J.R., Ronca-Testoni, S., Lin, E.T., Hatton, D., Zucchi, R., Grandy, D.K. (2004) 3-Iodothyronamine is an endogenous and rapid-acting derivative of thyroid hormone. *Nature Medicine*. **10**(6), 638–642.

Schéle, E., Bake, T., Rabasa, C., Dickson, S.L. (2016) Centrally Administered Ghrelin Acutely Influences Food Choice in Rodents M. López, ed. *PLOS ONE*.

11(2), e0149456.

Schwartz, M.W., Woods, S.C., Porte, D., Seeley, R.J., Baskin, D.G. (2000) Central nervous system control of food intake. *Nature*. **404**(6778), 661–671.

Seoane, L.M., Tovar, S., Baldelli, R., Arvat, E., Ghigo, E., Casanueva, F.F., Dieguez, C. (2000) Ghrelin elicits a marked stimulatory effect on GH secretion in freely-moving rats. *European journal of endocrinology*. **143**(5), R7-9.

Sgarbi, G., Giannone, F., Casalena, G.A., Baracca, A., Baldassare, M., Longobardi, P., Caraceni, P., Derenzini, M., Lenaz, G., Trerè, D., Solaini, G. (2011) Hyperoxia fully protects mitochondria of explanted livers. *Journal of Bioenergetics and Biomembranes*. **43**(6), 673–682.

Shimbara, T., Mondal, M.S., Kawagoe, T., Toshinai, K., Koda, S., Yamaguchi, H., Date, Y., Nakazato, M. (2004) Central administration of ghrelin preferentially enhances fat ingestion. *Neuroscience Letters*. **369**(1), 75–79.

Smith, J.E., Jansen, A.S., Gilbey, M.P., Loewy, A.D. (1998) CNS cell groups projecting to sympathetic outflow of tail artery: neural circuits involved in heat loss in the rat. *Brain research*. **786**(1–2), 153–64.

Soleimanpour, H., Rahmani, F., Safari, S., EJ Golzari, S. (2014) Hypothermia After Cardiac Arrest as a Novel Approach to Increase Survival in Cardiopulmonary Cerebral Resuscitation: A Review. *Iranian Red Crescent Medical Journal*. **16**(7), e17497.

Stachniak, T.J., Ghosh, A., Sternson, S.M. (2014) Chemogenetic Synaptic Silencing of Neural Circuits Localizes a Hypothalamus→Midbrain Pathway for Feeding Behavior. *Neuron*. **82**(4), 797–808.

Stamper, J.L., Dark, J., Zucker, I. (1999) Photoperiod modulates torpor and food intake in Siberian hamsters challenged with metabolic inhibitors. *Physiology & behavior*. **66**(1), 113–8.

Standish, A., Enquist, L.W., Escardo, J.A., Schwaber, J.S. (1995) Central neuronal circuit innervating the rat heart defined by transneuronal transport of

pseudorabies virus. *The Journal of neuroscience : the official journal of the Society for Neuroscience*. **15**(3 Pt 1), 1998–2012.

Staples, J.F., Brown, J.C.L. (2008) Mitochondrial metabolism in hibernation and daily torpor: a review. *Journal of Comparative Physiology B*. **178**(7), 811–827.

Sternson, S.M., Atasoy, D. (2014) Agouti-Related Protein Neuron Circuits That Regulate Appetite. *Neuroendocrinology*. **100**(2–3), 95–102.

Sternson, S.M., Eiselt, A.-K. (2017) Three Pillars for the Neural Control of Appetite. *Annual Review of Physiology*. **79**(1), 401–423.

Stitt, J.T. (1973) Prosaglandin E1 fever induced in rabbits. *The Journal of physiology*. **232**(1), 163–79.

Storey, K.B., Storey, J.M. (1990) Metabolic Rate Depression and Biochemical Adaptation in Anaerobiosis, Hibernation and Estivation. *The Quarterly Review of Biology*. **65**(2), 145–174.

Stornetta, R.L., Rosin, D.L., Simmons, J.R., McQuiston, T.J., Vujovic, N., Weston, M.C., Guyenet, P.G. (2005) Coexpression of vesicular glutamate transporter-3 and γ-aminobutyric acidergic markers in rat rostral medullary raphe and intermediolateral cell column. *The Journal of Comparative Neurology*. **492**(4), 477–494.

Stuber, G.D., Wise, R.A. (2016) Lateral hypothalamic circuits for feeding and reward. *Nature neuroscience*. **19**(2), 198–205.

Swoap, S.J., Rathvon, M., Gutilla, M. (2007) AMP does not induce torpor. *AJP: Regulatory, Integrative and Comparative Physiology*. **293**(1), R468–R473.

Tamura, Y., Shintani, M., Nakamura, A., Monden, M., Shiomi, H. (2005) Phase-specific central regulatory systems of hibernation in Syrian hamsters. *Brain research*. **1045**(1–2), 88–96.

Tanaka, M., McAllen, R.M. (2005) A subsidiary fever center in the medullary raphe? *AJP: Regulatory, Integrative and Comparative Physiology*. **289**(6), R1592–R1598.

Tanaka, M., Nagashima, K., McAllen, R.M., Kanosue, K. (2002) Role of the medullary raphé in thermoregulatory vasomotor control in rats. *The Journal of physiology*. **540**(Pt 2), 657–64.

Tanaka, M., Owens, N.C., Nagashima, K., Kanosue, K., McAllen, R.M. (2006) Reflex activation of rat fusimotor neurons by body surface cooling, and its dependence on the medullary raphé. *The Journal of Physiology*. **572**(2), 569–583.

Tang-Christensen, M., Vrang, N., Ortmann, S., Bidlingmaier, M., Horvath, T.L., Tschöp, M. (2004) Central Administration of Ghrelin and Agouti-Related Protein (83–132) Increases Food Intake and Decreases Spontaneous Locomotor Activity in Rats. *Endocrinology*. **145**(10), 4645–4652.

Tao, Z., Zhao, Z., Lee, C.C. (2011) 5'- Adenosine monophosphate induced hypothermia reduces early stage myocardial ischemia/reperfusion injury in a mouse model. *American journal of translational research*. **3**(4), 351–61.

Tokita, K., Armstrong, W.E., St. John, S.J., Boughter Jr., J.D. (2014) Activation of lateral hypothalamus-projecting parabrachial neurons by intraorally delivered gustatory stimuli. *Frontiers in Neural Circuits*. **8**, 86.

Tóth, I.E., Tóth, D.E., Boldogkoi, Z., Hornyák, A., Palkovits, M., Blessing, W.W. (2006) Serotonin-synthesizing neurons in the rostral medullary raphé/parapyramidal region transneuronally labelled after injection of pseudorabies virus into the rat tail. *Neurochemical research*. **31**(2), 277–86.

Tsubone, T., Masaki, T., Katsuragi, I., Tanaka, K., Kakuma, T., Yoshimatsu, H. (2005) Ghrelin regulates adiposity in white adipose tissue and UCP1 mRNA expression in brown adipose tissue in mice. *Regulatory Peptides*. **130**(1–2), 97–103.

Tupone, D., Madden, C.J., Morrison, S.F. (2013) Central Activation of the A1 Adenosine Receptor (A1AR) Induces a Hypothermic, Torpor-Like State in the Rat. *Journal of Neuroscience*. **33**(36), 14512–14525.

Vianna, D.M.L., Carrive, P. (2005) Changes in cutaneous and body temperature

during and after conditioned fear to context in the rat. *European Journal of Neuroscience*. **21**(9), 2505–2512.

Volkow, N.D., Morales, M. (2015) The Brain on Drugs: From Reward to Addiction. *Cell*. **162**(4), 712–725.

Walker, H.C., Romsos, D.R. (1993) Similar effects of NPY on energy metabolism and on plasma insulin in adrenalectomized ob/ob and lean mice. *The American journal of physiology*. **264**(2 Pt 1), E226-30.

Wang, L., Saint-Pierre, D.H., Taché, Y. (2002) Peripheral ghrelin selectively increases Fos expression in neuropeptide Y – synthesizing neurons in mouse hypothalamic arcuate nucleus. *Neuroscience Letters*. **325**(1), 47–51.

Williams, J.W., Rudy, T.A., Yaksh, T.L., Viswanathan, C.T. (1977) An extensive exploration of the rat brain for sites mediating prostaglandin-induced hyperthermia. *Brain research*. **120**(2), 251–62.

Williams, K.W., Elmquist, J.K. (2012) From neuroanatomy to behavior: central integration of peripheral signals regulating feeding behavior. *Nature Neuroscience*. **15**(10), 1350–1355.

Wilz, M., Heldmaier, G. (2000) Comparison of hibernation, estivation and daily torpor in the edible dormouse, Glis glis. *Journal of comparative physiology. B, Biochemical, systemic, and environmental physiology*. **170**(7), 511–21.

Yakimova, K.S., Sann, H., Pierau, F.K. (1996) Neuronal basis for the hyperthermic effect of mu-opioid agonists in rats: decrease in temperature sensitivity of warm-sensitive hypothalamic neurons. *Neuroscience letters*. **218**(2), 115–8.

Yamamoto, T., Shimura, T., Sako, N., Yasoshima, Y., Sakai, N. (1994) Neural substrates for conditioned taste aversion in the rat. *Behavioural brain research*. **65**(2), 123–37.

Yasuda, T., Masaki, T., Kakuma, T., Yoshimatsu, H. (2003) Centrally administered ghrelin suppresses sympathetic nerve activity in brown adipose tissue of rats. *Neuroscience letters*. **349**(2), 75–8.

Zee, P.C., Manthena, P. (2007) The brain's master circadian clock: Implications and opportunities for therapy of sleep disorders. *Sleep Medicine Reviews*. **11**(1), 59–70.

Zhang, F., Wang, S., Luo, Y., Ji, X., Nemoto, E.M., Chen, J. (2009) When hypothermia meets hypotension and hyperglycemia: the diverse effects of adenosine 5'-monophosphate on cerebral ischemia in rats. *Journal of cerebral blood flow and metabolism : official journal of the International Society of Cerebral Blood Flow and Metabolism*. **29**(5), 1022–34.

Zhang, Y., Proenca, R., Maffei, M., Barone, M., Leopold, L., Friedman, J.M. (1994) Positional cloning of the mouse obese gene and its human homologue. *Nature*. **372**(6505), 425–432.

Zhu, X., Ottenheimer, D., DiLeone, R.J. (2016) Activity of D1/2 Receptor Expressing Neurons in the Nucleus Accumbens Regulates Running, Locomotion, and Food Intake. *Frontiers in Behavioral Neuroscience*. **10**, 66.

ACKNOWLEDGEMENTS

First and foremost, I would like to thank deeply my lab group. My tutor, Professor Roberto Amici, that always had time and wise advices whenever needed, Dr. Matteo Cerri, who to taught me curiosity, Dr. Marco Luppi, who taught me scientific rigorousness and method. Prof. Giovanni Zamboni, Prof. Emanuele Perez, Dr. Davide Martelli and Dr. Domenico Tupone, who were always there when I needed help.

Special thanks go to the best colleague in the world, Dr. Alessia di Cristoforo, who has been a true friend in difficult moments.

Lastly, my gratitude goes to my parents, my boyfriend, and my friends, that supported every my decision and made this possible.